Aus der Neurochirurgischen Klinik und Poliklinik, Klinik der

Ludwig-Maximilians-Universität München

Vorstand: Prof. Dr. Jörg-Christian Tonn

Investigating the Effect of Cannabidiol on NF-κB Phosphorylation and Nuclear Translocation in Glioblastoma Cells

Dissertation
zum Erwerb des Doktorgrades der Medizin
an der Medizinischen Fakultät der
Ludwig-Maximilians-Universität zu München

vorgelegt von

Haitham Alenezi

aus

Madinah

Jahr

2022

Mit Genehmigung der Medizinischen Fakultät
der Universität München

Berichterstatter:	Prof. Dr. Rainer Glaß
Mitberichterstatter/in:	Prof. Dr. Claus Schäfer Prof. Dr. Nathalie Albert
Mitbetreuung durch den promovierten Mitarbeiter:	Dr. Roland Kälin
Dekan:	Prof. Dr. med. Thomas Gudermann
Tag der mündlichen Prüfung:	29.09.2022

Table of Contents

List of Figures

List of Tables

IV. Abbreviations

Bcl-3	B-cell lymphoma 3-encoded protein
BCR	B Cell Receptor
CBD	Cannabidiol
CDKN2A	Cyclin-Dependent Kinase Inhibitor 2A
cIAP1	Baculoviral IAP repeat-containing protein 2
CKII	Casein Kinase II
CT	Computed Tomography
DAPI	4′,6-Diamidin-2-phenylindol
DTI	Diffusion Tensor Imaging
EGFR	Epidermal Growth Factor Receptor
GBM	Glioblastoma
ICC	Immunocytochemistry
IDH1	Isocitrate Dehydrogenase-1
Ig	immunoglobulin
IKK	Inhibitor of kappa-B Kinase
IκB	Inhibitor of kappa-B
LPS	Lipopolysaccharide
LTβR	Lymphotoxin B receptor
MRI	Magnetic Resonance Imaging
MS	Multiple Sclerosis
NF-κB	Nuclear Factor kappa-B
NIK	NF-κB Inducing Kinase
PDGF	Platelet-Derived Growth Factor
PDGFRA	Platelet-Derived Growth Factor Receptor α
RANKL	Receptor Activator of Nuclear factor kappa-B Ligand
RHD	Rel Homology Domain
SETD6	(SET Domain-containing 6)
TACE	TNFα converting enzyme

THC	delta-9 tetrahydrocannabinol
TLR	Toll-Like Receptor
TMZ	Temozolomide
TNFR	Tumour Necrosis Factor Receptor
TNFα	Tumour Necrosis Factor alpha
TP53	Tumour Protein p53
TRADD	Tumour Necrosis Factor Receptor type 1-associated Death Domain
TRAF2	TNF Receptor-Associated Factor 2
TRPA1	Transient Receptor Potential Ankyrin 1

1. Introduction

1.1 Glioblastoma

Glioblastoma (GBM) is the most common primary malignant brain tumour, which has a bad chance of survival once diagnosed (Sinigaglia, et al. 2019); (Sundar, et al. 2014). GBM is assigned the highest severity (Grade 4) by the World Health Organization (WHO) for its fast spreading and destructive nature (Louis, et al. 2021); (Molinaro, et al. 2019); (Young, et al. 2015).

1.1.1 Symptoms

General symptoms caused by GBM can vary and include derangement, headaches, lethargy, dizziness, nausea, loss of vision, stroke-like symptoms or memory loss (Young, et al. 2015). The severity of these symptoms depends on a variety of factors, for example the size and the location of the tumour (Young, et al. 2015). The intracerebral edema caused by the tumour may also cause different neurological symptoms (Young, et al. 2015).

1.1.2 Classification

The WHO classification 2021 of brain and spinal cord tumours is based on histopathologic appearance and established molecular biomarkers (Louis, et al. 2021). Particularly the WHO classification includes three genetic parameters beside the invasive microvascular proliferation and necrosis as criteria for the diagnosis of GBM, isocitrate dehydrogenase (IDH) wildtype (Grade 4) (Louis, et al. 2021). These are Telomerase Reverse Transcriptase (TERT) promoter mutation, Epidermal Growth Factor Receptor (EGFR) gene amplification, combined gain of entire chromosome 7 and loss of entire chromosome 10 (+7/−10) (Louis, et al. 2021). The IDH-mutation is associated with favourable prognosis and mainly found in lower-grade gliomas (Louis, et al. 2021); (Brito, et al. 2019); (Molinaro, et al. 2019).

The molecular classification of GBM provides many clinical and therapeutic benefits for better understanding of the malignant tumour, accurate diagnosis and choosing the appropriate procedure for treatment (Lee, et al. 2018); (Verhaak, et al. 2010). There are many mutations and abnormalities in tumour suppressor genes and oncogenes,

which were investigated and categorized into gene expression profiles (Lee, et al. 2018); (Verhaak, et al. 2010). These gene expression profiles enable a characterisation of GBM into several subtypes such as classical, proneural and mesenchymal (Wang, et al. 2017); (Verhaak, et al. 2010). The classical subtype is known for its overexpression of Epidermal Growth Factor Receptor (EGFR), deletion of Cyclin-Dependent Kinase Inhibitor 2A (CDKN2A) and absence of Tumour Protein p53 (TP53) mutation (Lee, et al. 2018); (Verhaak, et al. 2010). The proneural subtype is described by several alteration markers such as the overexpression of Platelet-Derived Growth Factor Receptor α (PDGFR α) (Lee, et al. 2018). Activation of PDGFRα triggers an intracellular signalling cascade leading to proliferation, regeneration and increased malignity in tumour cells (Heldin 2013). DNA methylation status is also involved in GBM subtype characterisation. Glioma cytosine-phosphate-guanine (CpG) island methylator phenotype (G-CIMP) is a molecular biomarker, which highly appears among the proneural subtype (Lee, et al. 2018). The appearance of G-CIMP methylation is associated with IDH mutation (Malta, et al. 2018). Both are related to a better prognosis (Malta, et al. 2018).

Furthermore, O^6-methylguanine-DNA methyltransferase (MGMT) is a protein that repairs the DNA by removing the most common alkylation on the O^6 position of guanine (O^6-meG) (Lee, et al. 2018). This protein supresses the activity of alkylating agent e.g. temozolomide (Lee, et al. 2018). The methylation of MGMT promoter is associated with a better response to temozolomide therapy and a favourable prognosis in GBM (Brito, et al. 2019); (Malta, et al. 2018).

Neurofibromin (NF1) gene is mutated in about 20% of GBM and it is mainly associated with the mesenchymal subtype (Wood, Mukherjee and Pieper 2018) and (Verhaak, et al. 2010). NF1 is a GTPase activating protein that downregulates the RAS signalling pathway and its pro-malignant effects under basal conditions (Wood, Mukherjee and Pieper 2018). The lack of NF1 activity causes neurofibromatosis type 1, predisposition to gliomas and aggressive tumorigenesis (Wood, Mukherjee and Pieper 2018).

Epidermal Growth Factor Receptor (EGFR) is a transmembrane protein receptor tyrosine kinases that can promote DNA transcription, anti-apoptosis and cell growth

(Zhang, et al. 2007). EGFR variant III mutation (EGFRvIII) is the most prominent EGFR mutation in GBM, in which the amino acids 6-273 are deleted from the N-terminal domain (Lee, et al. 2018). This mutation causes structure changes rendering the receptor independence from extracellular ligand and expanded activity (Lee, et al. 2018).

Cyclin-dependent kinase inhibitor 2A (CDKN2A) is a gene located on chromosome 9p21 and encodes two proteins p16 and p14ARF which are involved in cell cycle inhibition and tumour suppression (Helgadottir, et al. 2018). A mutated CDKN2A is associated with tumour cells growth and metastases (Helgadottir, et al. 2018). TP53 gene encodes the protein tumour p53 which plays an important role in cell cycle, angiogenesis inhibition, tumour suppression and apoptosis (Jesionek-Kupnicka, et al. 2014). Mutated TP53 gene disables p53 from fulfilling its role (Jesionek-Kupnicka, et al. 2014).

1.2 NF- κB

Nuclear Factor kappa-B (NF-κB) is a transcription factor that is practically found in all mammalian cells (Gilmore 2006). Its importance is observed in inflammation, immune response and autoimmunity (Evans, et al. 2018).

1.2.1 Structure

NF-κB is not a single molecule (Liu, et al. 2017). NF-κB but represents a family of five different protein subunits namely RelA (p65), RelB, c-Rel, NF-κB1 (p50/p105), and NF-κB2 (p52/p100) (Liu, et al. 2017). These protein subunits bind in different combinations to form homodimeric and heterodimeric NF-κB complexes (Liu, et al. 2017). All these protein subunits contain a Rel Homology Domain (RHD) which is a domain of approximately 300 amino acids located toward the N terminus of the protein (Oeckinghaus and Ghosh 2009). RHD plays a major role in dimerization, interaction with IκB (Inhibitor of κB) and binding to DNA (Oeckinghaus and Ghosh 2009). The protein subunits p100 and p105 have inhibitory domains which restrict the nuclear localisation and DNA binding (Mussbacher, et al. 2019). These protein subunits undergo to activation processes by proteasomes to generate p52 from p100

and p50 from p105 (Mussbacher, et al. 2019). Dimers of p50 and p52 act as transcriptional repressors (Mussbacher, et al. 2019). Although p50 and p52 can bind to promoter regions of DNA, they are unable to activate transcription processes due to the absence of transactivation domain (Mussbacher, et al. 2019). The other three NF-κB protein subunits p65 (RelA), RelB, and c-Rel do not have these inhibitory domains (Mussbacher, et al. 2019). Therefore, p50 and p52 have to form dimers with one of the other three NF-κB protein subunits to enhance a transcription of target genes (Mussbacher, et al. 2019). The heterodimer p50/p65 is the common NF-κB form (Korc 2016); (Lash 2010). Most unstimulated cells contain NF-κB dimers bound with the inhibitor IκB which keep p50/p65 in the cytoplasm (Mussbacher, et al. 2019). Activation of NF-κB signalling is induced by release of p50/p65 from the cytoplasmic chaperones and translocation to the nucleus (Oeckinghaus and Ghosh 2009); (Hayden and Ghosh 2004).

The IκB family consists of IκBα, IκBβ, IκBε, IκB-ζ and B-cell lymphoma 3-encoded protein (Bcl-3) (Bremner and Heinrich 2010); (Yamazaki, Muta and Takeshige 2001). The inducible post-translational modification specifically the phosphorylation of NF-κB protein subunits is important for an efficient transcription of desired genes (Hochrainer, et al. 2013). The NF-κB protein subunit p65 which has the highest potency of transcriptional activation compared to other NF-κB protein subunits has 12 phospho-acceptor sites of serine (ser) and threonine (thr) amino acids (Hochrainer, et al. 2013). There are five sites (ser-205, thr-254, ser-276, ser-281, and ser-311) located toward the N-terminal of RHD while seven sites (thr-435, ser-468, thr-505, ser-529, ser-535, ser-536, and ser-547) are located toward the C-terminal of transcriptional activation domains (Hochrainer, et al. 2013). The phosphorylation of these serine sites plays a major role in controlling modulation, activation and inhibition of NF-κB transcription functions (Alexander V. Bagaev, et al. 2019); (Christian, Smith and Carmody 2016).

1.2.2 NF-κB Signalling Pathway

The activity of NF-κB is regulated by the canonical (classical) pathway and the non-canonical (alternative) pathway (Liu, et al. 2012). The activation of the NF-κB in the canonical pathway is e.g. induced by several pro-inflammatory receptors like T Cell Receptor (TCR), B Cell Receptor (BCR), Toll-Like Receptor (TLR), Interleukin-1 Receptor IL-1R (IL-1R) and Tumour Necrosis Factor Receptor (TNFR1) (Leon-Boenig, et al. 2012).

A signalling cascade through the canonical NF-κB pathways initiates an activation of IκB kinase complex (IKK) that consists of several subunits IKKα, IKKβ, and the regulatory subunit IKKγ (Mussbacher, et al. 2019); (Prescott and Cook 2018). Activating the IKK inactivates IκB by phosphorylation leading to the release of NF-κB from the cytoplasmic chaperon and allowing its nuclear translocation (see Figure 1) (Prescott and Cook 2018). On the other hand, the NF-κB non-canonical pathway can be stimulated by several receptors e.g. B-cell activating factor receptor (BAFFR), Lymphotoxin B receptor (LTβR) and Receptor Activator of Nuclear factor kappa-B Ligand (RANKL) (Tegowski and Baldwin 2018). After receptor stimulation a signalling cascade is initiated to activate the NF-κB Inducing Kinase (NIK) (Tegowski and Baldwin 2018). The NIK and IKKα induce the proteasome of p100 into RelB/p52 NF-κB complex (Tegowski and Baldwin 2018). Then the RelB/p52 NF-κB complex can translocate to the nucleus and induce transcription processes (see Figure 1) (Tegowski and Baldwin 2018).

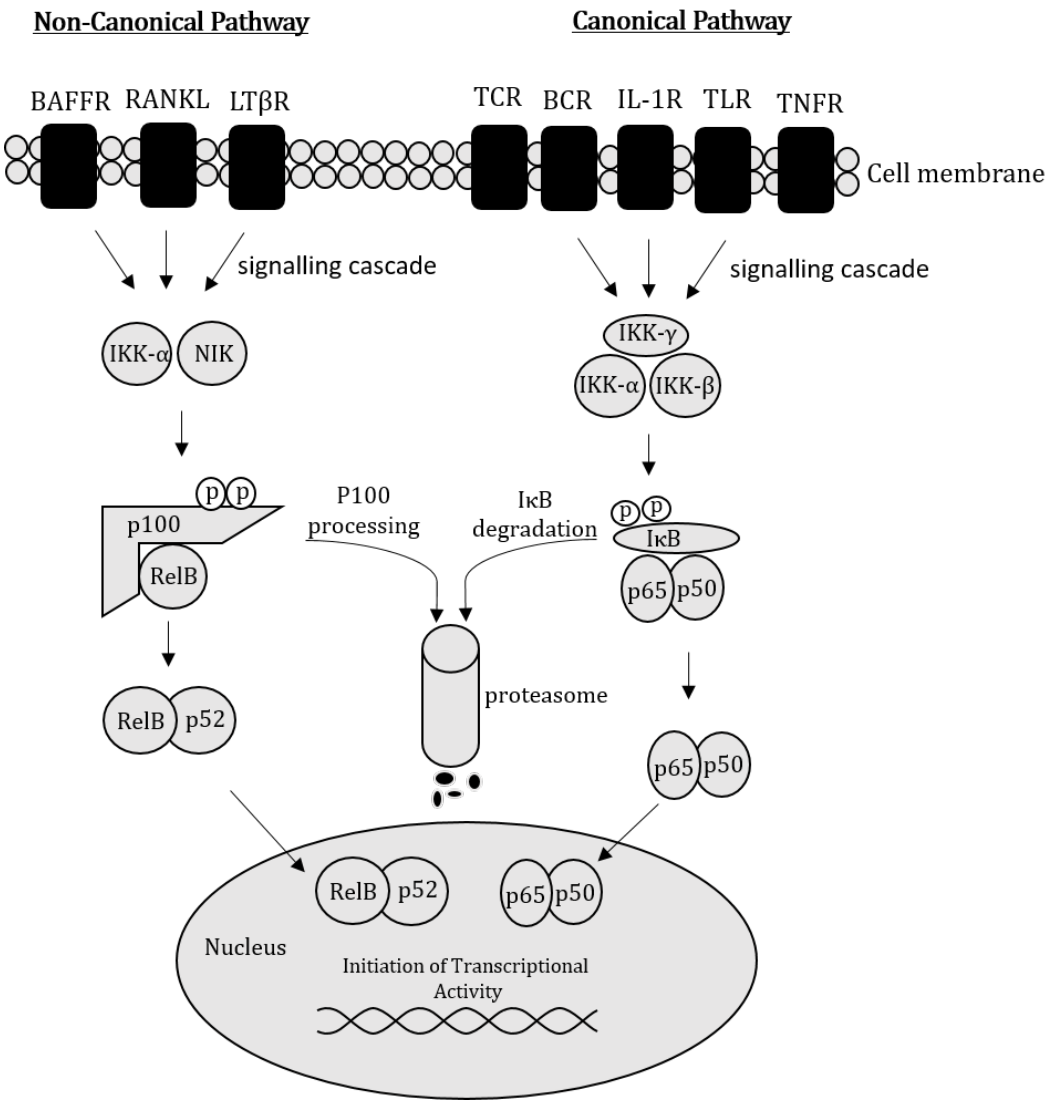

Figure 1 Overview of the activation of NF-κB through the canonical and the non-canonical pathways. Both pathways are initiated by binding of different ligands to the extracellular domain of the receptor in the cell membrane, where a signalling cascade starts. The canonical pathway of NF-κB activation is induced by several pro-inflammatory receptors like T Cell Receptor (TCR), B Cell Receptor (BCR), Toll-Like Receptor (TLR), Interleukin-1 Receptor (IL-1R) and Tumour Necrosis Factor Receptor (TNFR1). A signalling cascade triggers the activation of the IκB kinase (IKK) complex that include several subunits IKKα, IKKβ, and the regulatory subunit IKKγ. This complex phosphorylates Inhibitor of kappa-B (IκB), which is consequently ubiquitinated and degraded through the proteasomes, releasing NF-κB (the common components of which in the canonical pathway are p65-p50 heterodimers), to translocate to the nucleus, where it plays a major role in the transcription of inflammatory and survival genes. The non-canonical pathway is stimulated by several receptors e.g. B-cell activating factor receptor (BAFFR), Lymphotoxin B receptor (LTβR) and Receptor Activator of Nuclear factor kappa-B Ligand (RANKL). Binding of these ligands to its particular receptors stimulates a signalling cascade which activate the NF-κB Inducing Kinase (NIK). The NIK and IKKα triggers the proteasome of p100 into RelB/p52 NF-κB complex. Hence the RelB/p52 NF-κB complex can translocate to the nucleus and to induce transcription processes. (modified from Fig.1 in (Tegowski and Baldwin 2018)).

1.2.3 NF-κB Activation

Cell stimuli such as Tumour Necrosis Factor α (TNFα), Interleukin-1 (IL-1) or Lipopolysaccharide (LPS) induce a signalling cascade that causes a release of NF-κB from its inhibitor IκB and allow its nuclear translocation (Diaz-Meco and Moscat 2012). NF-κB as a dimer contains two of the subunits RelA (p65), RelB, c-Rel, p50/p105 (NF-κB1) or p52/p100 (NF-κB2) (Liu, et al. 2017). The heterodimer containing p50 and p65 subunits is the most common form of NF-κB (Korc 2016); (Lash 2010); (Vermeulen, et al. 2003). Phosphorylation of the Rel Homology Domain (RHD) of RelA (p65) is important for NF-κB transcriptional activity (Duran, Diaz-Meco and Moscat 2003). The NF-κB phosphorylation is induced by several enzymes such as Protein Kinase A (PKA) which phosphorylates RelA/p65 on serine 276 (Duran, Diaz-Meco and Moscat 2003) or Casein Kinase II (CKII) which phosphorylates RelA/p65 on serine 529 (Wang, et al. 2000). Protein Kinase C zeta (PKCζ) is an important member of Protein Kinase C enzymes (PKC) (Diaz-Meco and Moscat 2012). In response to TNFα stimulation, PKCζ triggers IκB degradation by its phosphorylation (Rimessi, et al. 2013); (Diaz-Meco and Moscat 2012).

Furthermore, PKCζ phosphorylates NF-κB p65 on serine 311 (ser311) which is an important step for NF-κB transcriptional activation (Reina-Campos, Diaz-Meco and Moscat 2019); (Rimessi, et al. 2013); (Diaz-Meco and Moscat 2012). Under basal conditions, the methyltransferase SET Domain-containing 6 (SETD6) methylates NF-κB p65 on Lysine 310 (Rimessi, et al. 2013); (Diaz-Meco and Moscat 2012); (Levy, et al. 2011). Methylated Lysine 310 is recognised by G9a-related methyltransferase (GLP), which induces histone-methylation and leads to transcription repression of NF-κB target genes (Rimessi, et al. 2013); (Levy, et al. 2011). The phosphorylated serine 311 supresses the methylation of Lysine 310 by SETD6 and thereby disables the recognition of Lysin 310 by GLP (Rimessi, et al. 2013); (Diaz-Meco and Moscat 2012); (Levy, et al. 2011). This allows the transcriptional coactivator CBP to acetylate Lysine 310 and other histone residues which leads to an opening of the chromatin structure and enhanced transcription of NF-κB regulated genes (see Figure 2) (Rimessi, et al. 2013); (Diaz-Meco and Moscat 2012); (Levy, et al. 2011).

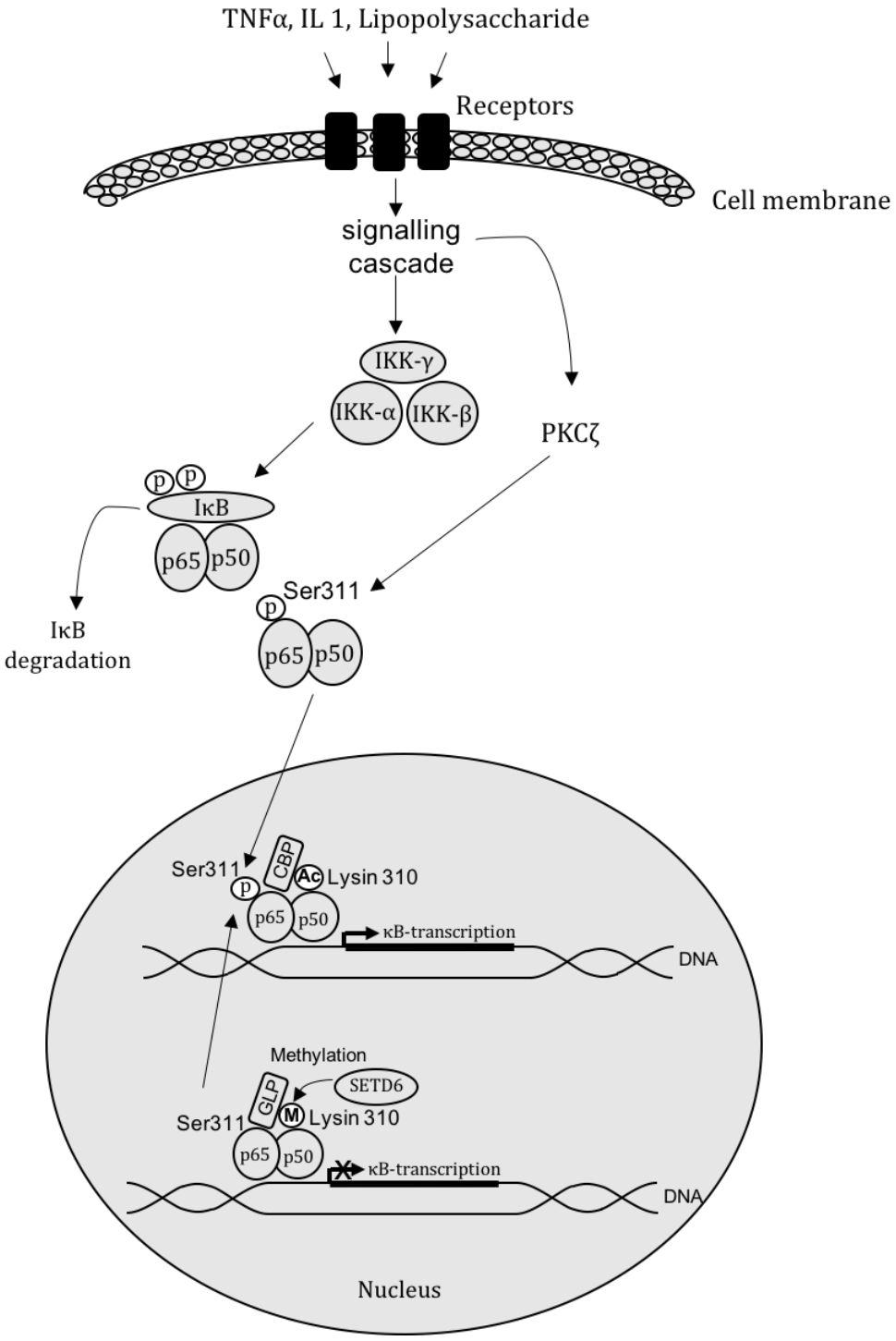

Figure 2 Phosphorylation of NF-κB by Protein Kinase C zeta (PKCζ). The binding of different ligands such as Tumour Necrosis Factor α (TNFα), Interleukin-1 (IL-1) or Lipopolysaccharide (LPS) to their specific receptors in the cell membrane induces the formation of a signal cascade, which comprises two catalytic subunits of the Inhibitor of kappa-B Kinase (IKKα and IKKβ) and one regulatory subunit (IKKγ). This cascade leads to phosphorylation of Inhibitor of kappa-B (IκB), which is then ubiquitinated and eliminated by the proteasome system. NF-κB (the most common components are p65-p50 heterodimers) is then free to translocate into the cell nucleus and to interact with elements in the promoter of inflammatory and survival genes that contain κB elements in their promoters. PKCζ phosphorylates NF-κB p65 on serine 311 (ser311) as an important step in the recruitment of the transcriptional coactivator CBP. This indicates the acetylation of Lysine 310 to activate transcription. Under basal conditions, NF-κB p65 is methylated (M) at Lysine 310 by SET Domain-containing 6 (SETD6), which induces the recruitment of G9a-related methyltransferase (GLP), which then leads to the inhibition of κB-dependent transcription. After ligand binding, the phosphorylation of serine 311 by PKCζ suppresses methylation to activate transcription. PKCζ is also capable of acting as an IKK kinase. (modified from Fig.3 in (Diaz-Meco and Moscat 2012)).

1.3 TNFα

Tumour Necrosis Factor α (TNFα) is a cytokine that plays an important role in cellular processes such as inflammatory, controlling of tumour growth, autoimmunity and immunological reactions in various cell types (Belmellat, et al. 2017).

1.3.1 Structure

TNFα begins its synthesis as a transmembrane protein in lymphocytes, activated macrophages and other types of cells (Mitoma, et al. 2018). The initial form is 233-amino acid-long (26-kDa) type II transmembrane protein called transmembrane TNFα (tmTNFα) (Mitoma, et al. 2018); (Caron, et al. 1999). The protease TNFα converting enzyme (TACE) cleaves tmTNFα between residues alanine 76 and valine 77 which results in the release of 157 amino acid long (17-kDa) soluble TNFα (sTNFα) peptide from the cell membrane (Mitoma, et al. 2018); (Mohan, et al. 2002). The remaining cytoplasmic domain of tmTNFα after TACE cleavage is subject to an additional cleavage by Signal Peptide Peptidase-Like 2B (SPPL2b) releasing Intracellular Domain (ICD) that migrates into the nucleus of the tmTNFα bearing cells where it triggers expression of pro-inflammatory genes (Horiuchi, et al. 2010); (Fluhrer, et al. 2006).

1.3.2 Signalling

TNFα mediates its biological activities by binding with two types of receptors: Tumour Necrosis Factor Receptor 1 (TNFR1) and Tumour Necrosis Factor Receptor 2 (TNFR2) (Deora, et al. 2017). TNFα mainly stimulates TNFR1 while tmTNF stimulates TNFR2 (Deora, et al. 2017). Activation of TNFR1 by TNFα mediates either cell survival by NF-κB activation or cell apoptosis by different pathways (Christofferson., Li and Yuan 2014); (McComb, et al. 2012). TNFR1 is interacting with an intercellular protein complex that contains Tumour Necrosis Factor Receptor type 1-associated Death Domain (TRADD), TNF Receptor-Associated Factor 2 (TRAF2), Receptor Interacting Protein Kinase1 (RIP1) and Baculoviral IAP repeat-containing protein 2 (cIAP1) (Zhou and Yuan 2014). This protein complex initiates a cascade after TNFR1 activation by TNFα which leads to IKK activation and the

release of NF-κb from IκB followed by transcription processes that serve the cell survival (Zhou and Yuan 2014).

1.4 Cannabidiol (CBD)

Since ancient times, preparations of the plant *Cannabis sativa* have been used in religious ceremonies and for therapy as a recreational drug (Devinsky, et al. 2014). The ancient chinese medicine used it to treat diseases such as rheumatic disorder, constipation and absent-mindedness (Devinsky, et al. 2014). Also in the medieval period, cannabis was used to treat pain, nausea, epilepsy and other diseases (Devinsky, et al. 2014). Cannabidiol (CBD) and delta-9 tetrahydrocannabinol (THC) are neuroactive cannabinoid components produced by *Cannabis sativa* beside more than 80 other cannabinoid compounds (Schoedel, et al. 2018). While THC induces euphoric effects, CBD has no psychoactivity (Schoedel, et al. 2018).

1.4.1 CBD as Clinical Therapeutic

Treatment using a drug containing CBD results in a positive outcome for patients with Multiple Sclerosis (MS) (Langford, et al. 2013). The treatment reduces the symptoms for the patients, enhances the performance of the daily activities and improves the quality of life (Zajicek and Apostu 2011); (Rog, et al. 2005).

CBD was involved in many clinical trials and showed beneficial effects on several types of epilepsy in adults and children (Szaflarski, et al. 2018); (Devinsky, et al. 2014). Furthermore, CBD showed an anti-inflammatory effect on mice *in vivo* as well as *in vitro* models (Pagano, et al. 2016); (Filippis, et al. 2011); (Jamontt, et al. 2010). The effect of CBD on GBM was investigated in some studies with *in vitro* models (Deng, Ng, et al. 2017); (Ivanov, Wu and Hei 2017). It was shown that CBD either reduced the cell proliferation or caused cell death (Deng, Ng, et al. 2017); (Ivanov, Wu and Hei 2017).

1.4.2 Pharmacology

Endocannabinoids and the phytocannabinoid THC bind to two types of receptors Cannabinoid-Receptor 1 (CB1) and Cannabinoid-Receptor 2 (CB2) (Dai, et al. 2017).

Both receptors are G protein-coupled receptors (Hillger, et al. 2017); (Dai, et al. 2017). CB1 is primarily found in the central nervous system while CB2 is located mainly in cells and tissue of the immune system (Guo, et al. 2018); (Deng, Guindon, et al. 2014). THC is an agonist to CB1 and CB2 (Devinsky, et al. 2014). On the other hand, the pharmacology of CBD is largely unclear. CBD has multiple effects on a variety of molecular signalling pathways, of which only some have been characterised, e.g. weak CB1 and CB2 antagonist, potential G Protein-Coupled Receptor 55 (GPR55) antagonist, potential moderator of Serotonin 1A Receptor (5-HT1A), potential inductor of Transient Receptor Potential Ankyrin 1 (TRPA1) and potential effector of proliferator-activated receptor (PPAR γ) (Ahmed, et al. 2018); (Ghovanloo, et al. 2018); (Ibeas Bih, et al. 2015).

1.5 Immunocytochemistry

Immunochemistry and particularly the immunocytochemistry (ICC) is a useful method to monitor and investigate cytological preparations using the immunoreactivity of antibodies (Renshaw 2017). The antibody isotype is an immunoglobulin (Ig) that binds to a specific antigen in previous fixed cells (Renshaw 2017). The antigens can be visualized through primary antibodies that binds directly to the antigens and secondary antibodies that binds to the primary antibodies (Renshaw 2017). The secondary antibodies are fluorescent labelled reporter which can be detected after exposure to a specific wavelength with selected sets of emission filters (Renshaw 2017). This allows the detection of the targeted antigen or protein bound to the primary antibody (Renshaw 2017). Selecting the emission filters allows the combination between two or more fluorescent dyes with different fluorochrome absorption and emission spectra without a significant overlap in the excitation e.g. DAPI (4′,6-Diamidin-2-phenylindol) and Alexa Fluor® 488 (Renshaw 2017). DAPI is used to stain the nuclei by its binding specifically to adenine–thymine (A-T) rich regions of double-stranded DNA (Renshaw 2017). It has a maximum absorption at wavelength of 359 nm and maximum emission at wavelength of 461 nm (blue) (Renshaw 2017). Whereas green fluorescent labels e.g. Alexa Fluor® 488 has a maximum absorption at a wavelength of 495 nm and maximum emission at a wavelength of 519 nm (green) (Renshaw 2017).

1.6 Aims and Objectives

NF-κB plays an essential role in inflammation and anti-apoptosis in many human malignant tumours such as the most aggressive brain tumour glioblastoma. NF-κB induces cell proliferation and cell survival by controlling transcriptional activity. Inhibition of NF-κB activity is associated with poor survival in malignant cells. Cannabidiol is an established drug for the treatment of neurological diseases. Previous studies have shown an anti-inflammatory effect of cannabidiol. This study investigates, by immunocytochemistry and immunofluorescence staining, the cannabidiol effects on NF-κB nuclear translocation and its phosphorylation on serine 311 in vitro models on a larger set of human glioblastoma cell cultures. These effects on NF-κB are compared to the effects achieved by TNFα. Furthermore, this study investigates the NF-κB response in a range of transgenic murine glioblastoma cells. The pharmacological responses to CBD or TNFα, as compared to relevant controls, are analysed in order investigate inter-individual differences in NF-κB signalling and to get a defter insight into CBD initiated signalling processes.

2. Materials

2.1 Laboratory Equipment and Devices

Table 1 Laboratory Equipment and Devices

Product	Type / Cat. Nr	Company
Automated cell counter	countess II FL	Life Technologies
Incubator	CB150	Binder
Microscope	Diavert	Leitz
Fluorescence Microscope	Axiovert 25 CFL	Zeiss
Fluorescence Microscope	Axiophot	Zeiss
Microscope camera	AxioCam MRm	Zeiss
Centrifuge	Rotana/S	Hettich
Minishaker	MS2	IKA
Freezing Container Mr. Frosty	5100-0001	Sigma Nalgene
Fume Hood	2-248-N	Köttermann
PH meter	Multi-cal	WTW
Water bath	VC/3	Julabo
Autoclave	DX23	Systec
Pipettes	10, 20, 100, 200 and 1000 µl	Eppendorf
Refrigerators	4°C, -20°C	Liebherr
Freezer	-80°C	Thermo Scientific
HERA safe Hood	KS 12	Thermo Scientific

2.2 Consumables

Table 2 Consumables

Product	Type / Cat. Nr	Company
Culture slides	354108	Falcon
Cell culture flask T25	90026	TPP
Cell culture flask T75	90976	TPP
Cell culture flask T150	909151	TPP
Cell culture dish	755923	Sigma-Aldrich
Cover slips	BBAD02400500#A1	Thermo Scientific
Pipette 5 ml	CLS4487	Costar
Pipette 10 ml	CLS4488	Costar
Pipette 25 ml	CLS4489	Costar
Tubes 0,5 ml	0030121.023	Eppendorf
Tubes 1,5 ml	0030121.694	Eppendorf
Tubes 2 ml	0030120.094	Eppendorf
Tubes 15 ml	91015	TPP
Tubes 50 ml	352070	Falcon
Pipette Tips	10, 20, 100, 200 and 1000 µl	Eppendorf

2.3 Chemicals and Reagents

Table 3 Chemicals and Reagents

Product	Type / Cat. Nr	Company
Cannabidiol		GW Pharmaceuticals
TNFα	300-01A	PeproTech
Poly-L-ornithinehydrobromide	P3655	Sigma-Aldrich
Tween 20	P9416	Sigma-Aldrich
Dimethyl sulfoxide (DMSO)	D8418	Sigma-Aldrich
Donkey Serum	017-000-121	Jackson ImmunoResearch
Paraformaldehyde (PFA)	P6148	Sigma-Aldrich
Sodium chloride (NaCl)	1.06404	Emsure
Tris base	77-86-1	Sigma-Aldrich
Laminin	L2020-IMG	Sigma-Aldrich
Trypan blue	T8154	Sigma-Aldrich
Phosphate-buffered saline (PBS)	APO-ST016	Apotheke Klinikum LMU
Cell Dissociation Reagent (Accutase)	A11105-01	Gibco
Fluorescence mounting medium	S3023	Dako
Antibody diulent	S3022	Dako

2.4 Cell Culture Media and Supplements

Table 4 Cell Culture Media and Supplements

Product	Cat.Nr.	Company
DMEM/F-12, no phenol red	21041025	Gibco
DMEM/F-12, with phenol red	11320074	Gibco
NeuroCult™ Basal Medium (Mouse)	05700	Stemcell Technologies
NeuroCult™ Proliferation Supplement (Mouse)	05701	Stemcell Technologies
B-27™ Supplement	17504044	Gibco
Penicillin-Streptomycin	15140122	Gibco
Fibroblast Growth Factor (FGF)	AF-100-18B	PeproTech
Epithelial Growth Factor (EGF)	AF-100-15	PeproTech

- **NPC culture medium:** DMEM/F-12, B-27™ Supplement, 1% Penicillin-Streptomycin, 10 ng/ml FGF, 10 ng/ml EGF.
- **NSC culture medium:** Basal Medium (Mouse), NeuroCult™ Proliferation Supplement (Mouse), 1% Penicillin-Streptomycin, 10 ng/ml FGF, 10 ng/ml EGF.

2.5 Antibodies

Table 5 Antibodies and Dyes

Antibody/Dye	Company	Cat.Nr.	Isotyp	Dilution
Purified anti-NFκB p65 Antibody	BioLegend	622601	Rabbit Polyclonal IgG	1:100
Phospho-NF-κB p65 (Ser311) Polyclonal Antibody	Thermo Fisher Scientific	PA5-37720	Rabbit / IgG	1:200
Hoechst 33342	Invitrogen	H3570		1-2 µg/ml
Alexa Fluor® 488	Jackson ImmunoResearch	711-545-152	Donkey Anti-Rabbit IgG (H+L)	1:200

2.6 Software

Table 6 Software

Software	Provider
AxioVision Microscopy Software	Carl Zeiss
GraphPad Prism	GraphPad Software, Inc.
ImageJ	Wayne Rasband
Microsoft Office (Word, Excel and PowerPoint)	Microsoft

2.7 Glioblastoma (GBM) Cell Culture

2.7.1 Human GBM Cell Cultures

The human GBM cell cultures (see Table 7) were derived from patients. The cells were stored after its isolation in NPC medium (5% DMSO) in liquid nitrogen freezer at -180° C.

Table 7 Human GBM Cell Cultures

Cell Culture	Subtype
Line#7	proneural
GBM13	proneural
NCH664	proneural
NCH421k	proneural
Line#2	classical
Line#6	mesenchymal
Line#10	mesenchymal
Line#11	mesenchymal
GBM441	unclassified
GBM14	unclassified

2.7.1 Murine GBM Cell Cultures

The murine cell cultures (see Table 8) were genetically manipulated to generate alterations described in human GBMs. The mice were modified by knocking-out or floxing several tumour suppressors such as p53, CDKN2A, PTEN, p65 and NF1. The cells were stored in NPC medium (5% DMSO) in liquid nitrogen freezer at -180° C after its isolation.

Table 8 Murine GBM Cell Cultures

Cell Culture	Subtype
$p53^{R172H}$, $p65^{\Delta/\Delta}$, PDGFB $^{\oplus}$	Proneural
$p53^{-/-}$,PDGFB$^{\oplus}$	Proneural
$cdkn2a^{-/-}$, EGFR$^{\oplus}$	Classical
$cdkn2a^{-/-}$, PDGFB $^{\oplus}$	Proneural
$p53^{R172H}$, $p65^{\Delta/\Delta}$, PDGFB $^{\oplus}$	Proneural

***R172H:** p53 R172H mutation, **Δ:** floxed gene, **-/-:** knocked out gene, **⊕:** Overexpression

3. Methods

3.1 Cell Culture

3.1.1 Cell Culture Conditions

This study incorporated ten human primary GBM cell cultures (Table 7) and five transgenic murine GBM cell cultures (Table 8). The GBM cells were cultured in NSC or NPC culture media. The human GBM cells labelled as (Line#) were cultured in NSC culture medium in T75 or T150 flasks while the murine cells were cultured on cell culture dishes in NPC culture medium. The cultures were maintained in an incubator at a temperature of 37° C and a humidified atmosphere of 5% CO_2. The culture media were changed every 1-2 days and the cells were passaged 2 to 3 times per week to keep a cell density of $0{,}03\text{-}0{,}05\times10^6$ cells/ml.

3.1.2 Changing the Cell Culture Media

The cell culture media changing was performed in a sterile environment. First, the cultured cell suspension was collected from the flask or the culture dish using a 10 ml pipette. Then, it was transferred to either a 15 or 50 ml tube. The tubes were centrifuged at room temperature. After centrifugation, the supernatant was discarded. The remaining cell pellets were resuspended in a fresh pre-warmed culture media, returned to a new flask or culture dish and placed in the incubator. The pre-warming of culture medium was done by placing it in a fresh water bath at 37° C.

3.2 Preparations of Immunofluorescence Staining

3.2.1 Slide Coating

Sterile chambered cell culture slides were placed under the hood in sterile conditions and each well was filled with 100 µl of Poly-ornithine (50 µg/ml in PBS). The cell culture slides were incubated for 24 hours at 37° C. Then, the Poly-ornithine was removed and each well was washed once gently with sterile PBS for 5 minutes. Then, each well was filled with 100 µl of laminin (5 µg/ml in PBS) and incubated for two hours at 37° C.

3.2.2 Cell Plating

Only if the cell viability was more than 90%, were the cells platted (50,000 cells per well in the pre-coated cell culture slides). The slides were placed in the cell culture incubator at 37° C for 24 hours in order to obtain a monolayer of adherent cells.

3.2.3 Drug Treatment

The treatment drugs and the vehicle control were diluted in culture medium (DMEM/F-12 no phenol red) and added to the cell culture slides for Treatment. The drugs used were CBD 10 (µmolar), TNFα (10 ng/ml) and the vehicle (DMSO 0,01%).

3.2.4 Fixation

After treatment (as indicated for individual experiments in results chapter) the supernatants were removed from the wells. Each well was washed once with PBS for 5 minutes followed by removing the PBS and drying the wells for 30 seconds. The cells were fixed with PFA (4%) for 10 minutes in a ventilated cabinet. After removing of PFA, the wells were washed 3 times with PBS for 5 minutes each time.

3.2.5 Permeabilisation

For cell permeabilisation, the cells were incubated with TBST (3% normal serum, 0,9% NaCl, 100 mM Tris Base, 1% tween 20) for 10 minutes at room temperature. Next, TBST was removed and the wells were washed 3 times with PBS for 5 minutes each time.

3.2.6 Antibody Staining

For the antibody staining the primary antibodies were diluted in Dako diluent and added to the wells. The culture slides were incubated over night at 4°C in the fridge. Then, the primary antibodies were removed and the cells were washed 3 times with PBS for 5 minutes each time followed by addition of the secondary antibodies. The

cells were incubated with the secondary antibodies in darkness for two hours at room temperature.

3.2.7 Mounting

After removing the antibodies and washing the cells 3 times with PBS for 5 minutes each time, the culture slides were placed in darkness to dry. Then, the chambers were removed from the culture slides. Finally, the culture slides were mounted by adding a drop of fluorescence mounting medium onto each well and covering it using cover slips. To avoid air bubbles the borders of the slides were sealed with clear nail polish.

3.3 Microscopy

In this study two type of microscopes were used: a transmitted light microscope and a fluorescence microscope. The transmitted light microscope was used to check the cell cultures vitality, while the fluorescence microscope was used to assess the immunofluorescence staining. The images for each cell culture experiment were taken by the fluorescence microscope with the same exposure time and 40x magnification.

3.4 Analysis

The software Image J was used for the quantification of the images taken on the fluorescence microscope. Excel was then used for the calculations of fold changes of different time periods and treatments. Graphpad Prism was used for the comparison between the different treatment groups and also for creating graphs of the cell cultures and treatments. The unpaired t-test was chosen for the comparison between two groups of different treatment or control. The difference is significant when (P-value < 0.05). The one-way analysis of variance (one-way ANOVA) was used to compare whether the means among the different treatment groups are significantly different (P-value < 0.05) or not.

For the quantification process, two analysis methods have been used within the experiments: Analysis of images stained with purified anti-NF-κB p65 antibody and analysis of images stained with phospho-NF-κB p65 (ser311) antibody. Figures 3, 4 and 5 are produced to show the effect and properties of each method.

3.4.1 Analysis of Images Stained with anti-NF-κB p65 Antibody

By splitting the blue and green channels using Image J, it was possible to compare the nuclear staining in treated cells versus control. The blue channel presents the nuclei locations, which are stained with DAPI (Figure 3). The green channel presents the staining with the anti-NF-κB p65 antibody (Figure 3). The nuclei staining is considered to be positive when the primary antibody staining is detected in the nucleus location (as in Figure 3). While it is considered to be negative when the primary staining is not detected in the nucleus location (as in Figure 3). Note that Image J and Excel were used for quantifying, counting and tabulating the fold changes of different time periods and treatments in comparison to the control.

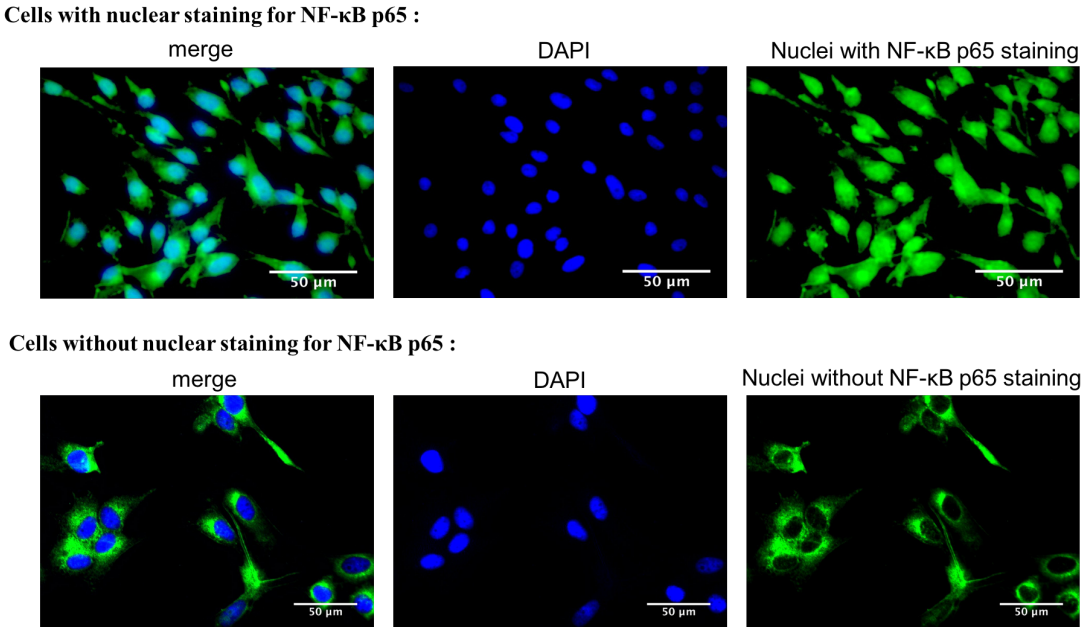

Figure 3 Explanation of the nuclear staining of NF-κB p65 in fixed GBM cells. The images were taken by fluorescence microscope. Microscope channels: merge, nuclei in DAPI staining and NF-κB p65 staining. The scale bar in the images is equal to 50µm.

3.4.2 Analysis of Images Stained with Phospho-NF-κB p65 (ser311) Antibody

In this section, Image J was used to compare nuclear NF-κB p65 phosphorylated on serine 311 (phspho-NF-κB p65 ser311) after different treatments and time periods. Phospho-NF-κB p65 (ser311) antibody was used as the primary antibody for the staining. The value compared was the Corrected Total Nucleus Fluorescence (CTNF), which is the integrated density of fluorescent staining of the nuclear region after subtracting the background staining.

After splitting of the channels using Image J, the CTNF calculation begins by using the drawing tools to select the nuclei areas in the blue channel, which is stained with DAPI. Followed by that, the Region of Interest (ROI) tool is used to mask the selected nuclei areas onto the green channel, in which the primary antibody staining (phspho-NF-κB p65 ser311) is presented (see Figure 4). After which, the integrated densities, areas and the mean of grey values are measured for the nuclear regions and the background. Excel is used to calculate the CTNF and its fold changes of different time periods and treatments (3 in Figure 4).

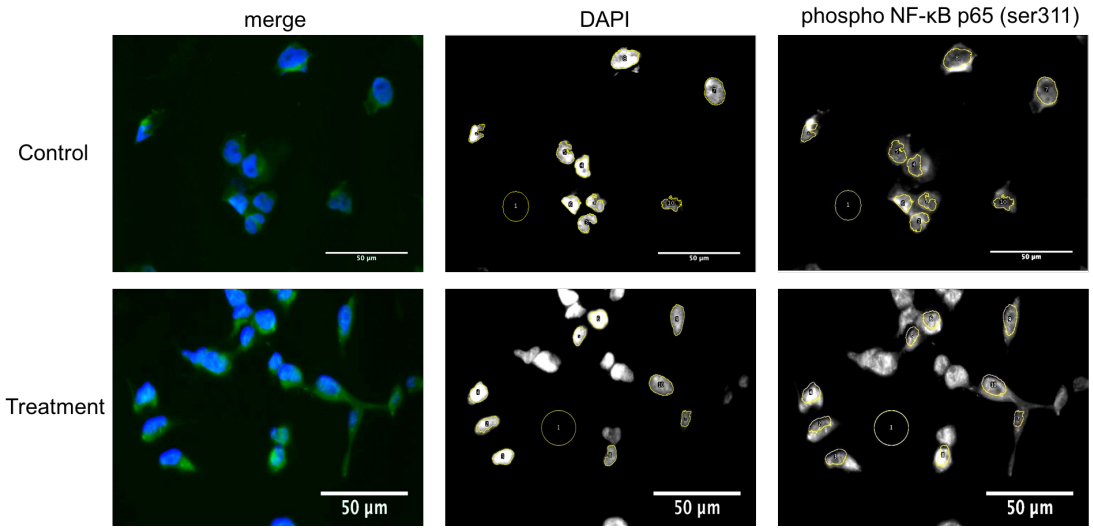

Figure 4 Explanation for images taken by fluorescence microscope and measurement of nuclear immunofluorescence staining in fixed GBM cells. Selecting the nuclear region in the DAPI channel, then masking the selected nuclear regions using ROI tool as in phospho- NF-κB p65 (ser311) channel. The scale bar in the images is equal to 50µm.

4. Results

4.1 Detection of NF-κB p65 Nuclear Translocation after TNFα Treatment

The GBM cell culture Line#2 (see Table 7) was treated with TNFα (10 ng/ml) to investigate the nuclear translocation of NF-κB p65 induced by TNFα. Selected time periods of treatment were 60 and 120 minutes. The anti-NF-κB p65 antibody was used as primary antibody. Image-analysis was performed by counting the stained nuclei (see 3.4.1). The cell culture Line#2 showed a significant increase of positively stained nuclei in the group treated with TNFα compared to the control group with the vehicle (0,01% DMSO) (see Figure 5).

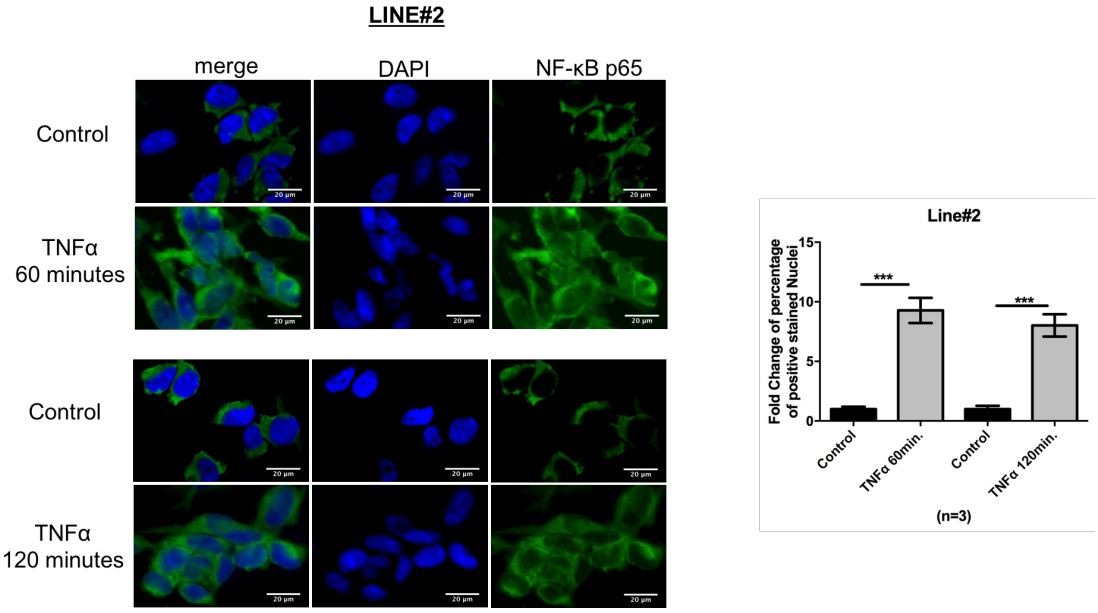

Figure 5 GBM Cell Culture Line#2. Microscope images (in different channels: merge, DAPI and NF-κB p65 antibody staining). The graph shows the fold changes of NF-κB p65 positive stained nuclei after TNFα (10 ng/ml) treatment for 60 and 120 minutes in GBM cell culture Line#2. TNFα led to a significant nuclear shift of NF-κB p65 after 60 minutes as well as after 120 minutes of treatment compared to the control groups. The unpaired t-test showed a significant different for both groups compared to the control groups (P-values < 0.0001). The scale bar in the images is equal to 20µm.

4.2 Detection of NF-κB p65 Nuclear Translocation after CBD/TNFα Treatments and Co-Treatments

The NF-κB p65 nuclear translocation was investigated by counting the positively stained nuclei (see 3.4.1). GBM cell culture Line#2 (see Table 7) was divided into two groups of treatments. The first group was treated with CBD (10 µmolar) for 6 hours followed by adding TNFα (10 ng/ml) for one hour (i.e. CBD and TNFα were co-applied for one hour). The second group was treated with TNFα (10 ng/ml) for one hour, where TNFα was added to the vehicle (DMSO 0,01%) as a control. Both groups were stained with anti-NF-κB p65 antibody as primary antibody. The cell culture Line#2 showed (see Figure 6) a significant elevation of NF-κB p65 nuclear translocation in the first group compared to the second group.

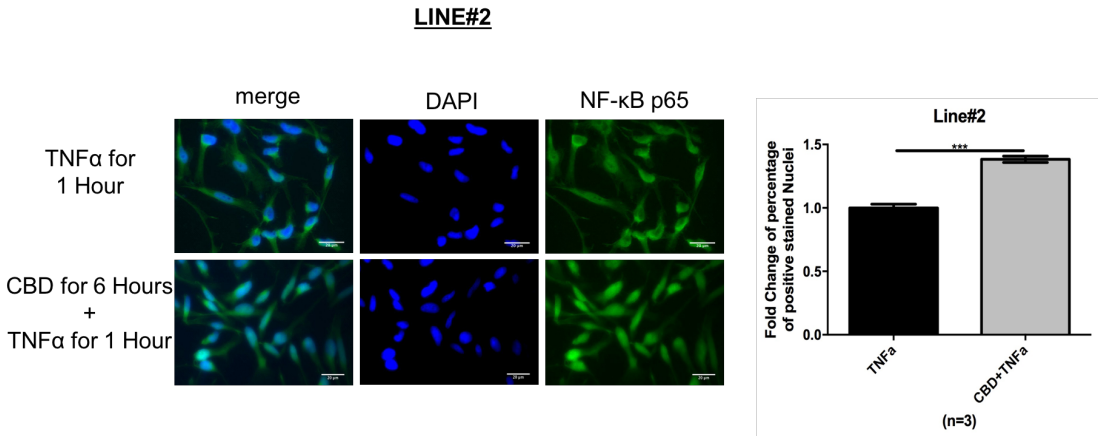

Figure 6 GBM Cell Culture Line#2. Microscope images in different channels: merge, DAPI and NF-κB p65 positive stained nuclei. The graph shows the fold changes of NF-κB p65 positive stained nuclei after TNFα treatment for one hour in cell culture Line#2. The group pre-treated with CBD for 6 hours followed by TNFα treatment for one hour shows a significant elevation of NF-κB p65 positive stained nuclei in comparison to the group treated only with TNFα for one hour. The unpaired t-test showed a significant difference (P-value <0.0001). The scale bar in the images is equal to 20µm.

4.3 Effect of CBD/TNFα Treatments and Co-Treatments on NF-κB p65 Nuclear Translocation

The GBM cell cultures (see Table 7 and 8) were divided into four groups to observe the effect of CBD, TNFα treatments and the co-treatment of CBD and TNFα on the NF-κB p65 nuclear translocation. The first group was the control and was treated only with the vehicle (DMSO 0,01%). The second group was treated with CBD (10 μmolar) for 16 hours. The third group was treated with TNFα (10 ng/ml) for one hour. Finally, the fourth group was pre-treated with CBD (10 μmolar) for 16 hours followed by a treatment with TNFα (10 ng/ml) for one hour as a co-treatment in addition to CBD. All groups were stained with anti-NFκB p65 antibody as primary antibody to detect the nuclear NF-κB p65. The nuclear translocation of NF-κB p65 was investigated by counting the positive stained nuclei ($DAPI^+$ area that is immunopositive for NF-κB) (see 3.4.1).

4.3.1 Cell Cultures Where CBD Treatment Affected the NF-κB p65 Nuclear Translocation

CBD was able to induce a significant elevation of NF-κB p65 nuclear translocation after 16 hours of treatment in both the human and murine GBM cell cultures. The effect on human cell cultures is shown in Line#2 (see Figure 7), Line#6 (see Figure 8), Line#7 (see Figure 9), Line#11 (see Figure 10), and NCH644 (see Figure 11). While the effect on murine cell cultures is shown in ($cdkn2a^{-/-}$, $EGFR^+$) *(-/-: signifies knock out gene, +: signifies Overexpression)* (see Figure 12) and ($p53^{-/-}$, $PDGFB^+$) (see Figure 14). Similar to the effect of TNFα, CBD led to an elevation of NF-κB p65 nuclear translocation. Vice versa, the murine cell culture ($cdkn2a^{-/-}$, $PDFGB^+$) (see Figure 13) showed significant elevation of NF-κB p65 nuclear translocation only in the group treated with CBD for 16 hours.

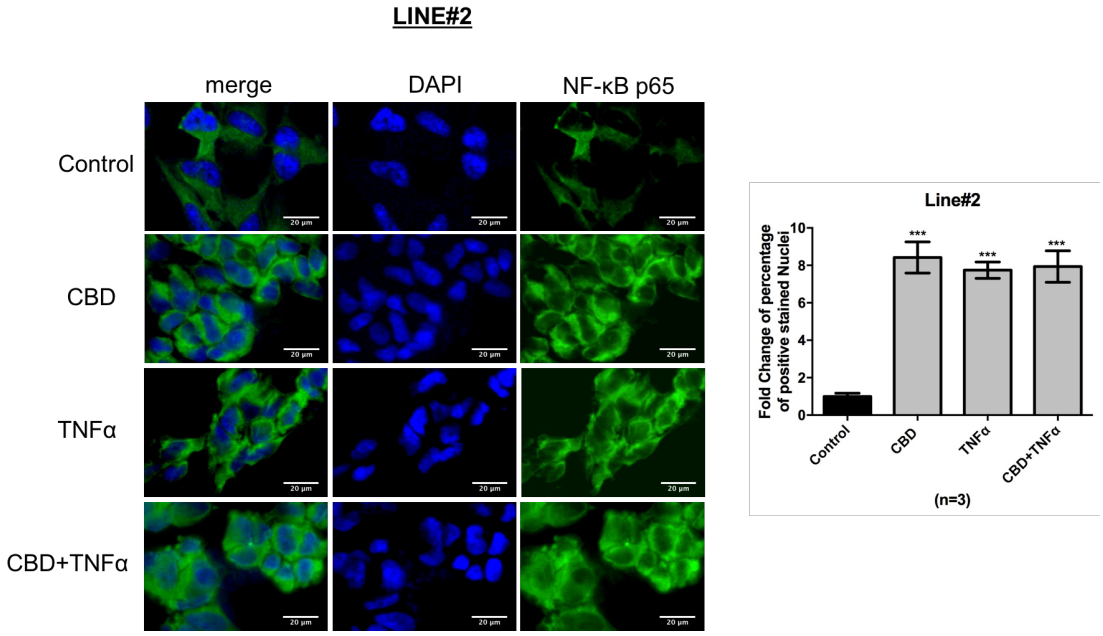

Figure 7 GBM Cell Culture Line#2. Microscope images of human cell culture Line#2 in separated channels: merge, DAPI and NF-κB p65 nuclear staining. The Treatments were as the following: CBD (10 µmolar) for 16 hours, TNFα (10 ng/ml) for one hour and pre-treatment of CBD (10 µmolar) for 16 hours followed by one hour co-treatment of CBD and TNFα (10 ng/ml). All treatments are compared to the control group in the first raw of the image. The unpaired t-test showed the following results. All treatments have led to a significant shift of NF-κB p65 to the nucleus comparing to the control group (P-value < 0.0001). The pre-treatment with CBD did not affect the ability of TNFα to induce a shift of NF-κB p65 to the nucleus after one hour of treatment. Considering CBD pre-treatment, there was no significant difference detected (P-value = 0.8411(ns)), whether the cells had been pre-treated with CBD for 16 hours or not. The applied One-way ANOVA was significant (P-value < 0.0001). The scale bar in the images is equal to 20µm.

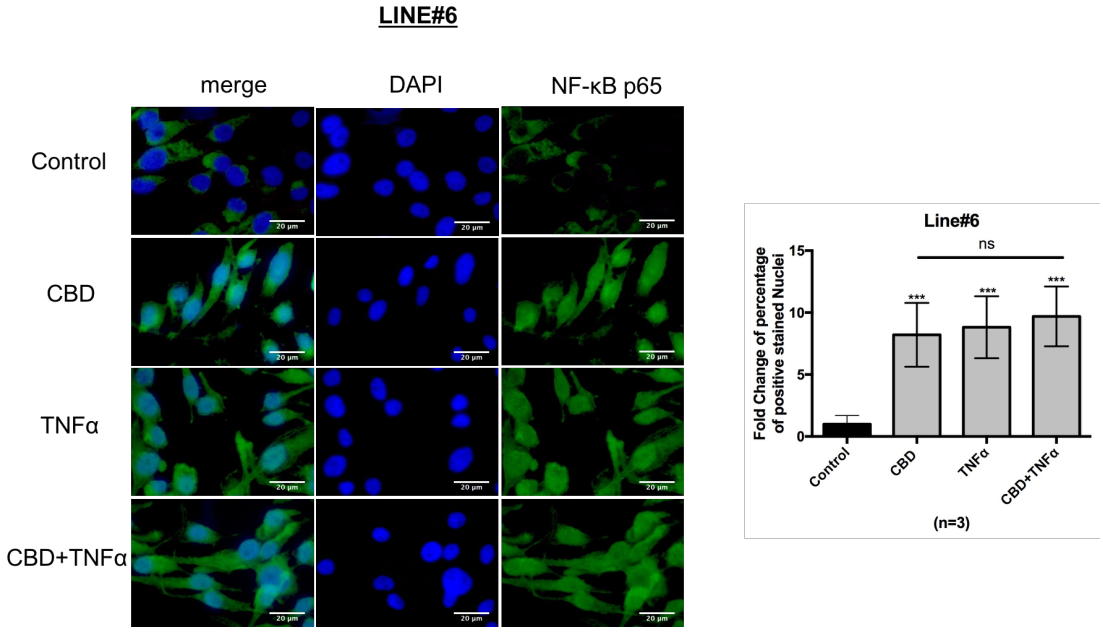

Figure 8 GBM Cell Culture Line#6. Microscope images of human cell culture Line#6 in separated channels: merge, DAPI and NF-κB p65 nuclear staining. The Treatments were as the following: CBD (µmolar) for 16 hours, TNFα (10 ng/ml) for one hour, and pre-treatment of CBD (10 µmolar) for 16 hours followed by one hour co-treatment of CBD and TNFα (10 ng/ml). All treatments are compared to the control group in the first raw of the image. The unpaired t-test showed the following results. All treatments have led to a significant shift of NF-κB p65 to the nucleus comparing to the control group (P-value < 0.0001). The pre-treatment with CBD for 16 hours did not affect the ability of TNFα to induce a shift of NF-κB p65 to the nucleus after one hour of treatment. Considering CBD pre-treatment, there was no significant difference detected (P-value = 0.4610 (ns)), whether the cells had been pre-treated with CBD for 16 hours or not. The applied One-way ANOVA test was significant (P-value < 0.0001). The scale bar in the images is equal to 20µm.

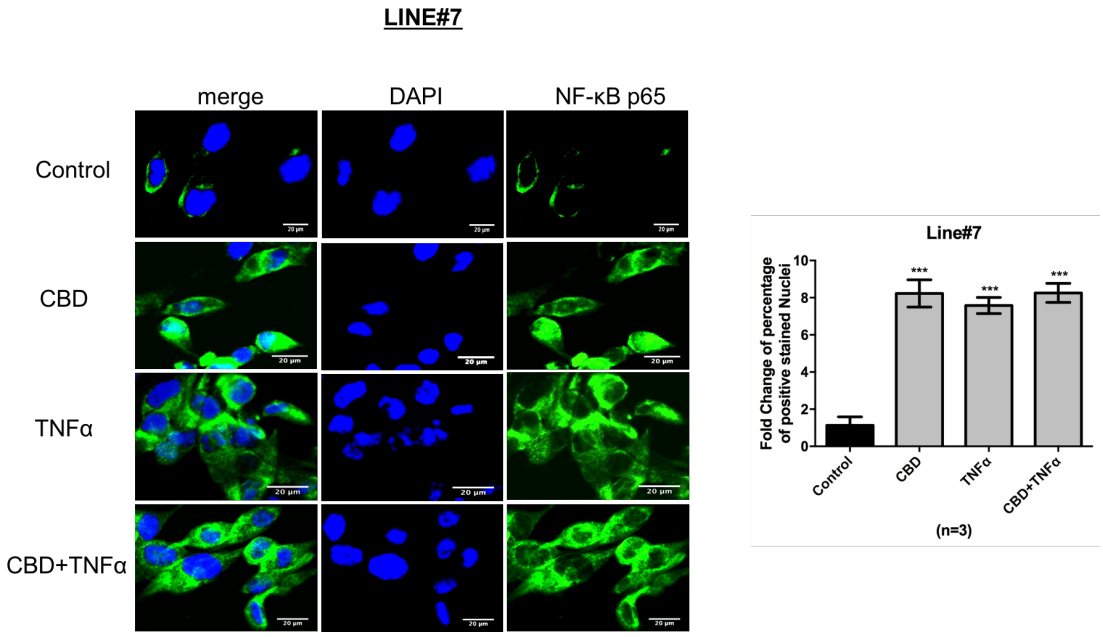

Figure 9 GBM Cell Culture Line#7. Microscope images of human cell culture Line#7 in separated channels: merge, DAPI and NF-κB p65 nuclear staining. The Treatments were as the following: CBD (10 µmolar) for 16 hours, TNFα (10 ng/ml) for one hour, and pre-treatment of CBD (10 µmolar) for 16 hours followed by one hour co-treatment of CBD and TNFα (10 ng/ml). The unpaired t-test showed the following results. All treatments are compared to the control group in the first raw of the image. All treatments have led to a significant shift of NF-κB p65 to the nucleus comparing to the control group (P-value < 0.0001). The pre-treatment with CBD for 16 hours did not affect the ability of TNFα to induce a shift of NF-κB p65 to the nucleus after one hour of treatment. Considering CBD pre-treatment, there was no significant difference detected (P-value = 0.3314(ns)), whether the cells had been pre-treated with CBD for 16 hours or not. The applied One-way ANOVA test was significant (P-value < 0.0001). The scale bar in the images is equal to 20µm.

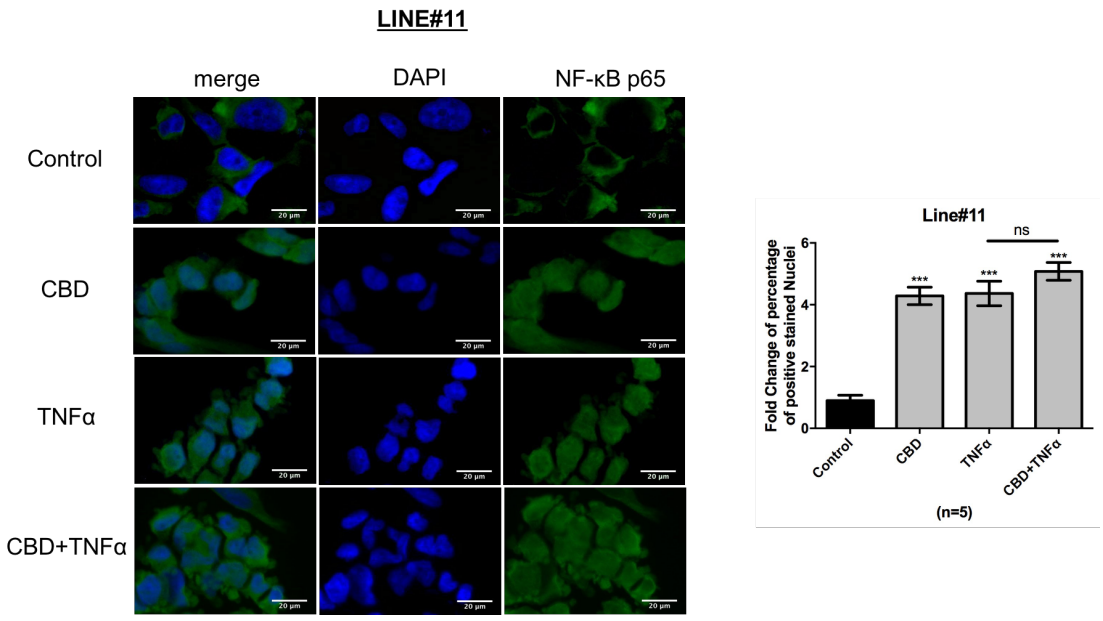

Figure 10 GBM Cell Culture Line#11. Microscope images of human cell culture Line#11 in separated channels: merge, DAPI and NF-κB p65 nuclear staining. The Treatments were as the following: CBD (µmolar) for 16 hours, TNFα (10 ng/ml) for one hour, and pre-treatment of CBD (10 µmolar) for 16 hours followed by one hour co-treatment of CBD and TNFα (10 ng/ml). All treatments are compared to the control group in the first raw of the image. The unpaired t-test showed the following results. All treatments have led to a significant shift of NF-κB p65 to the nucleus comparing to the control group (P-value < 0.0001). The pre-treatment with CBD for 16 hours did not affect the ability of TNFα to induce a shift of NF-κB p65 to the nucleus after one hour of treatment. Considering CBD pre-treatment, there was no significant difference detected (P-value = 0.1573 (ns)), whether the cells had been pre-treated with CBD for 16 hours or not. The applied One-way ANOVA test was significant (P-value < 0.0001). The scale bar in the images is equal to 20µm.

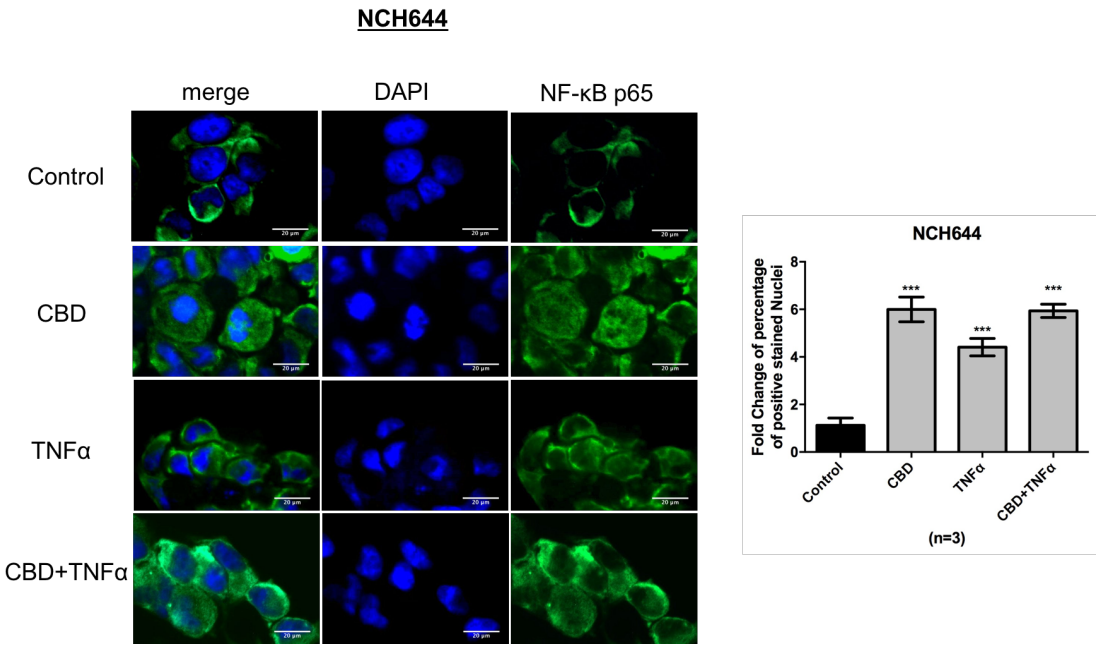

Figure 11 GBM Cell Culture NCH644. Microscope images of human cell culture NCH644 in separated channels: merge, DAPI and NF-κB p65 nuclear staining. The Treatments were as the following: CBD (10 µmolar) for 16 hours, TNFα (10 ng/ml) for one hour, and pre-treatment of CBD (10 µmolar) for 16 hours followed by one hour co-treatment of CBD and TNFα (10 ng/ml). All treatments are compared to the control group in the first raw of the image. The unpaired t-test showed the following results. All treatments have led to a significant shift of NF-κB p65 to the nucleus comparing to the control group (P-value < 0.0001). The pre-treatment with CBD for 16 hours increased the ability of TNFα to induce a shift of NF-κB p65 to the nucleus after one hour of treatment. Considering CBD pre-treatment, there was a significant difference between the group pre-treated with CBD in comparison to the group with no CBD pre-treatment (P-value = 0,0084(ns)). The applied One-way ANOVA test was significant (P-value < 0.0001). The scale bar in the images is equal to 20µm.

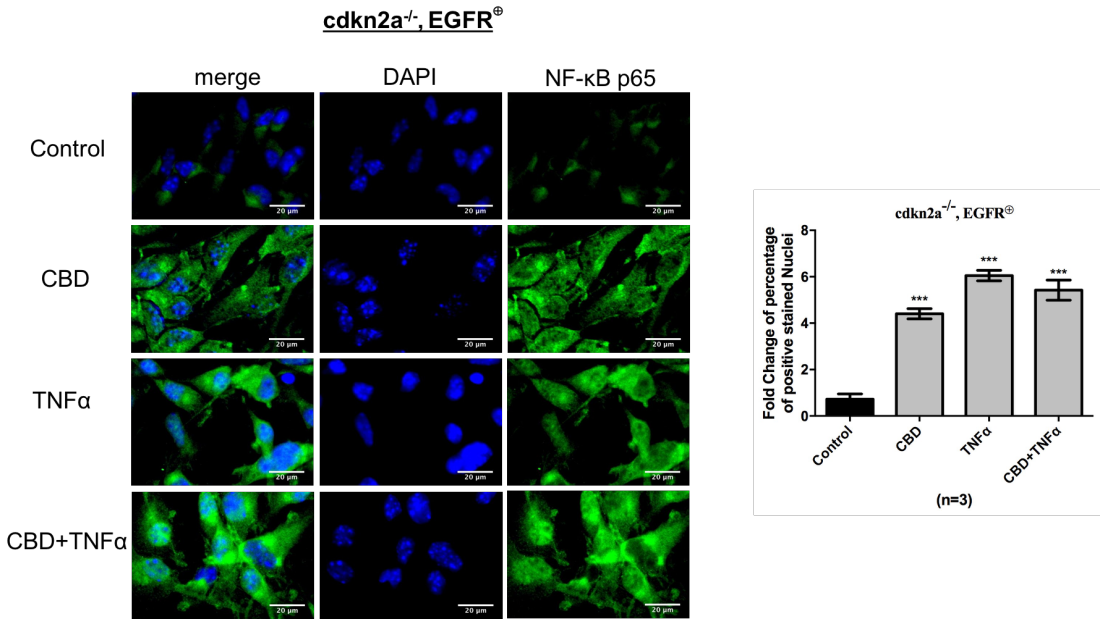

Figure 12 GBM Cell Culture (cdkn2a$^{-/-}$, EGFR^{+}). Microscope images of murine cell culture (cdkn2a$^{-/-}$, EGFR^{+}) in separated channels: merge, DAPI and NF-κB p65 nuclear staining. The Treatments were as the following: CBD (10 µmolar) for 16 hours, TNFα (10 ng/ml) for one hour, and pre-treatment of CBD (10 µmolar) for 16 hours followed by one hour co-treatment of CBD and TNFα (10 ng/ml). All treatments are compared to the control group in the first raw of the image. The unpaired t-test showed the following results. All treatments have led to a significant shift of NF-κB p65 to the nucleus comparing to the control group (P-value < 0.0001). The pre-treatment with CBD for 16 hours did not affect the ability of TNFα to induce a shift of NF-κB p65 to the nucleus after one hour of treatment. Considering CBD pre-treatment, there was no significant difference detected (P-value = 0.2284 (ns)), whether the cells had been pre-treated with CBD for 16 hours or not. The applied One-way ANOVA test was significant (P-value < 0.0001). The scale bar in the images is equal to 20µm.

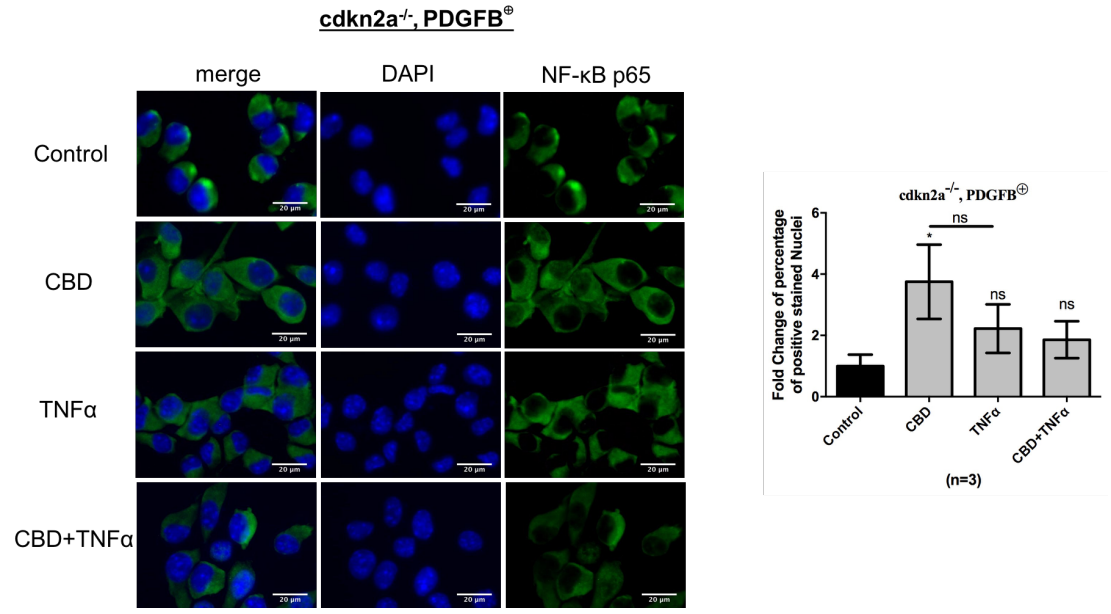

Figure 13 GBM Cell Culture (cdkn2a$^{-/-}$, PDGFB^{+}). Microscope images of murine cell culture (cdkn2a$^{-/-}$, PDGFB^{+}) in separated channels: merge, DAPI and NF-κB p65 nuclear staining. The treatments were as the following: CBD (10 µmolar) for 16 hours, TNFα (10 ng/ml) for one hour and pre-treatment of CBD (10 µmolar) for 16 hours followed by one hour co-treatment of CBD and TNFα (10 ng/ml). All treatments are compared to the control group in the first raw of the image. Only the group treated with CBD for 16 hours showed a low significant shift of NF-κB p65 to the nucleus compared to the control group, the unpaired t-test showed a (P-value = 0.0456). The other treatment groups did not show a significant difference of positive stained nuclei in comparison to the control group. The unpaired t-test results are as following: the group treated with TNFα for one hour vs control showed a (P-value = 0.1821 (ns)), the group pre-treated with CBD for 16 hours followed by one hour co-treatment of CBD and TNFα vs control showed a (P-value = 0.2441 (ns)). There was no significant difference detected between the group treated with CBD for 16 hours and the group treated with TNFα for one hour (P-value = 0.3059 (ns)). The applied One-way ANOVA test was non-significant (P-value=0.1291 (ns)). The scale bar in the images is equal to 20µm.

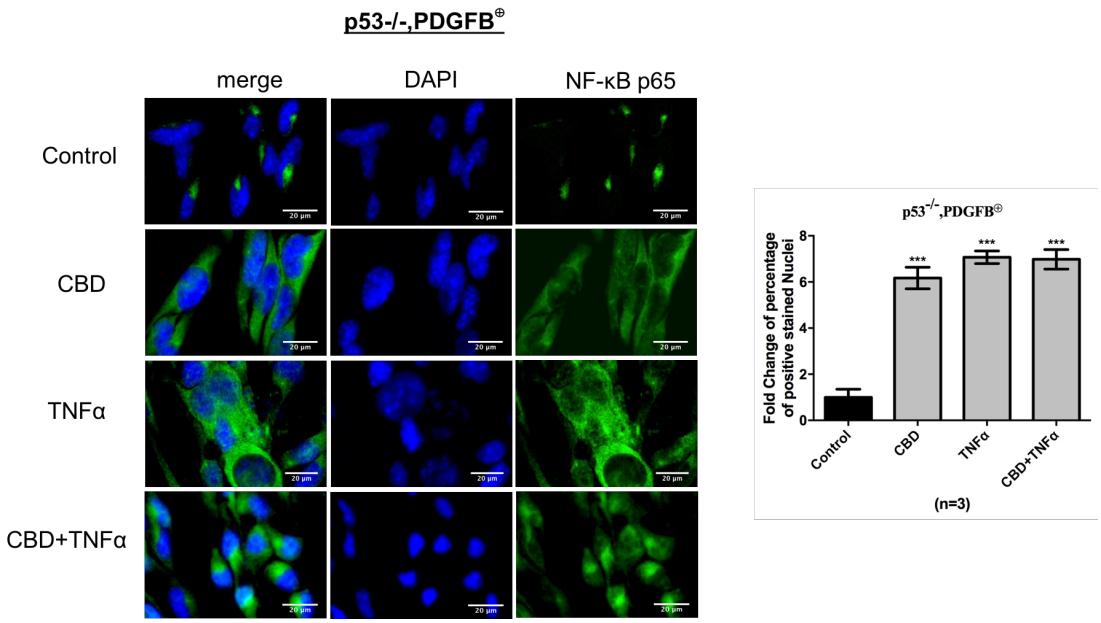

Figure 14 GBM Cell Culture ($p53^{-/-}$, $PDGFB^{+}$). Microscope images of murine cell culture ($p53^{-/-}$, $PDGFB^{+}$) in separated channels: merge, DAPI and NF-κB p65 nuclear staining. The treatments were as the following: CBD (10 µmolar) for 16 hours, TNFα (10 ng/ml) for one hour and pre-treatment of CBD (10 µmolar) for 16 hours followed by one hour co-treatment of CBD and TNFα (10 ng/ml). All treatments are compared to the control group in the first raw of the image. The unpaired t-test showed the following results. All treatments have led to a significant shift of NF-κB p65 to the nucleus comparing to the control group (P-value < 0.0001). The pre-treatment with CBD for 16 hours did not affect the ability of TNFα to induce a shift of NF-κB p65 to the nucleus after one hour of treatment. Considering CBD pre-treatment, there was no significant difference detected (P-value = 0.8645 (ns)), whether the cells had been pre-treated with CBD for 16 hours or not. The applied One-way ANOVA test was significant (P-value < 0.0001). The scale bar in the images is equal to 20µm.

4.3.2 Cell Cultures Where CBD Treatment Did not Affect the NF-κB p65 Nuclear Translocation

For another subset of the GBM cell cultures, the CBD (10 µmolar) treatment for 16 hours showed no effect on the nuclear translocation of NF-κB p65. This was noticed in the human cell cultures Line#10 (see Figure 15), GBM13 (see Figure 16), GBM14 (see Figure 17) and NCH421k (see Figure 18). On the other hand, TNFα induced the NF-κB p65 nuclear translocation after one hour of treatment also when the cells were pre-treated with CBD for 16 hours. The human cell culture NCH441 (see Figure 19) showed a high level of nuclear NF-κB p65 in the control with no changes after treatments. Both murine cell cultures ($p53^{R172H}$, $p65^{\Delta/\Delta}$ $PDGFB^{+}$) *(R172H: signifies p53 R172H mutation, Δ: signifies floxed gene, + : signifies Overexpression)* are NF-κB p65 knocked-out and showed no nuclear staining of NF-κB p65 (see Figure 20 and Figure 21).

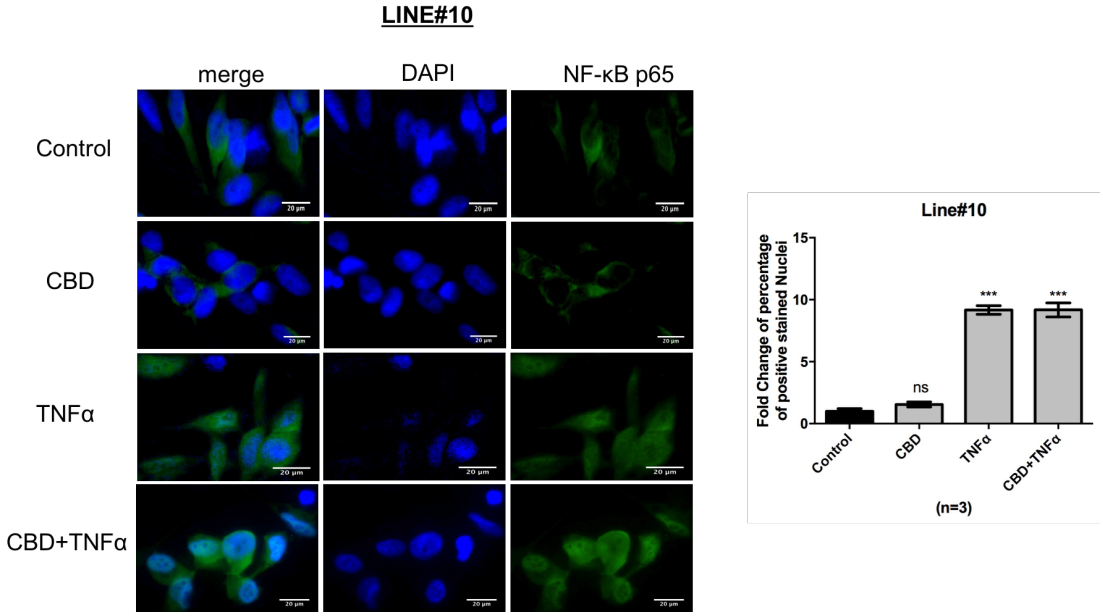

Figure 15 GBM Cell Culture Line#10. Microscope images of human cell culture Line#10 in separated channels: merge, DAPI and NF-κB p65 nuclear staining. The treatments were as the following: CBD (10 µmolar) for 16 hours, TNFα (10 ng/ml) for one hour and pre-treatment of CBD (10 µmolar) for 16 hours followed by one hour co-treatment of CBD and TNFα (10 ng/ml). All treatments are compared to the control group in the first raw of the image. The unpaired t-test showed the following results. The CBD treatment for 16 hours have not led to a significant shift of NF-κB p65 to the nucleus comparing to the control group (P-value = 0.0789 (ns)). TNFα was able to induce a shift of NF-κB p65 to the nucleus after one hour of treatment (P-value <0.0001). TNFα was also able to induce a shift of NF-κB p65 to the nucleus after one hour in the group pre-treated with CBD for 16 hours (P-value < 0.0001). Considering CBD pre-treatment, there was no significant difference detected, whether the cells had been pre-treated with CBD for 16 hours or not (P-value = 0.9933 (ns)). The applied One-way ANOVA was significant (P-value < 0.0001). The scale bar in the images is equal to 20µm.

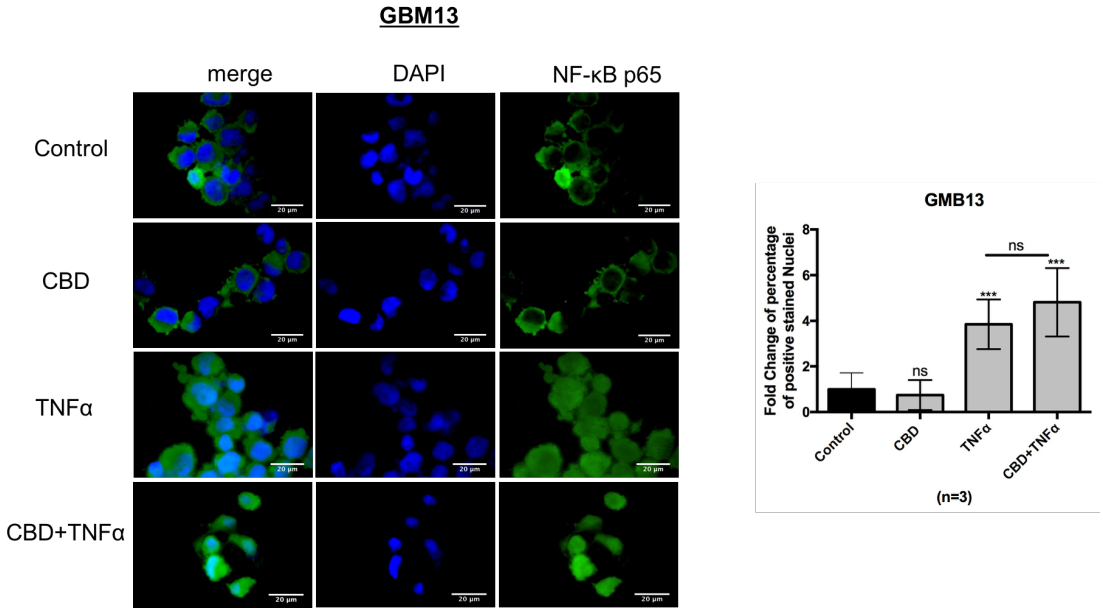

Figure 16 GBM Cell Culture GBM13. Microscope images of human cell culture GBM 13 in separated channels: merge, DAPI and NF-κB p65 nuclear staining. The treatments were as the following: CBD (10 µmolar) for 16 hours, TNFα (10 ng/ml) for one hour and pre-treatment of CBD (10 µmolar) for 16 hours followed by one hour co-treatment of CBD and TNFα (10 ng/ml). All treatments are compared to the control group in the first raw of the image. The unpaired t-test showed the following results. The CBD treatment for 16 hours have not led to a significant shift of NF-κB p65 to the nucleus comparing to the control group (P-value = 0.4456 (ns)). TNFα was able to induce a shift of NF-κB p65 to the nucleus after one hour of treatment (P-value <0.0001). TNFα was also able to induce a shift of NF-κB p65 to the nucleus after one hour in the group pre-treated with CBD for 16 hours (P-value < 0.0001). Considering CBD pre-treatment, there was no significant difference detected, whether the cells had been pre-treated with CBD for 16 hours or not (P-value = 0.1366 (ns)). The applied One-way ANOVA test was significant (P-value < 0.0001). The scale bar in the images is equal to 20µm.

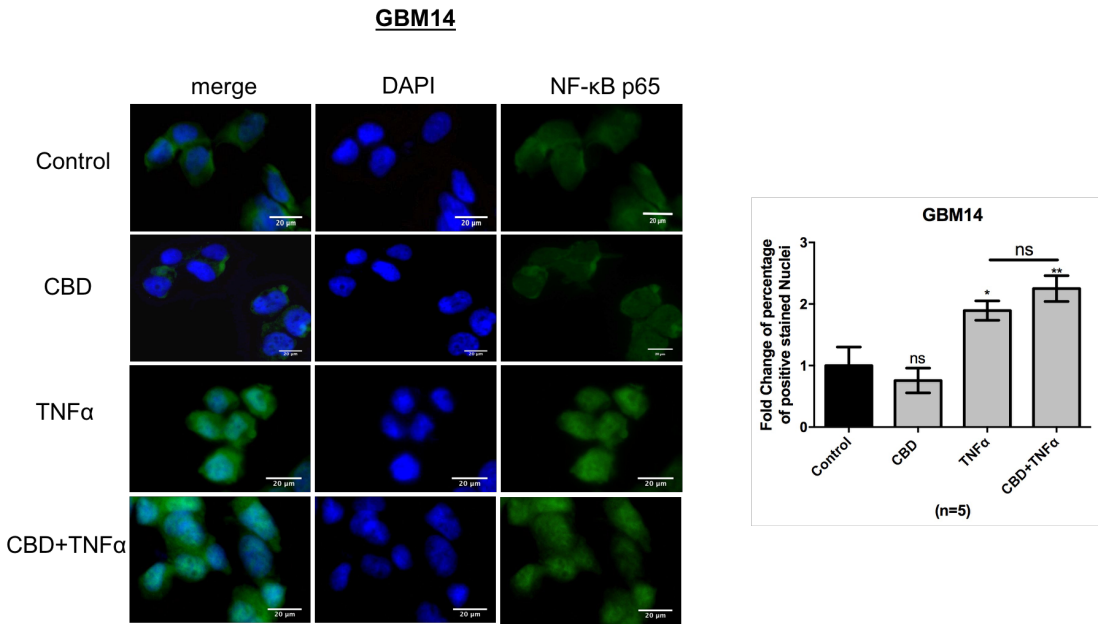

Figure 17 GBM Cell Culture GBM14. Microscope images of human cell culture GBM 14 in separated channels: merge, DAPI and NF-κB p65 nuclear staining. The treatments were as the following: CBD (10 µmolar) for 16 hours, TNFα (10 ng/ml) for one hour and pre-treatment of CBD (10 µmolar) for 16 hours followed by one hour co-treatment of CBD and TNFα (10 ng/ml). All treatments are compared to the control group in the first raw of the image. The unpaired t-test showed the following results. The CBD treatment for 16 hours have not led to a significant shift of NF-κB p65 to the nucleus comparing to the control group (P-value = 0.5076 (ns)). TNFα was able to induce a shift of NF-κB p65 to the nucleus after one hour of treatment (P-value = 0.0138). TNFα was also able to induce a shift of NF-κB p65 to the nucleus after one hour in the group pre-treated with CBD for 16 hours (P-value = 0.0021). Considering CBD pre-treatment, there was no significant difference detected, whether the cells had been pre-treated with CBD for 16 hours or not (P-value = 0.1846 (ns)). The applied One-way ANOVA was significant (P-value < 0.0001). The scale bar in the images is equal to 20µm.

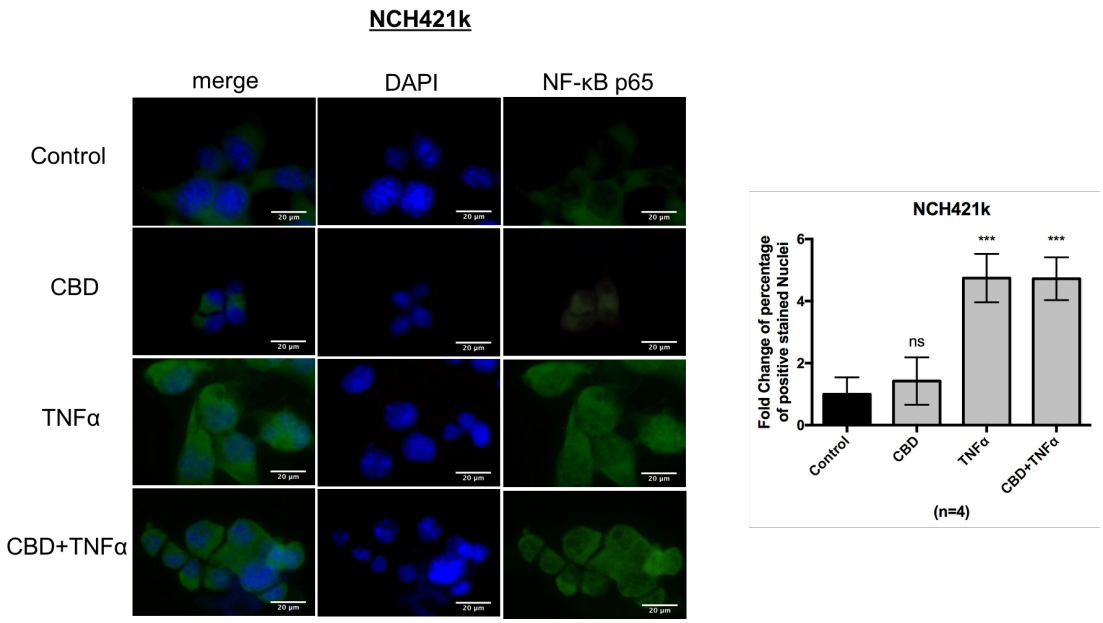

Figure 18 GBM Cell Culture NCH421k. Microscope images of human cell culture NCH421k in separated channels: merge, DAPI and NF-κB p65 nuclear staining. The treatments were as the following: CBD (10 µmolar) for 16 hours, TNFα (10 ng/ml) for one hour and pre-treatment of CBD (10 µmolar) for 16 hours followed by one hour co-treatment of CBD and TNFα (10 ng/ml). All treatments are compared to the control group in the first raw of the image. The unpaired t-test showed the following results. The CBD treatment for 16 hours have not led to a significant shift of NF-κB p65 to the nucleus comparing to the control group (P-value = 0.1322 (ns)). TNFα was able to induce a shift of NF-κB p65 to the nucleus after one hour of treatment (P-value <0.0001). TNFα was also able to induce a shift of NF-κB p65 to the nucleus after one hour in the group pre-treated with CBD for 16 hours (P-value < 0.0001). Considering CBD pre-treatment, there was no significant difference detected, whether the cells had been pre-treated with CBD for 16 hours or not (P-value = 0.9516 (ns)). The applied One-way ANOVA test was significant (P-value < 0.0001). The scale bar in the images is equal to 20µm.

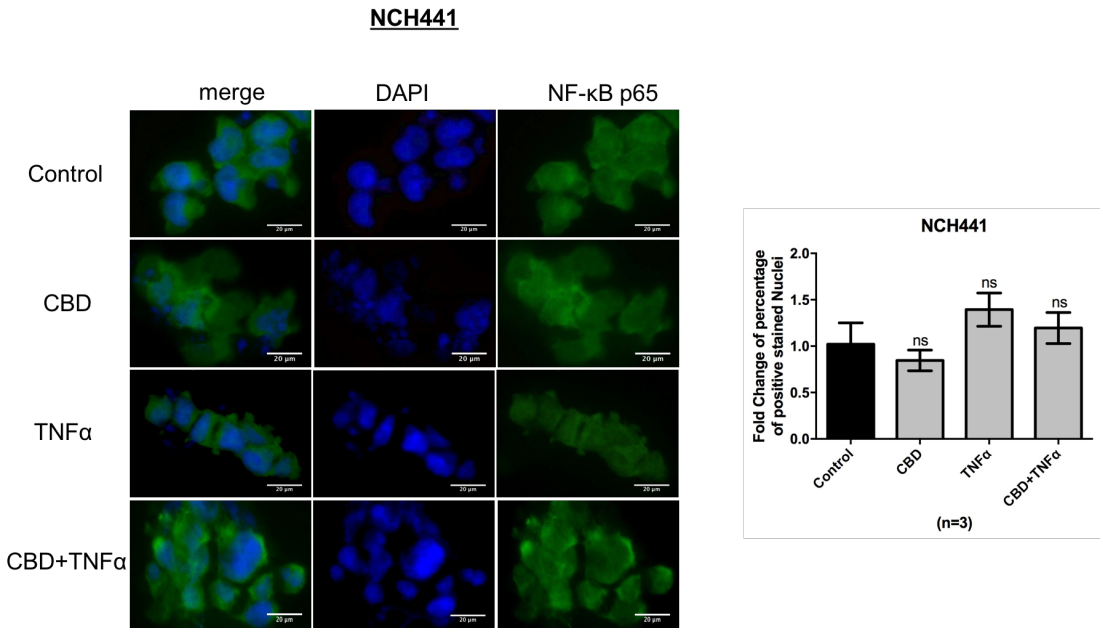

Figure 19 GBM Cell Culture NCH441. Microscope images of human cell culture NCH441 in separated channels: merge, DAPI and NF-κB p65 nuclear staining. The treatments were as the following: CBD (10 µmolar) for 16 hours, TNFα (10 ng/ml) for one hour and pre-treatment of CBD (10 µmolar) for 16 hours followed by one hour co-treatment of CBD and TNFα (10 ng/ml). All treatments are compared to the control group in the first raw of the image. All treatment groups did not show a significant difference of positive stained nuclei in comparison to the control group in the unpaired t-test. The unpaired t-test results are as following: the group treated with CBD for 16 hours vs control (P-value = 0.5054 (ns)), the group treated with TNFα for one hour vs control (P-value = 0.2389 (ns)), the group pre-treated with CBD for 16 hours followed by one hour co-treatment of CBD and TNFα vs control (P-value = 0.5637 (ns)). Considering the TNFα for one hour there was no significant difference detected, whether the cells had been pre-treated with CBD for 16 hours or not (P-value = 0.4385 (ns)). The applied One-way ANOVA test was non-significant (P-value=0.1916 (ns)). The scale bar in the images is equal to 20µm.

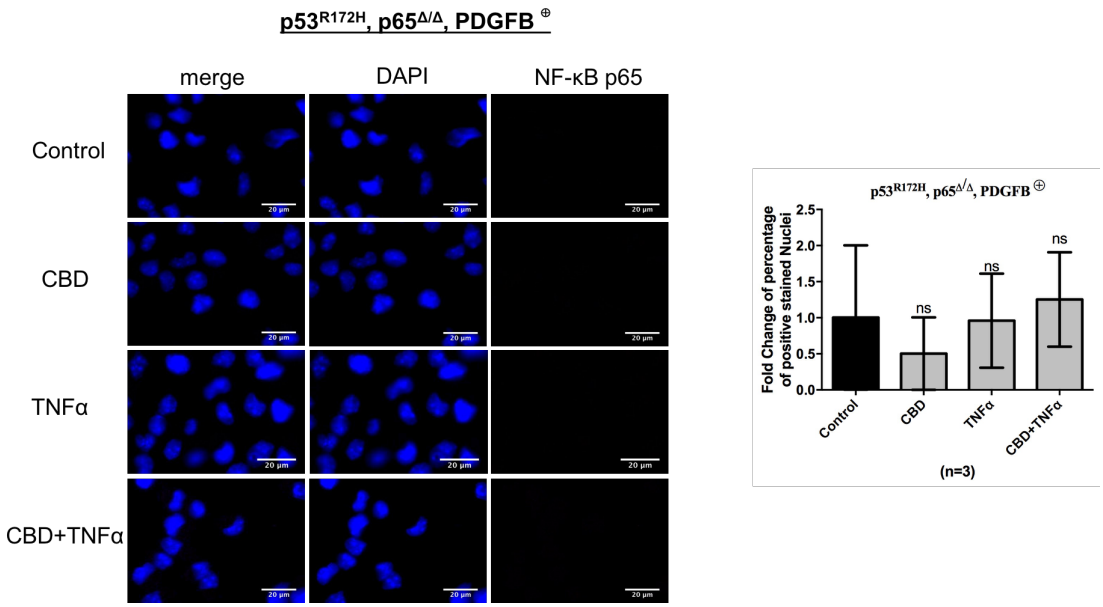

Figure 20 GBM Cell Culture p53^{R172H}, p65$^{\Delta/\Delta}$ PDGFB^{+}. Microscope images of murine cell culture p53^{R172H}, p65$^{\Delta/\Delta}$ PDGFB^{+} (NF-κB p65 knocked-out) in separated channels: merge, DAPI and NF-κB p65 nuclear staining. The treatments were as the following: CBD (10 µmolar) for 16 hours, TNFα (10 ng/ml) for one hour and pre-treatment of CBD (10 µmolar) for 16 hours followed by one hour co-treatment of CBD and TNFα (10 ng/ml). All treatments are compared to the control group in the first raw of the image. Nuclear staining of NF-κB p65 could not be seen in the images. All treatment groups did not show a significant difference of positive stained nuclei in comparison to the control group in the unpaired t-test. The unpaired t-test results are as following: the group treated with CBD for 16 hours vs control (P-value = 0.6754 (ns)), the group treated with TNFα for one hour vs control (P-value = 0.9753 (ns)), the group pre-treated with CBD for 16 hours followed by one hour co-treatment of CBD and TNFα vs control (P-value = 0.8350 (ns)). The applied One-way ANOVA test was non-significant (P-value = 0.9121 (ns)). The scale bar in the images is equal to 20µm.

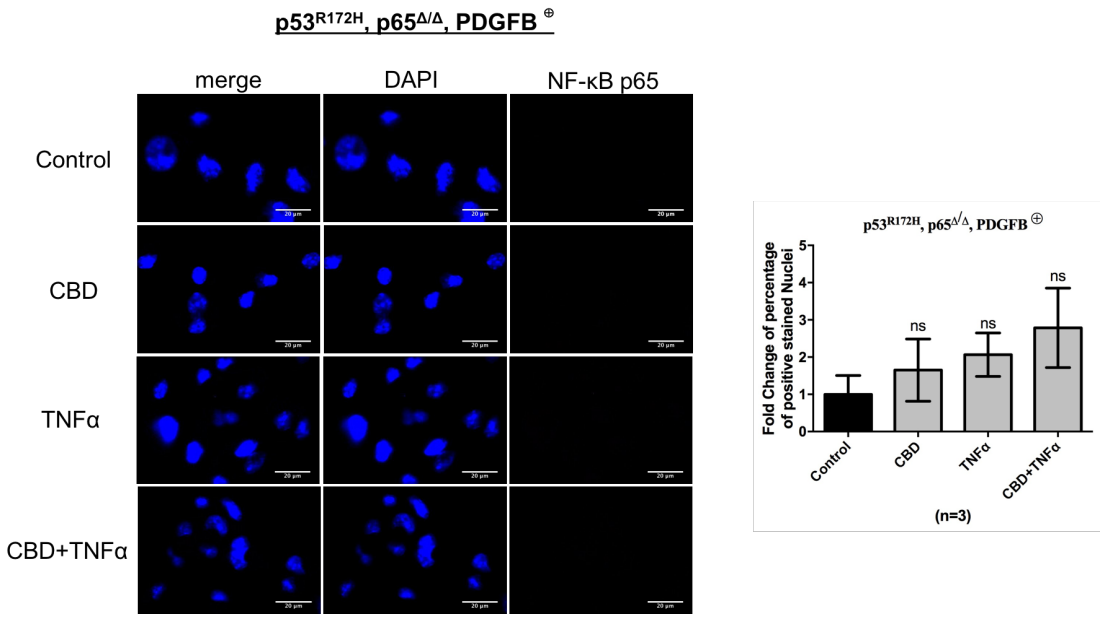

Figure 21 GBM Cell Culture $p53^{R172H}$, $p65^{\Delta/\Delta}$ $PDGFB^{+}$. Microscope images of murine cell culture $p53^{R172H}$, $p65^{\Delta/\Delta}$ $PDGFB^{+}$ (NF-κB p65 knocked-out) in separated channels: merge, DAPI and NF-κB p65 nuclear staining. The treatments were as the following: CBD (10 µmolar) for 16 hours, TNFα (10 ng/ml) for one hour and pre-treatment of CBD (10 µmolar) for 16 hours followed by one hour co-treatment of CBD and TNFα (10 ng/ml). All treatments are compared to the control group in the first raw of the image. Nuclear staining of NF-κB p65 could not be seen in the images. All treatment groups did not show a significant difference of positive stained nuclei in comparison to the control group in the unpaired t-test. The unpaired t-test results are as following: the group treated with CBD for 16 hours vs control (P-value = 0.5157 (ns)), the group treated with TNFα for one hour vs control (P-value = 0.1870 (ns)), the group pre-treated with CBD for 16 hours followed by one hour co-treatment of CBD and TNFα vs control (P-value = 0.1505 (ns)). The applied One-way ANOVA test was non-significant (P-value=0.4425 (ns)). The scale bar in the images is equal to 20µm.

4.4 Detection of Nuclear Accumulation of NF-κB p65 Phosphorylated on Serine 311 after TNFα Treatment

4.4.1 Nuclear Accumulation of NF-κB p65 Phosphorylated on Serine 311 within 60 minutes after TNFα Treatment

To detect the time point of nuclear accumulation of NF-κB p65 phosphorylated on serine 311 (phospho-NF-κB p65 ser311), the human GBM cell culture Line#2 was treated with TNFα (10 ng/ml) for several times ranging from 10 to 60 minutes. The image-analysis was obtained by counting the Corrected Total Nucleus Fluorescence (CTNF) (see 3.4.2). The cells were stained with phospho-NF-κB p65 (ser311) antibody as primary antibody. It is noticed that TNFα induced a significant elevation of the nuclear phospho-NF-κB p65 ser311 signal in the range from 10 to 60 minutes (see Figure 22). The highest nuclear phospho-NF-κB p65 ser311 signal was detected at 60 minutes (see Figure 22 and Figure 23).

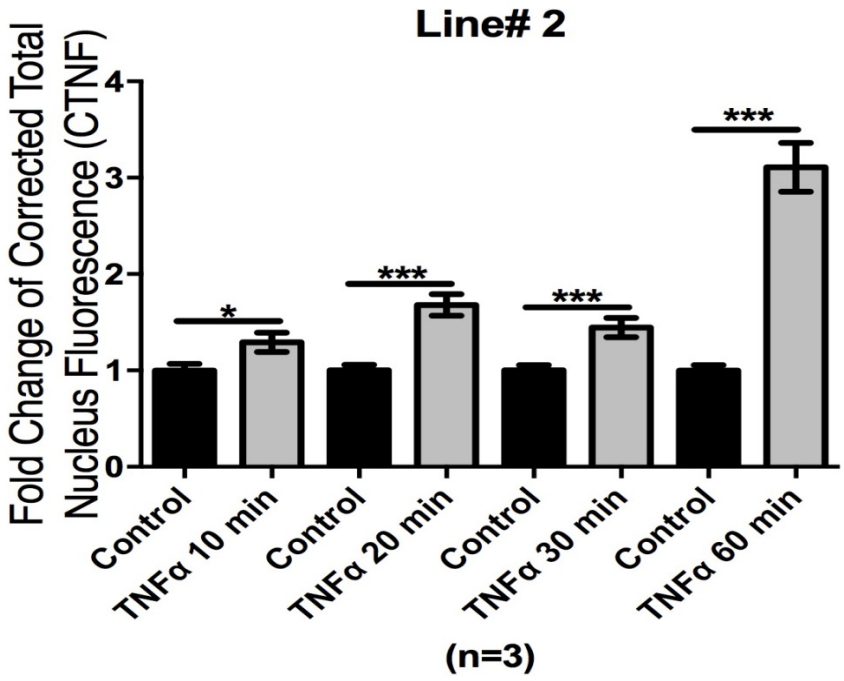

Figure 22 GBM Cell Culture Line#2. Fold changes of nuclear accumulation of NF-κB p65 phosphorylated on serine 311 (phospho-NF-κB p65 ser311) after TNFα (10 ng/ml) treatment for 10 to 60 minutes in cell culture Line#2. The unpaired t-tests showed significant elevation of nuclear phospho-NF-κB p65 ser311 in all treatment groups as following: TNFα for 10 minutes vs control (P-value = 0.0171(*)), TNFα for 20 minutes vs control (P-value <0.0001(***)), TNFα for 30 minutes vs control (P-value = 0.0002(***)), TNFα for 60 minutes vs control (P-value <0.0001 (***)).

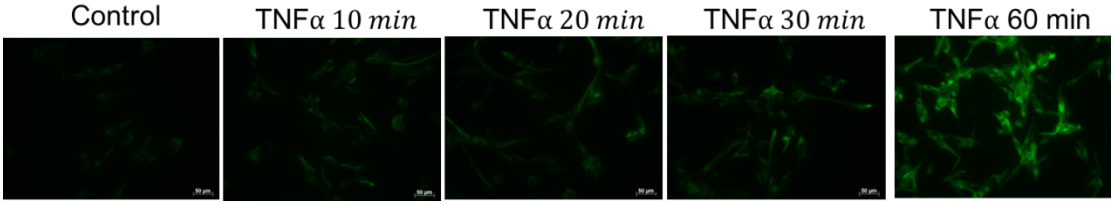

Figure 23 GBM Cell Culture Line#2. The images of cell culture Line#2 in the pospho-NF-κB p65 ser311 staining channel. Cells stained with phospho-NF-κB p65 ser311 antibody as primary antibody and Alexa Fluor® 488 as the secondary antibody. Treatment with TNFα (10 ng/ml) for 10 to 60 minutes. The scale bar in the images is equal to 50µm.

4.4.2 Nuclear Accumulation of NF-κB p65 Phosphorylated on Serine 311 after TNFα Treatment for 60 and 120 minutes

For further observation of phospho-NF-κB p65 ser311 nuclear accumulation over time, the cell culture Line#2 was treated with TNFα (10 ng/ml) for 60 and 120 minutes, then stained with phospho-NF-κB p65 (ser311) antibody as the primary antibody. By counting the CTNF, the nuclear accumulation of phospho-NF-κB p65 ser311 increased significantly after TNFα treatment in comparison to the controls at both time points (see Figure 24).

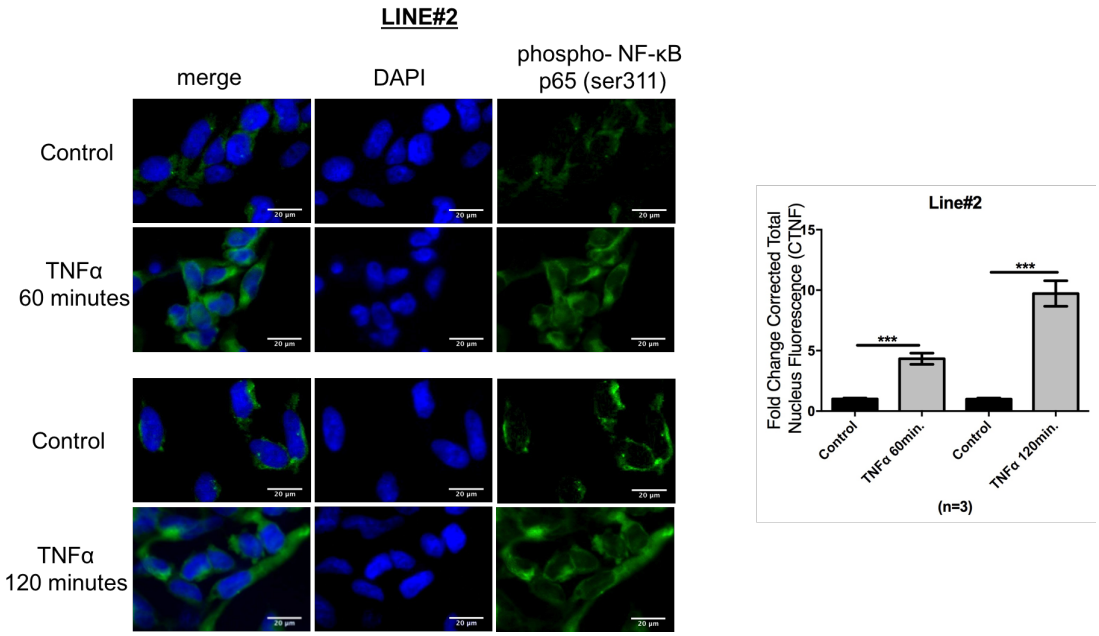

Figure 24 GBM Cell Culture Line#2. Microscope images and graph cell culture Line#2 show the fold changes of nuclear accumulation of NF-κB p65 phosphorylated on serine 311 (phspho NF-κB p65 ser311) after TNFα (10 ng/ml) treatment for 60 and 120 minutes. Both treatment groups showed a significant elevation of the nuclear accumulation of phspho NF-κB p65 ser311 in comparison to the control groups. The unpaired t-test showed a (P-value < 0,0001) for both groups. The scale bar in the images is equal to 20µm.

4.5 Detection of NF-κB p65 Phosphorylated on Serine 311 Nuclear Accumulation after CBD/TNFα Treatments and Co-Treatments

The accumulation of NF-κB p65 phosphorylated on serine 311 (phospho-NF-κB p65 ser311) was observed initially in the human GBM cell culture Line#2 by staining with phospho-NF-κB p65 (ser311) antibody as primary antibody and counting the Corrected Total Nucleus Fluorescence (CTNF) according to the method (in 3.4.2). The cell culture Line#2 was divided into two treatment groups. The first group was treated with TNFα (10 ng/ml) for one hour added to the vehicle (DMSO 0,01%) as a control. The second group was pre-treated with CBD (10 µmolar) for 6 hours followed by a co-treatment of CBD and TNFα (10 ng/ml) for one hour. CBD was unable to affect the nuclear accumulation of phospho-NF-κB p65 ser311 after 6 hours of treatment (see Figure 25).

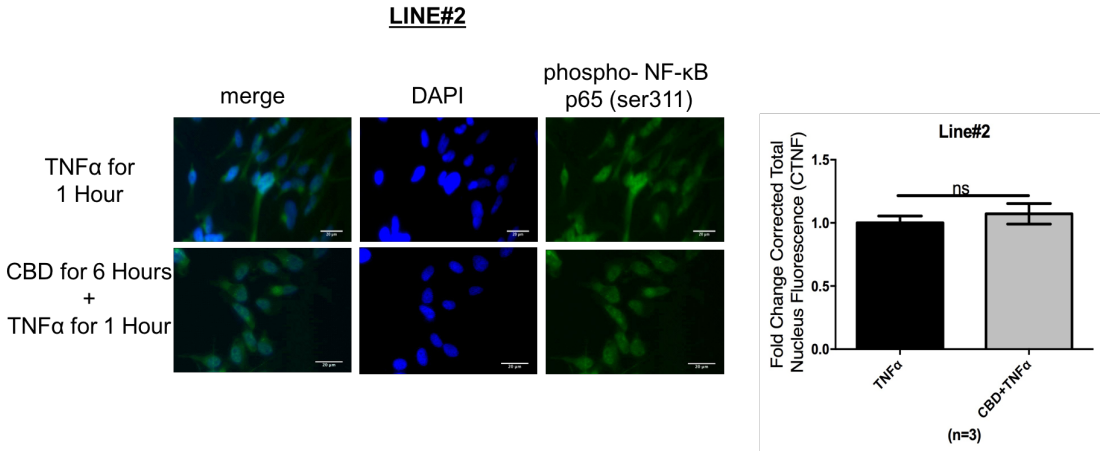

Figure 25 GBM Cell Culture Line#2. Microscope images of cell culture Line#2 in different channels: merge, DAPI and phospho-NF-κB p65 ser311 staining. The treatment groups were TNFα (10 ng/ml) for one hour as a control in comparison to the other group which was pre-treated with CBD (10 µmolar) for 6 hours followed by adding TNFα (10 ng/ml) for one hour as co-treatment. The graph shows the fold changes of nuclear phospho-NF-κB p65 ser311 accumulation after TNFα treatment for one hour with no significant effect of CBD pre-treatment for 6 hours. The P-value of unpaired t-test was (0,4609) (ns). The scale bar in the images is equal to 20µm.

4.6 Effect of CBD/TNFα Treatments and Co-treatments on the Nuclear Accumulation of NF-κB p65 Phosphorylated on Serine 311

For further evaluation of the effect of CBD on the nuclear accumulation of NF-κB p65 phosphorylated on serine 311 (phospho-NF-κB p65 ser311), the treatment time with CBD was increased to 16 hours. Here the GBM cell culture Line#2 was divided into four groups of treatments; 1) A control group that only has the vehicle (DMSO 0.01%); 2) a group treated with CBD (10 μmolar) for 16 hours; 3) a group treated with TNFα (10 ng/ml) for one hour and 4) a group treated with CBD (10 μmolar) for 16 hours followed by a co-treatment treatment of CBD and TNFα (10 ng/ml) for one hour. All groups were stained with NF-κB p65 (ser311) antibody as primary antibody. In the cell culture Line#2, the 16 hours treatment with CBD not only showed an inhibition of the nuclear accumulation phospho-NF-κB p65 ser311, but also a significant reduction of nuclear accumulation of phospho-NF-κB p65 ser311 caused by TNFα (see Figure 26). The nuclear accumulation of phospho-NF-κB p65 ser311 was investigated by analysing CTNF (see 3.4.2). To expand these findings, the GBM cell cultures (Table 7 Human GBM Cell Cultures and Table 8 Murine GBM Cell Cultures) were treated for the same periods and under the same conditions.

4.6.1 Cell Cultures where CBD Treatment Inhibited the Nuclear Accumulation of NF-κB p65 Phosphorylated on Serine 311

This part shows the effect of CBD on the nuclear accumulation of phospho-NF-κB p65 ser311 after 16 hours of treatment in both human and murine cell cultures. In the human cell cultures Line#2 (see Figure 26), Line#6 (see Figure 27), Line#7 (see Figure 28), Line#11 (see Figure 29) and NCH644 (see Figure 30) was it noticed that CBD inhibited the nuclear accumulation of phospho-NF-κB p65 ser311 after 16 hours. Similar findings were observed in the murine cell cultures (cdkn2a$^{-/-}$, EGFR^{+}) *(-/-: signifies knock out, +: signifies Overexpression)* (see Figure 31) and (cdkn2a$^{-/-}$, PDGFB^{+}) (see Figure 32). While TNFα enhanced the nuclear accumulation of phospho-NF-κB p65 ser311 after one hour of treatment, it was unable to reach the same effect in the groups pre-treated with CBD for 16 hours.

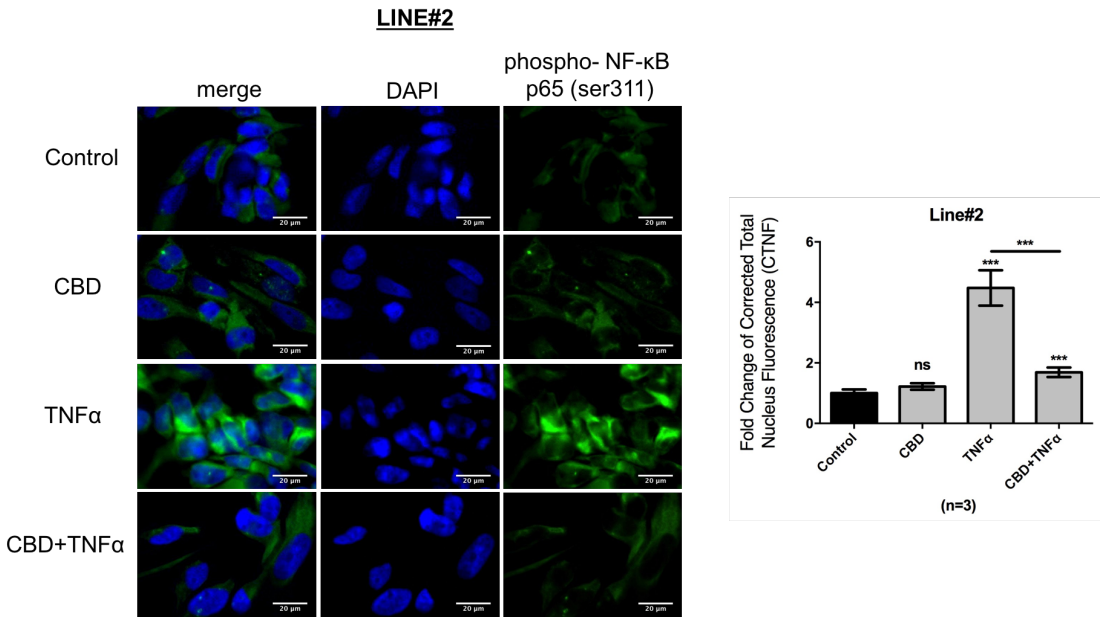

Figure 26 GBM Cell Culture Line#2. Microscope images of human cell culture Line#2 in separated channels: merge, DAPI and nuclear NF-κB p65 phosphorylated on serine 311 (phospho-NF-κB p65 ser311). The Treatments were as the following: CBD (10 µmolar) for 16 hours, TNFα (10 ng/ml) for one hour and pre-treatment of CBD (10 µmolar) for 16 hours followed by one hour co-treatment of CBD and TNFα (10 ng/ml). All treatments are compared to the control group in the first raw of the image. The CBD treatment for 16 hours have not led to a significant accumulation of nuclear NF-κB p65 ser311 in comparison to the control group (P-value = 0.1731 (ns)). TNFα elevated significantly the nuclear accumulation of NF-κB p65 ser311 after one hour in comparison to the control group (P-value < 0.0001). Furthermore, TNFα could elevate significantly the nuclear accumulation of NF-κB p65 ser311 after one hour in the group pre-treated with CBD for 16 hours comparing to the control group (P-value = 0.0006). The pre-treatment with CBD for 16 hours reduced significantly the ability of TNFα to induce a nuclear accumulation of NF-κB p65 ser311 after one hour in comparison to the group which was not pre-treated with CBD (P-value < 0.0001). The applied One-way ANOVA test showed a significant P-value (< 0.0001). The scale bar in the images is equal to 20µm.

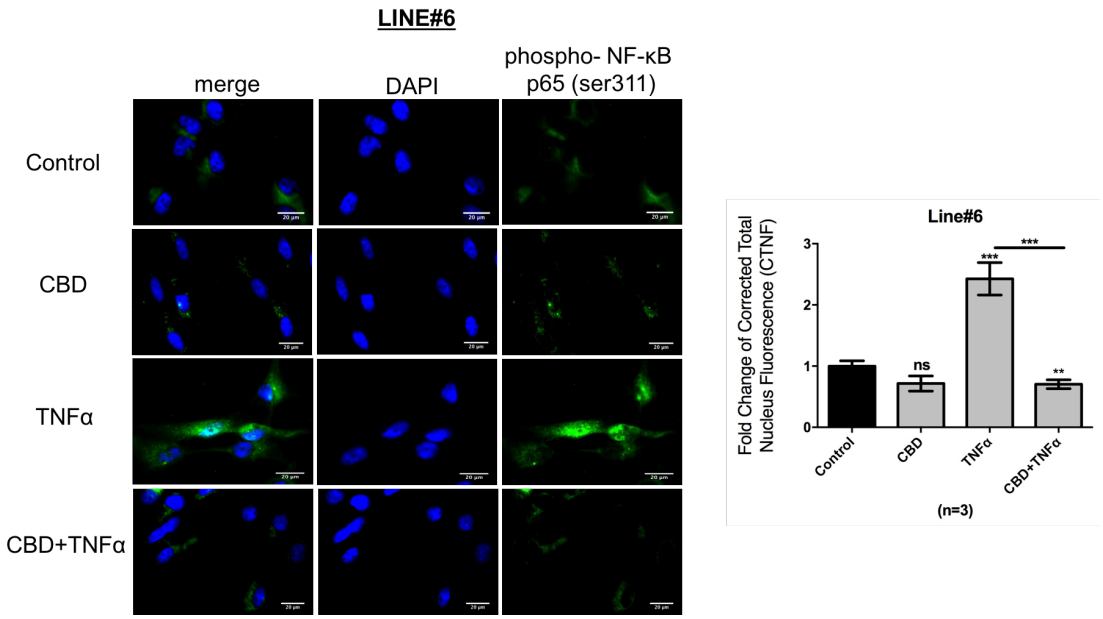

Figure 27 GBM Cell Culture Line#6. Microscope images of human cell culture Line#6 in separated channels: merge, DAPI and nuclear NF-κB p65 phosphorylated on serine 311 (phospho-NF-κB p65 ser311). The Treatments were as the following: CBD (10 µmolar) for 16 hours, TNFα (10 ng/ml) for one hour and pre-treatment of CBD (10 µmolar) for 16 hours followed by one hour co-treatment of CBD and TNFα (10 ng/ml). All treatments are compared to the control group in the first raw of the image. The unpaired t-tests showed the following results. The CBD treatment for 16 hours have not led to a significant accumulation of nuclear NF-κB p65 ser311 in comparison to the control group (P-value = 0.0602 (ns)). TNFα elevated significantly the nuclear accumulation of NF-κB p65 ser311 after one hour in comparison to the control group (P-value < 0.0001). The pre-treatment with CBD for 16 hours reduced significantly the nuclear accumulation of NF-κB p65 ser311 comparing to the control group (P-value = 0.0088). Furthermore, it reduced the ability of TNFα to induce a nuclear accumulation of NF-κB p65 ser311 after one hour of treatment in comparison to the group which was not pre-treated with CBD (P-value < 0.0001). The applied One-way ANOVA test showed a significant P-value (< 0.0001). The scale bar in the images is equal to 20µm.

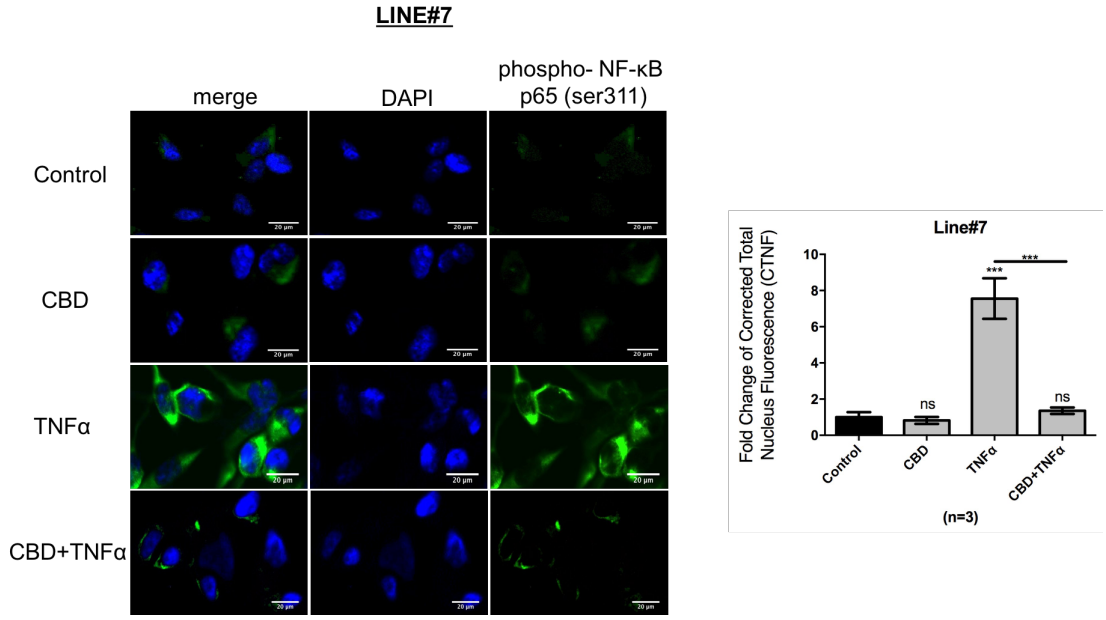

Figure 28 GBM Cell Culture Line#7. Microscope images of human cell culture Line#7 in separated channels: merge, DAPI and nuclear NF-κB p65 phosphorylated on serine 311 (phospho-NF-κB p65 ser311). The Treatments were as the following: CBD (10 µmolar) for 16 hours, TNFα (10 ng/ml) for one hour and pre-treatment of CBD (10 µmolar) for 16 hours followed by one hour co-treatment of CBD and TNFα (10 ng/ml). All treatments are compared to the control group in the first raw of the image. The unpaired t-tests showed the following results. The CBD treatment for 16 hours have not led to a significant accumulation of nuclear NF-κB p65 ser311 in comparison to the control group (P-value = 0.5743 (ns)). TNFα elevated significantly the nuclear accumulation of NF-κB p65 ser311after one hour in comparison to the control group (P-value < 0.0001). The pre-treatment with CBD for 16 hours inhibited the ability of TNFα to induce a nuclear accumulation of NF-κB p65 ser311 after one hour of treatment in comparison to the control group (P-value = 0.2866 (ns)). Considering TNFα treatment for one hour, a significant difference was detected between the group pre-treated with CBD for 16 hours and the group which was not pre-treated with CBD (P-value < 0.0001). The applied One-way ANOVA test showed a significant P-value (< 0.0001). The scale bar in the images is equal to 20µm.

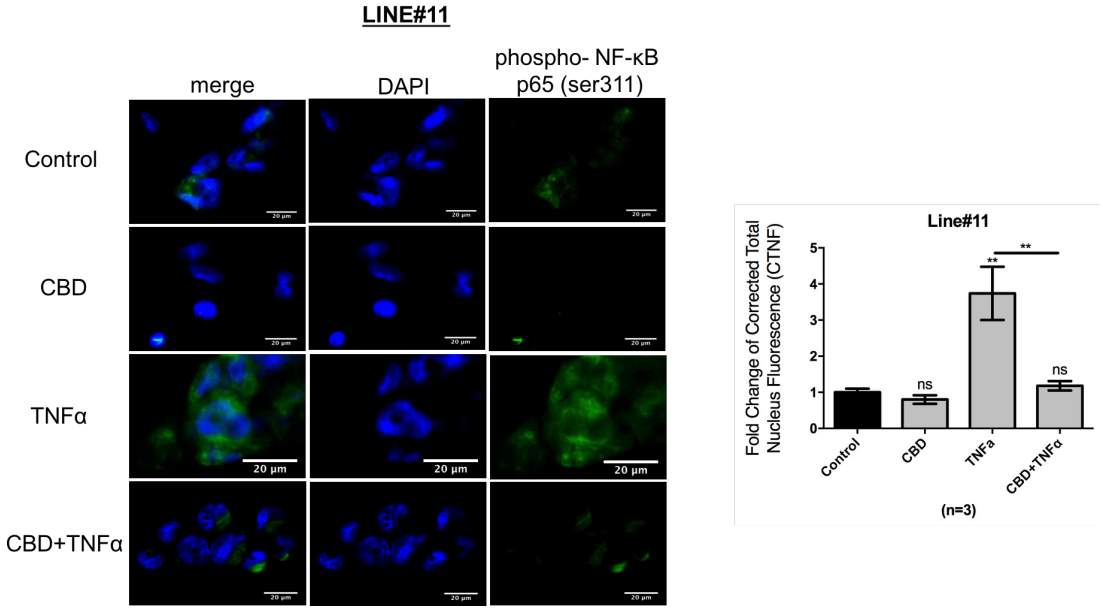

Figure 29 GBM Cell Culture Line#11. Microscope images of human cell culture Line#11 in separated channels: merge, DAPI and nuclear NF-κB p65 phosphorylated on serine 311 (phospho-NF-κB p65 ser311). The Treatments were as the following: CBD (10 µmolar) for 16 hours, TNFα (10 ng/ml) for one hour and pre-treatment of CBD (10 µmolar) for 16 hours followed by one hour co-treatment of CBD and TNFα (10 ng/ml). All treatments are compared to the control group in the first raw of the image. The unpaired t-tests showed the following results. The CBD treatment for 16 hours have not led to a significant accumulation of nuclear NF-κB p65 ser311 in comparison to the control group (P-value = 0.1989 (ns)). TNFα elevated significantly the nuclear accumulation of NF-κB p65 ser311 after one hour in comparison to the control group (P-value = 0.0014). The pre-treatment with CBD for 16 hours inhibited the ability of TNFα to induce a nuclear accumulation of NF-κB p65 ser311 after one hour of treatment in comparison to the control group (P-value = 0.2887 (ns)). Considering TNFα treatment for one hour, a significant difference was detected between the group pre-treated with CBD (10 µmolar) for 16 hours and the group which was not pre-treated with CBD (P-value = 0.0021). The applied One-way ANOVA was significant (P-value < 0.0001). The scale bar in the images is equal to 20µm.

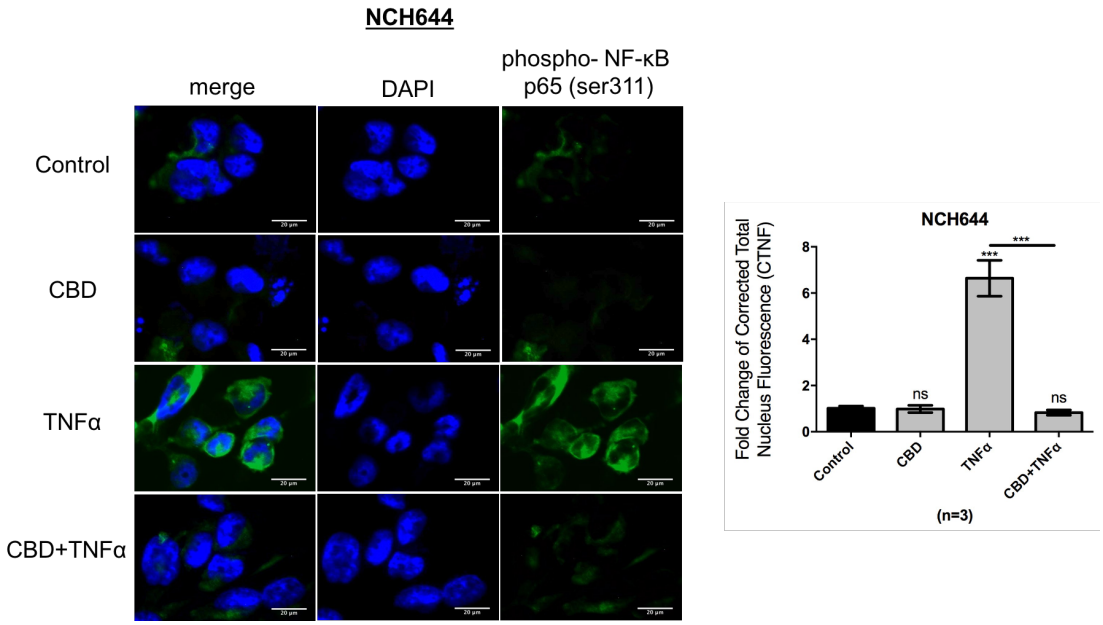

Figure 30 GBM Cell Culture NCH644. Microscope images of human cell culture NCH644 in separated channels: merge, DAPI and nuclear NF-κB p65 phosphorylated on serine 311 (phospho-NF-κB p65 ser311). The Treatments were as the following: CBD (10 µmolar) for 16 hours, TNFα (10 ng/ml) for one hour and pre-treatment of CBD (10 µmolar) for 16 hours followed by one hour co-treatment of CBD and TNFα (10 ng/ml). All treatments are compared to the control group in the first raw of the image. The unpaired t-tests showed the following results. The CBD treatment for 16 hours have not led to a significant accumulation of nuclear NF-κB p65 ser311 in comparison to the control group (P-value = 0.8606 (ns)). TNFα elevated significantly the nuclear accumulation of NF-κB p65 ser311 after one hour in comparison to the control group (P-value < 0.0001). The pre-treatment with CBD for 16 hours inhibited the ability of TNFα to induce a nuclear accumulation of NF-κB p65 ser311 after one hour of treatment in comparison to the control group (P-value = 0.2050 (ns)). Considering TNFα treatment for one hour, a significant difference was detected between the group pre-treated with CBD for 16 hours and the group which was not pre-treated with CBD (P-value <0.0001). The applied One-way ANOVA was significant (P-value < 0.0001). The scale bar in the images is equal to 20µm.

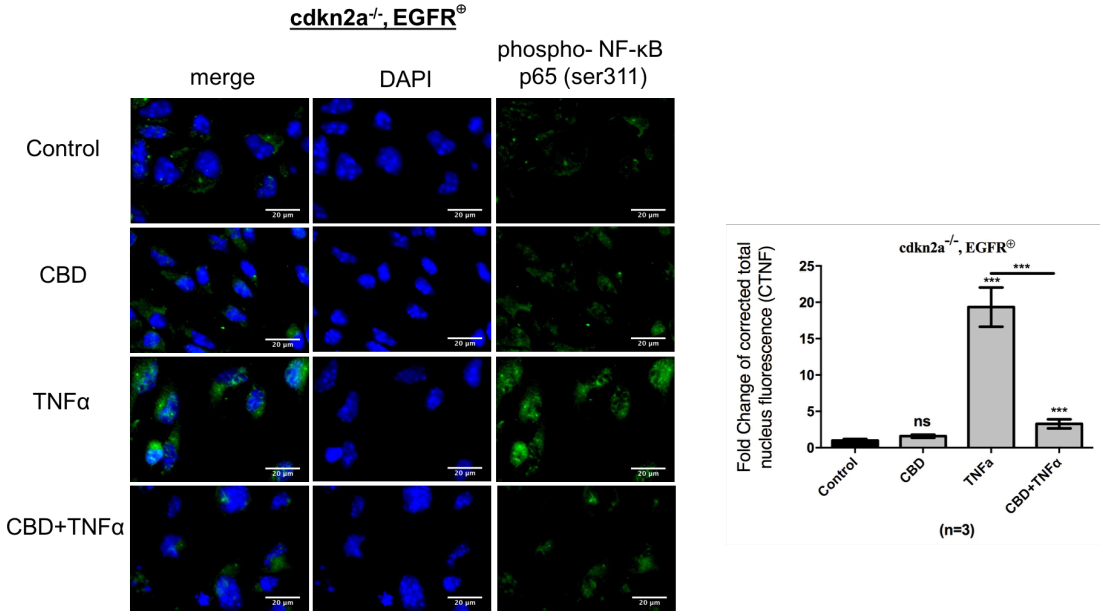

Figure 31 GBM Cell Culture (cdkn2a$^{-/-}$, EGFR^{+}). Microscope images of murine cell culture (cdkn2a$^{-/-}$, EGFR^{+}) in separated channels: merge, DAPI and nuclear NF-κB p65 phosphorylated on serine 311 (phospho-NF-κB p65 ser311). The Treatments were as the following: CBD (10 µmolar) for 16 hours, TNFα (10 ng/ml) for one hour and pre-treatment of CBD (10 µmolar) for 16 hours followed by one hour co-treatment of CBD and TNFα (10 ng/ml). All treatments are compared to the control group in the first raw of the image. The unpaired t-tests showed the following results. The CBD treatment for 16 hours have not led to a significant accumulation of nuclear NF-κB p65 ser311 in comparison to the control group (P-value = 0.0541 (ns)). TNFα elevated significantly the nuclear accumulation of NF-κB p65 ser311 after one hour in comparison to the control group (P-value <0.0001). Furthermore, TNFα could elevate significantly the nuclear accumulation of NF-κB p65 ser311 after one hour in the group pre-treated with CBD for 16 hours comparing to the control group (P-value = 0.0007). The pre-treatment with CBD for 16 hours reduced significantly the ability of TNFα to induce a nuclear accumulation of NF-κB p65 ser311 after one hour in comparison to the group which was not pre-treated with CBD (P-value <0.0001). The applied One-way ANOVA test showed a significant P-value (< 0.0001). The scale bar in the images is equal to 20µm.

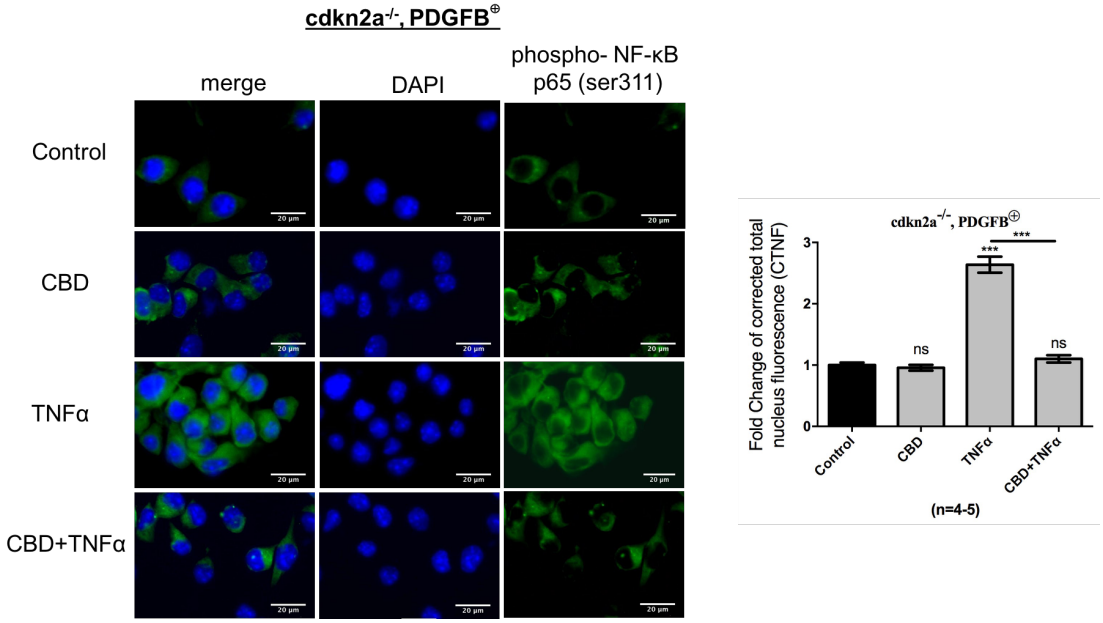

Figure 32 GBM Cell Culture (cdkn2a$^{-/-}$, PDGFB^{+}). Microscope images of murine cell culture (cdkn2a$^{-/-}$, PDGFB^{+}) in separated channels: merge, DAPI and nuclear NF-κB p65 phosphorylated on serine 311 (phospho-NF-κB p65 ser311). The Treatments were as the following: CBD (10 µmolar) for 16 hours, TNFα (10 ng/ml) for one hour and pre-treatment of CBD (10 µmolar) for 16 hours followed by one hour co-treatment of CBD and TNFα (10 ng/ml). All treatments are compared to the control group in the first raw of the image. The unpaired t-tests showed the following results. The CBD treatment for 16 hours have not led to a significant accumulation of nuclear NF-κB p65 ser311 in comparison to the control group (P-value = 0.4650 (ns)). TNFα elevated significantly the nuclear accumulation of NF-κB p65 ser311 after one hour in comparison to the control group (P-value < 0.0001). The pre-treatment with CBD for 16 hours inhibited the ability of TNFα to induce a nuclear accumulation of NF-κB p65 ser311 after one hour of treatment in comparison to the control group (P-value = 0.1450 (ns)). Considering TNFα treatment for one hour a significant difference was detected between the group pre-treated with CBD for 16 hours and the group which was not pre-treated with CBD (P-value <0.0001). The applied One-way ANOVA test showed a significant P-value (< 0.0001). The scale bar in the images is equal to 20µm.

4.6.2 Cell Cultures Where CBD Treatment Has no Effect on the Nuclear Accumulation of NF-κB p65 Phosphorylated on Serine 311

When observing the human cell cultures: Line#10 (see Figure 33), GBM13 (see Figure 34), GBM14 (see Figure 35), NCH421k (see Figure 36) and NCH441 (see Figure 37), it was noticed that there are no significant changes of the nuclear accumulation of NF-κB p65 phosphorylated on serine 311 (phospho-NF-κB p65 ser311) after treatment with CBD for 16 hours. Similarly, there were no significant changes in the murine cell culture ($p53^{-/-}$, $PDGFB^{+}$) (see Figure 38).

On the other hand, when observing the group pre-treated with CBD for 16 hours, it was noticed that TNFα induced a significant nuclear accumulation of phospho-NF-κB p65 ser311 in the human cell cultures: Line#10 (see Figure 33), GBM13 (see Figure 34) and GBM14 (see Figure 35). In a similar manner, TNFα had the same effect on the murine cell culture ($p53^{-/-}$, $PDGFB^{+}$) (see Figure 38). The same effects were noticed when observing the group pre-treated with CBD for 16 hours.

The human cell cultures, NCH421k (see Figure 36) and NCH441 (see Figure 37) showed no changes of the nuclear phospho-NF-κB p65 ser311 after treatments.

Both murine cell cultures ($p53R^{172H}$, $p65^{\Delta/\Delta}$, $PDGFB^{+}$) *(R172H: signifies p53 R172H mutation, Δ: signifies floxed gene, + : signifies Overexpression)* (see Figure 39 and Figure 40) are NF-κB p65 knocked-out and showed no nuclear staining.

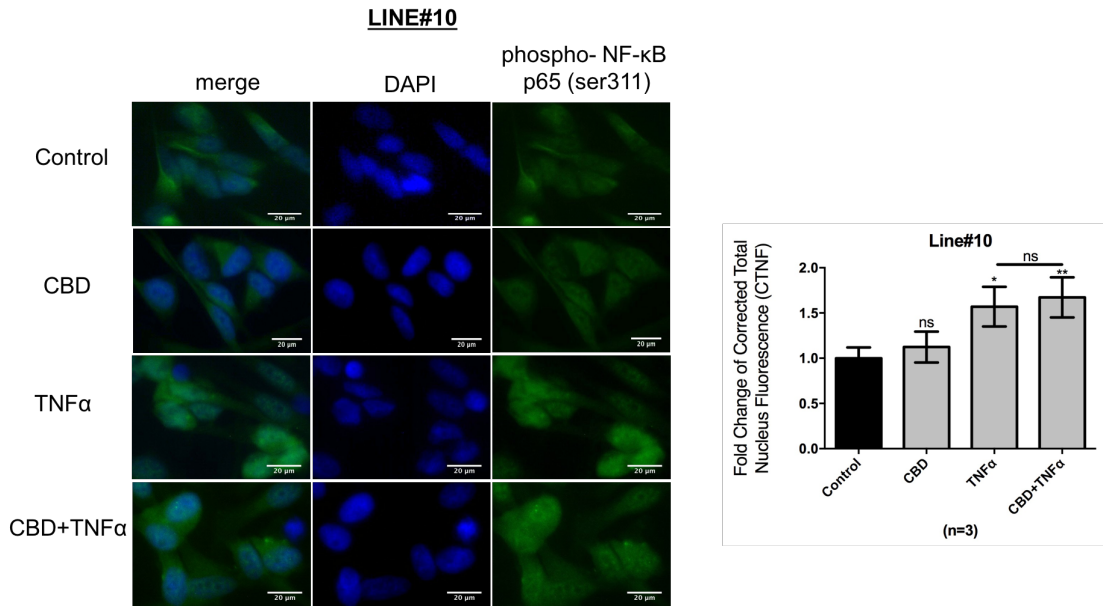

Figure 33 GBM Cell Culture Line#10. Microscope images of human cell culture Line #10 in separated channels: merge, DAPI and nuclear NF-κB p65 phosphorylated on serine 311 (phospho-NF-κB p65 ser311). The treatments were as the following: CBD (10 µmolar) for 16 hours, TNFα (10 ng/ml) for one hour and pre-treatment of CBD (10 µmolar) for 16 hours followed by one hour co-treatment of CBD and TNFα (10 ng/ml). All treatments are compared to the control group in the first raw of the image. The unpaired t-tests showed the following results. The CBD treatment for 16 hours did not affect the nuclear accumulation phospho-NF-κB p65 ser311 comparing to the control group (P-value = 0.5540 (ns)). TNFα could induce a significant accumulation of nuclear phospho-NF-κB p65 ser311 after one hour of treatment comparing to the control group (P-value = 0.0240). Moreover, TNFα induced an accumulation of nuclear phospho-NF-κB p65 ser311 after one hour in the group pre-treated with CBD for 16 hours compared to the control group (P-value = 0.0085). Considering CBD pre-treatment, there was no significant difference detected, whether the cells had been pre-treated with CBD for 16 hours or not (P-value = 0.7438 (ns)). The applied One-way ANOVA test was significant (P-value = 0.0275). The scale bar in the images is equal to 20µm.

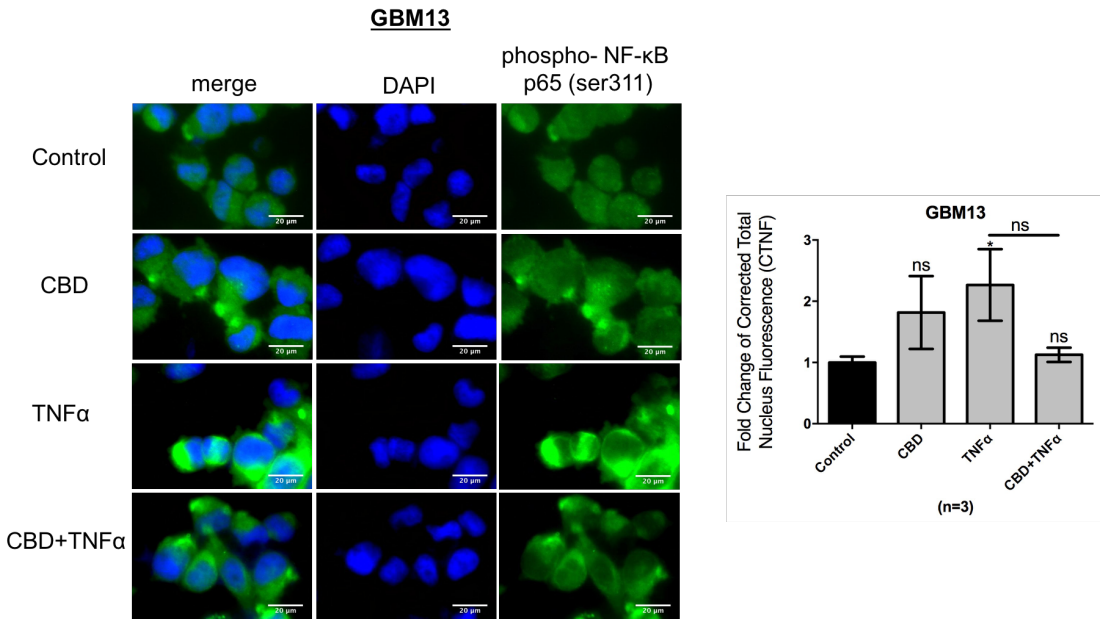

Figure 34 GBM Cell Culture GBM13. Microscope images of human cell culture GBM13 in separated channels: merge, DAPI and nuclear NF-κB p65 phosphorylated on serine 311 (phospho-NF-κB p65 ser311). The treatments were as the following: CBD (10 µmolar) for 16 hours, TNFα (10 ng/ml) for one hour and pre-treatment of CBD (10 µmolar) for 16 hours followed by one hour co-treatment of CBD and TNFα (10 ng/ml). All treatments are compared to the control group in the first raw of the image. The unpaired t-tests showed the following results. The CBD treatment for 16 hours did not affect the nuclear accumulation phospho-NF-κB p65 ser311 comparing to the control group (P-value = 0.1622 (ns)). TNFα could induce a low significant accumulation of nuclear phospho-NF-κB p65 ser311 after one hour of treatment comparing to the control group (P-value = 0.0343). However, TNFα could not show a significant accumulation of nuclear phospho-NF-κB p65 ser311 after one hour of treatment in the group pre-treated with CBD for 16 hours compared to the control group (P-value = 0.4056 (ns)). Considering CBD pre-treatment, there was no significant difference detected, whether the cells had been pre-treated with CBD for 16 hours or not (P-value = 0.0688 (ns)). The applied One-way ANOVA test was non-significant (P-value = 0.1129 (ns)). The scale bar in the images is equal to 20µm.

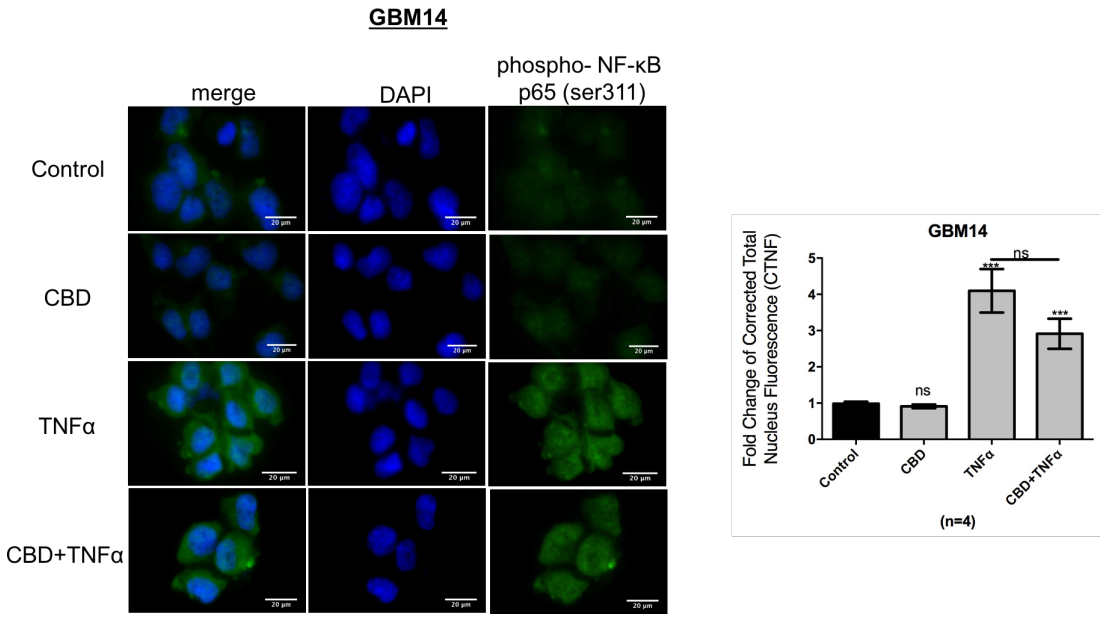

Figure 35 GBM Cell Culture GBM14. Microscope images of human cell culture GBM14 in separated channels: merge, DAPI and nuclear NF-κB p65 phosphorylated on serine 311 (phospho-NF-κB p65 ser311). The treatments were as the following: CBD (10 µmolar) for 16 hours, TNFα (10 ng/ml) for one hour and pre-treatment of CBD (10 µmolar) for 16 hours followed by one hour co-treatment of CBD and TNFα (10 ng/ml). All treatments are compared to the control group in the first raw of the image. The unpaired t-tests showed the following results. The CBD treatment for 16 hours did not affect the nuclear accumulation phospho-NF-κB p65 ser311 comparing to the control group (P-value = 0.3308 (ns)). TNFα could induce a significant accumulation of nuclear phospho-NF-κB p65 ser311 after one hour of treatment comparing to the control group (P-value < 0.0001). Moreover, TNFα induced an accumulation of nuclear phospho-NF-κB p65 ser311 after one hour in the group pre-treated with CBD for 16 hours compared to the control group (P-value < 0.0001). Considering CBD pre-treatment, there was no significant difference detected, whether the cells had been pre-treated with CBD for 16 hours or not (P-value = 0.1326 (ns)). The applied One-way ANOVA test was significant (P-value < 0.0001). The scale bar in the images is equal to 20µm

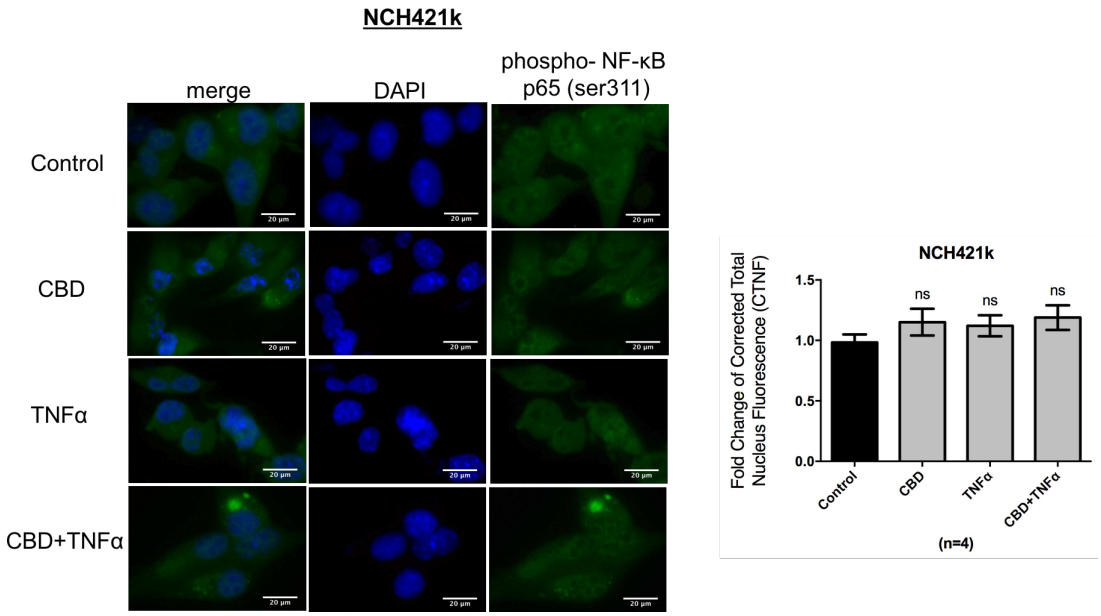

Figure 36 GBM Cell Culture NCH421k. Microscope images of human cell culture NCH421k in separated channels: merge, DAPI and nuclear NF-κB p65 phosphorylated on serine 311 (phospho-NF-κB p65 ser311). The treatments were as the following: CBD (10 µmolar) for 16 hours, TNFα (10 ng/ml) for one hour and pre-treatment of CBD (10 µmolar) for 16 hours followed by one hour co-treatment of CBD and TNFα (10 ng/ml). All treatments are compared to the control group in the first raw of the image. None of the treatment groups showed a significant difference of the nuclear phospho-NF-κB p65 ser311 level in comparison to the control group in the unpaired t-test. The unpaired t-test results are as following: the group treated with CBD for 16 hours vs control showed a (P-value = 0.1913 (ns)), the group treated with TNFα for one hour vs control showed a (P-value = 0.2133 (ns)), the group pre-treated with CBD for 16 hours followed by one hour co-treatment of CBD and TNFα vs control showed a (P-value = 0.0881 (ns)). Considering the TNFα for one hour there was no significant difference detected, whether the cells had been pre-treated with CBD for 16 hours or not (P-value = 0.6100 (ns)). The applied One-way ANOVA test was a non-significant (P-value = 0.4222 (ns)). The scale bar in the images is equal to 20µm.

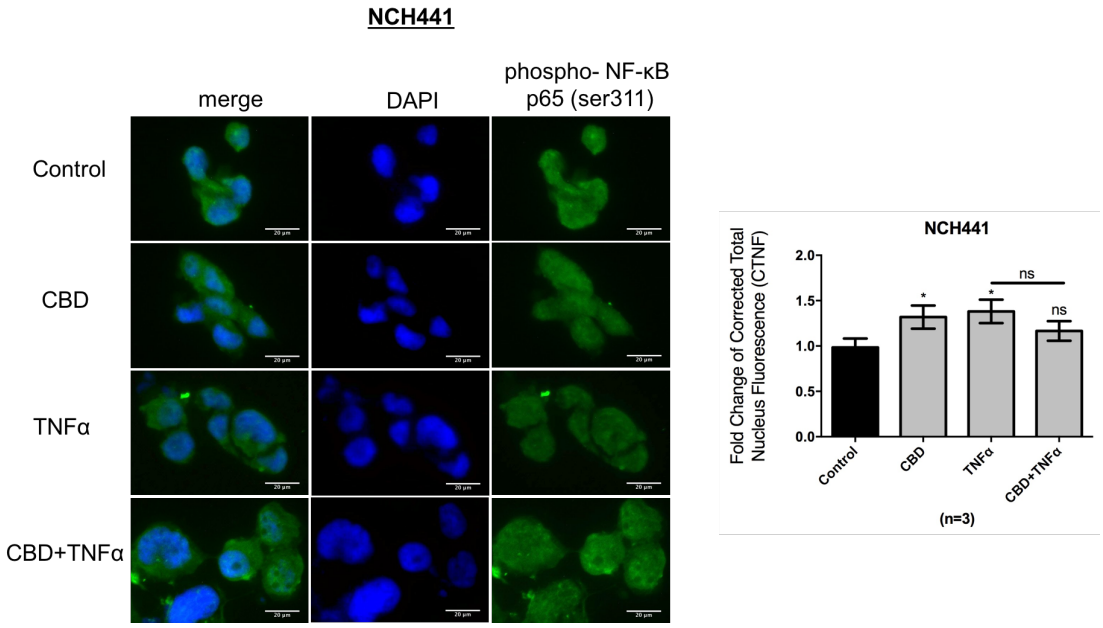

Figure 37 GBM Cell Culture NCH441. Microscope images of human cell culture NCH441 in separated channels: merge, DAPI and nuclear NF-κB p65 phosphorylated on serine 311 (phospho-NF-κB p65 ser311). The treatments were as the following: CBD (10 µmolar) for 16 hours, TNFα (10 ng/ml) for one hour and pre-treatment of CBD (10 µmolar) for 16 hours followed by one hour co-treatment of CBD and TNFα (10 ng/ml). All treatments are compared to the control group in the first raw of the image. The unpaired t-tests showed the following results. The CBD treatment for 16 hours showed a low significant accumulation of nuclear phospho-NF-κB p65 ser311 comparing to the control group (P-value = 0.0380). Furthermore, TNFα could induce a low significant accumulation of nuclear phospho-NF-κB p65 ser311 after one hour of treatment comparing to the control group (P-value = 0,0142). However, the group pre-treated with CBD for 16 hours followed by TNFα treatment for one hour in a co-treatment showed no significant difference of the nuclear phospho-NF-κB p65 ser311 in comparison to the control group (P-value = 0,2128) (ns)). Considering CBD pre-treatment, there was no significant difference detected, whether the cells had been pre-treated with CBD for 16 hours or not (P-value = 0.2029 (ns)). The applied One-way ANOVA test was non-significant (P-value = 0.0713 (ns)). The scale bar in the images is equal to 20µm.

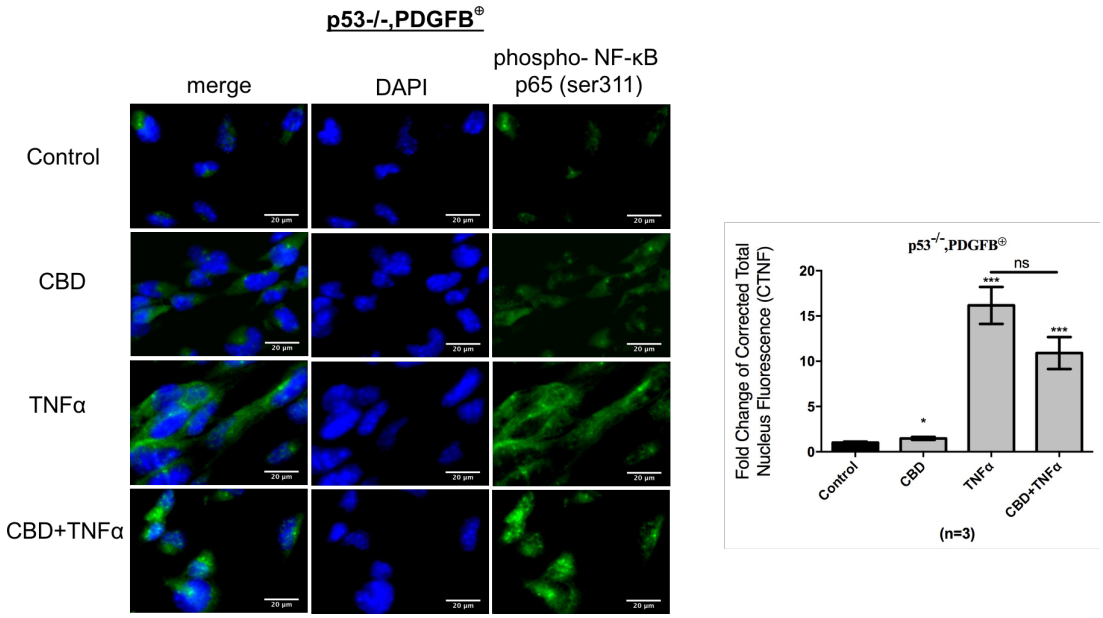

Figure 38 GBM Cell Culture (p53$^{-/-}$, PDGFB^{+}). Microscope images of the murine cell culture (p53-/-, PDGFB^{+}) in separated channels: merge, DAPI and nuclear NF-κB p65 phosphorylated on serine 311 (phospho-NF-κB p65 ser311). The treatments were as the following: CBD (10 µmolar) for 16 hours, TNFα (10 ng/ml) for one hour and pre-treatment of CBD (10 µmolar) for 16 hours followed by one hour co-treatment of CBD and TNFα (10 ng/ml). All treatments are compared to the control group in the first raw of the image. The unpaired t-tests showed the following results. The CBD treatment for 16 hours showed a low significant accumulation of nuclear phospho-NF-κB p65 ser311 comparing to the control group (P-value = 0.0217). On the other hand, TNFα could induce a significant accumulation of nuclear phospho-NF-κB p65 ser311 after one hour of treatment comparing to the control group (P-value < 0,0001). Moreover, the group pre-treated with CBD for 16 hours followed by TNFα treatment for one hour in a co-treatment showed significant difference of the nuclear phospho-NF-κB p65 ser311 in comparison to the control group (P-value < 0,0001). Considering CBD pre-treatment, there was no significant difference detected, whether the cells had been pre-treated with CBD for 16 hours or not (P-value = 0.0527 (ns)). The applied One-way ANOVA test was significant (P-value < 0,0001). The scale bar in the images is equal to 20µm.

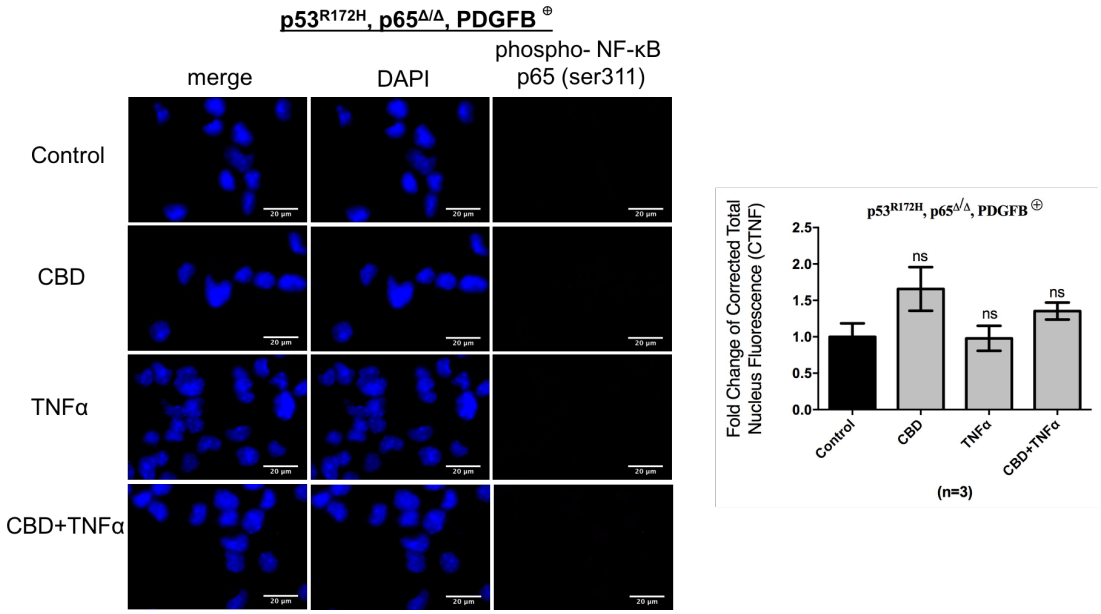

Figure 39 GBM Cell Culture $p53^{R172H}$, $p65^{\Delta/\Delta}$, $PDGFB^{+}$. Microscope images of murine cell culture $p53^{R172H}$, $p65^{\Delta/\Delta}$, $PDGFB^{+}$ (NF-κB p65 knocked-out) in separated channels: merge, DAPI and nuclear NF-κB p65 phosphorylated on serine 311 (phospho-NF-κB p65 ser311). The treatments were as the following: CBD (10 µmolar) for 16 hours, TNFα (10 ng/ml) for one hour and pre-treatment of CBD (10 µmolar) for 16 hours followed by one hour co-treatment of CBD and TNFα (10 ng/ml). All treatments are compared to the control group in the first raw of the image. The nuclear staining of phospho-NF-κB p65 ser311could not be seen in the images. All treatment groups did not show a significant nuclear accumulation in comparison to the control group. The unpaired t-test results are as following: the group treated with CBD for 16 hours vs control (P-value = 0.0635 (ns)), the group treated with TNFα for one hour vs control (P-value = 0.9319 (ns)), the group pre-treated with CBD for 16 hours followed by one hour co-treatment of CBD and TNFα vs control (P-value = 0.1104 (ns)). The applied One-way ANOVA test was non-significant (P-value=0.0599 (ns)). The scale bar in the images is equal to 20µm.

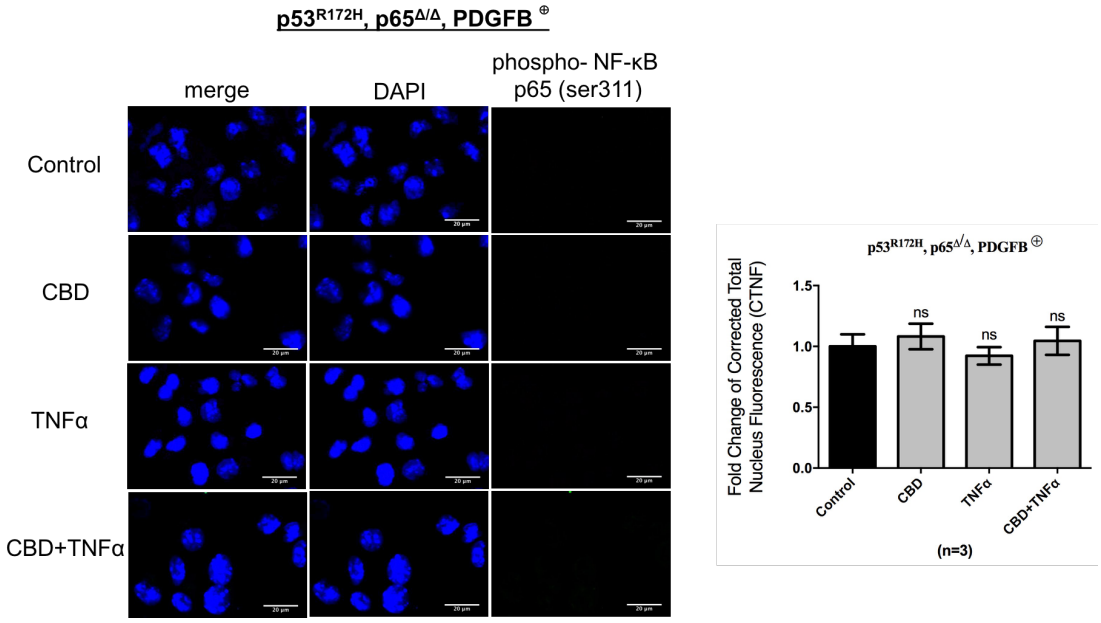

Figure 40 GBM Cell Culture $p53^{R172H}$, $p65^{\Delta/\Delta}$, $PDGFB^{+}$. Microscope images of murine cell culture $p53^{R172H}$, $p65^{\Delta/\Delta}$, $PDGFB^{+}$ (NF-κB p65 knocked-out) in separated channels: merge, DAPI and nuclear NF-κB p65 phosphorylated on serine 311 (phospho-NF-κB p65 ser311). The treatments were as the following: CBD (10 µmolar) for 16 hours, TNFα (10 ng/ml) for one hour and pre-treatment of CBD (10 µmolar) for 16 hours followed by one hour co-treatment of CBD and TNFα (10 ng/ml). All treatments are compared to the control group in the first raw of the image. The nuclear staining of phospho-NF-κB p65 ser311could not be seen in the images. All treatment groups did not show a significant nuclear accumulation in comparison to the control group. The unpaired t-test results are as following: the group treated with CBD for 16 hours vs control (P-value = 0.5704 (ns)), the group treated with TNFα for one hour vs control (P-value = 0.5289 (ns)), the group pre-treated with CBD for 16 hours followed by one hour co-treatment of CBD and TNFα vs control (P-value = 0.7625 (ns)). The applied One-way ANOVA test was non-significant (P-value=0.6936 (ns)). The scale bar in the images is equal to 20µm.

5. Discussion

This section reveals the quantification and analysis, antibody control, time course of TNFα activation, NF-κB as a survival factor and CBD effect on nuclear NF-κB in several GBM (Glioblastoma) cell cultures.

Activated NF-κB regulates cell proliferation, inflammation and has been noted in numerous human cancers as a major factor that induces cell survival and treatment resistance (Vlahopoulos, et al. 2015). These findings were also observed in GBMs (da Nóbrega, et al. 2018). On the other hand, inhibiting or blocking NF-κB in malignant cells is associated with better response to therapy, proliferation reduction and hence cell death (Zeligs, Neuman and Annunziata 2016). This set NF-κB as a target for this study by investigating its phosphorylation and nuclear translocation in GBM cells.

These investigations were carried out on fixed cells that were treated in vital state without cell lysing or damaging. The used methods were immunofluorescence staining and immunocytochemistry. This method was applied to this study to investigate the effect of CBD on the nuclear translocation of NF-κB p65. Also to investigate the nuclear accumulation of NF-κB p65 phosphorylated on serine 311 in GBM cells by staining with different immunofluorescent antibodies.

The quantification and the analysis of immunofluorescence staining to detect the localisation or expression levels of different proteins in fixed cells were also used in (Zeng, et al. 2018); (Ruiz-Perera, et al. 2018); (Lee, et al. 2014). In this study, Image J software was used to analyse the images taken on fluorescence microscope of fixed cells after treatments. The images of each cell culture experiment were taken on the fluorescence microscope with the same exposure time for the control and the treatment. Image J allowed the separation of the different colour channels and the quantification of stained nuclei as well as the density of nuclear staining. This method allows converting the collected results from the fixed cells images into numbers that can be analysed and compared using Excel and Graphpad Prism.

One of the best methods to control the specificity of the primary antibodies is to knock-out the genes coding for the antigen (Burry 2011). The advantage of this method is that the primary antibody can be tested on knocked-out samples under the same conditions as otherwise used for the genetically unmanipulated samples in the experiments (Burry 2011). However, in some cases the knocked-out cells/tissues were still able to express mutated non-functional proteins and protein-epitopes (Burry 2011). Two of the several GBM cell cultures used in this study are NF-κB p65 knocked-out cell cultures. None of these two cell cultures showed NF-κB p65 nuclear staining. On the other hand, the remaining cell cultures in which NF-κB p65 had not been genetically manipulated showed different levels of nuclear staining for NF-κB p65. Therefore, the control method was adequate to test the specificity of the used primary antibodies.

TNFα is a cytokine that induces cellular proliferation, inflammatory response and anti-apoptotic functions via NF-κB (Chatterjee, et al. 2019). The activation and nuclear translocation of NF-κB p65 in response to TNFα were observed within ~30-60 minutes in several studies (Maguire, O'Loughlin and Minderman 2015); (Moreno, et al. 2010); (Noursadeghi, et al. 2008). This study shows similar findings when investigating nuclear accumulation of unphosphorylated NF-κB p65 or NF-κB p65 phosphorylated on serine 311 after TNFα treatments. The highest increase of nuclear NF-κB p65 phosphorylated on serine 311 was observed after 60 minutes of TNFα treatment when compared to shorter periods of time.

There are several drugs that show an inhibitory effect on NF-κB. For example, Denosumab as monoclonal antibody inhibiting Receptor Activator of NF-κB Ligand (RANKL) is a drug used in form of subcutaneous injection to treat osteoporosis (Boyce 2017). By inhibition of RANKL, denosumab reduces the inflammatory and improves the therapy response (Bonnet, et al. 2019). Although this work considers brain tumour (GBM), the denosumab is found to be associated with better therapeutic outcome for bone tumour patients e.g. for giant-cell tumour of bone (Chinder, et al. 2019). Potential side effects of denosumab i.a. are atypical femur fractures, osteonecrosis of the jaw, severe symptomatic hypocalcaemia, and anaphylaxis (Kalayanamitra, et al. 2019); (Abe, et al. 2019); (Zaheer, LeBoff and Lewiecki 2015).

Moreover, cortisol, the glucocorticoid hormone is known for its anti-inflammatory and anti-rheumatic effects (Gualtierotti, Parisi and Ingegnoli 2018); (Dong, et al. 2019). Eventually cortisol shows a downregulation of NF-κB by inhibiting the expression of various proinflammatory prostaglandins, interleukins, cytokines and the suppression of pro-inflammatory genes like cyclooxygenase (Dong, et al. 2019). Note that it is not possible to ignore the side effects of cortisol such as mood changes, osteoporosis, altered metabolism and the increased susceptibility to diabetes and Cushing's syndrome (Oprea, et al. 2019).

Furthermore, the activation of NF-κB pathway can also be downregulated by immunosuppressants such as the calcineurin inhibitors cyclosporine and tacrolimus. Also, the NF-κB pathway can be downregulated by the inhibitor of mammalian Target Of Rapamycin (mTOR) everolimus (Wu, Tong and Ran 2020); (Emal, et al. 2019); (Spadazzi, et al. 2019). The calcineurin inhibitors have many benefits such as immunosuppression after organ transplantation and autoimmune diseases. However, they may cause side effects such as hepatotoxicity, nephrotoxicity and gingival hyperplasia (Nastasio, et al. 2019); (Lee, et al. 2019).

Moreover, the monoclonal antibodies that inhibit TNFα (e.g. adalimumab), which are widely used to treat autoimmune diseases and intestinal inflammation (e.g. crohn's disease) show eventual inhibition of NF-κB (Urbano, Soccol and Azevedo 2014); (Park, et al. 2019). On the other hand, these monoclonal antibodies downregulate the immune response, which probably activate a latent tuberculosis and facilitates infections (Sator 2018); (Colombel, et al. 2017).

In comparison to the aforementioned drugs, the considered cannabidiol (CBD) in this study is an active ingredient in the cannabinoids group with anticonvulsant and neuroprotective properties (Sekar and Pack 2019). CBD can be administered orally, buccally and by inhalation (Urits, et al. 2019). CBD and tetrahydrocannabinol (THC) are the components of the oromucosal cannabinoid spray nabiximols (Sativex®) (Urits, et al. 2019). Nabiximols (Sativex®) is approved in Canada and some European countries for treating multiple sclerosis spasticity (Urits, et al. 2019).

Unlike THC, CBD is not psychoactive. Lately, CBD (Epidiolex®) was approved in the United States by the US Food and Drug Administration (FDA) and in the European Union for the treatment of epilepsy in children caused by Dravet and Lennox-Gastaut syndromes (European Medicines Agency 2021); (Greenwich Biosciences 2018). Administering the epilepsy agent Epidiolex® does not cause serious side effects in comparison to the side effects caused by the aforementioned drugs. Some of these non-serious side effects are diarrhea, drowsiness, poor appetite, fever and vomiting (European Medicines Agency 2021); (Thiele, et al. 2019); (Sekar and Pack 2019).

The effects of CBD as an anti-proliferative and pro-apoptotic agent were observed in numerous human cancers (Chakravarti, Ravi and Ganju 2014); (Massi, et al. 2013). Furthermore, CBD shows a cytotoxicity in GBM cells (Nabissi, et al. 2013); (Marcu, et al. 2010). In regards to the anti-inflammatory effects, CBD was able to reduce the NF-κB activation, which is induced by epidermal growth factor (Elbaz, et al. 2015). In GBM cells, CBD was shown to have minor effects on the level of NF-κB-p65 phosphorylated on serine 568 and NF-κB-p65 phosphorylated on serine 536 (Ivanov, Wu and Hei 2017). However, it was able to induce apoptosis in these cells after the suppression of NF-κB activation (Ivanov, Wu and Hei 2017).

This study investigated the effect of CBD on NF-κB nuclear translocation. It includes a number of GBM cell cultures for this purpose. The GBM as a malignant tumour shows different mutations and subclasses. The responses to the treatments vary from one mutation to another. CBD induced NF-κB nuclear translocation in some GBM cell cultures, which was also comparable to TNFα effects, while other cell cultures were not affected by CBD. As for TNFα effect, it was noticed that there is no induction of NF-κB nuclear translocation in part of the observed GBM cell cultures. This can be due to the high level of nuclear NF-κB in these GBM cells. The high level of nuclear NF-κB could be attributed to the deletion of NFKBIA, which is the gene encoding the IκBα (NF-KB inhibitor alpha). Note that this deletion is detected in approximately 25% of GBMs (Masilamani, et al. 2017). The absence of NF-κB inhibition is associated with high level of NF-κB activity, increased therapy resistance and poor survival (Kinker, et al. 2016); (Cahill, Morshed and Yamini 2015); (Bredel, et al. 2010).

Since NF-κB requires phosphorylation to initiate its full transcriptional activity, the effect of CBD on the nuclear accumulation of NF-κB p65 phosphorylated on serine 311 has also been investigated. Similarly, the GBM cell cultures showed various responses. In most GBM cell cultures that were affected by CBD, it was noticed that CBD inhibited the nuclear accumulation of NF-κB p65 phosphorylation on serine 311 induced by TNFα. Note that this inhibition was achieved after CBD pre-treatment for 16 hours. CBD could not show an inhibition of nuclear NFκB p65 phosphorylation on serine 311 in shorter time periods, specifically after pre-treatment for 6 hours.

The molecular biomarkers in transgenic murine glioblastoma cells included in this study show different responses to the CBD treatment. The GBM cells with mutated tumour protein p53 reacted to CBD by elevation of the nuclear NFκB p65. But nevertheless, CBD could not inhibit the phosphorylation of NFκB p65 on serine 311 in this cells. Moreover, the overexpression of Platelet-Derived Growth Factor Receptor (PDGFB) is not expected to play an obvious role in response to the CBD treatment, as it was specified in groups that responded to CBD treatment and also in another groups that did not respond. Glioblastoma cells with a lack of Cyclin-dependent kinase inhibitor 2A (CDKN2A) and an overexpression of the Epidermal Growth Factor Receptor (EGFR) showed an inhibition of the phosphorylation of NFκB p65 on serine 311 caused by CBD.

Summary

Glioblastoma is classified by the World Health Organization (WHO) as a grade 4 tumour. NF-κB as a transcription factor plays a major role in glioblastoma surviving by inducing inflammatory and anti-apoptotic pathways. This study investigates the effect of cannabidiol as a therapeutic option on the transduction signals at a molecular level in the highly malignant glioblastoma. In particular, the effect of cannabidiol on the nuclear translocation of NF-κB and its phosphorylation.

This study was performed on free glioblastoma cells *in vitro*. The chosen methods that have been used for this study were the immunocytochemistry and immunofluorescence staining. The used methods allowed investigating the nuclear NF-κB on fixed cells without lysing or damaging their structure. Furthermore, this study investigated the effect of TNF alpha as a positive control on the phosphorylation and nuclear translocation of NF-κB.

The vital glioblastoma cells were treated with cannabidiol for different time periods prior to fixing them. The corresponding antibodies were selected for the immunofluorescence staining. In particular, anti NF-κB antibody and phospho NF-κB serin 311 antibody. The analysis was performed on images taken by immunofluorescent microscope using Image J software for quantification and measurements of nuclear staining.

Glioblastoma cells shown different responses to cannabidiol treatment. In some of the glioblastoma cell cultures, cannabidiol could induce the nuclear translocation of NF-κB, which is comparable to the effect of TNF alpha. On the other hand, cannabidiol inhibit the nuclear accumulation of NF-κB phosphorylated on serine 311 in most of these cells. However, other glioblastoma cell cultures show no response to the cannabidiol in terms of phosphorylation and nuclear translocation of NF-κB. Some of these cell cultures do not even show response to TNF alpha.

Zusammenfassung

Glioblastom wird von der Weltgesundheitsorganisation (WHO) als Tumorgrad 4 eingestuft. NF-κB als Transkriptionsfaktor spielt eine wichtige Rolle beim Überleben der Glioblastomen, indem es entzündliche und anti-apoptotische Signalwege induziert. Diese Studie untersucht die Wirkung von Cannabidiol als therapeutische Option auf die Transduktionssignale auf molekularer Ebene im hochmalignen Glioblastomzellen. Insbesondere die Wirkung von Cannabidiol auf die nukleare Translokation von NF-κB sowie auf seine Phosphorylierung.

Diese Studie wurde an nicht-adhärenten Glioblastomzellen *in vitro* durchgeführt. Zu den angewendeten Methoden zählten die Immunzytochemie und Immunfluoreszenzfärbung. Sie ermöglichten die Untersuchung von NF-κB in fixierten Zellen, ohne die Zellen zu lysieren oder ihre Struktur zu beschädigen. Weiterhin wurde der Effekt von TNF-alpha als Positivkontrolle für die NF-κB Phosphorylierung und nukleäre Translokation untersucht. Hierfür wurden zahlreiche Glioblastom-Zellkulturen analysiert.

Die Glioblastomzellen wurden in verschiedene Behandlungsgruppen aufgeteilt. Die Behandlungsgruppen wurden mit Cannabidiol, TNFα, und mit beiden für jeweils verschiedene Zeiträume behandelt. Nach der Behandlung wurden die Glioblastomzellen fixiert und mit zwei verschiedenen NF-κB p65 Antiköpern gefärbt. Die Antikörper dienen der Detektion der nukleären Lokalisation von NF-κB. Der erste Antikörper wird für die Detektion des Gesamt-NF-κB p65 verwendet, während der zweite Antiköper für die Detektion des phosphorylierten Phospho-NF-κB-p65-Serin 311 verwendet wird.

Nach der Immunfluoreszenzfärbung wurden Bilder der Zellen mit einem Immunfluoreszenzmikroskop aufgenommen. Diese wurden mit einem Imaging Programm analysiert - dies beinhaltet das Zählen der Zellen und die Messung der Intensität der Immunfluoreszenzfärbung. Nach der Analyse wurden die Ergebnisse der verschiedenen Behandlungsgruppen mit der Kontrolle verglichen.

Das Glioblastom zeigt verschiedene Mutationen und Unterklassen, wodurch das Ansprechen auf verschiedene Medikamente variiert. Cannabidiol zeigte in einigen Glioblastom-Zelllinien einen Effekt auf NF-κB nukleäre Translokation. Dies war auch vergleichbar mit dem Effekt von TNFα. Andere Glioblastom-Zelllinien waren nicht betroffen. In einigen von ihnen induzierte sogar TNFα keine nukleäre Translokation von NF-κB. Ein Teil dieser Zelllinien zeigte durchwegs einen hohen Anteil an nukleärem NF-κB.

Authour's Publication

This work has been published in:

- Marie N. M. Volmar, Jiying Cheng, Haitham Alenezi, Sven Richter, Alisha Haug, Zonera Hassan, Maria Goldberg, Yuping Li, Mengzhuo Hou, Christel Herold-Mende, Cecile L Maire, Katrin Lamszus, Charlotte Flüh, Janka Held-Feindt, Gaetano Gargiulo, Geoffrey J Topping, Franz Schilling, Dieter Saur, Günter Schneider, Michael Synowitz, Joel A Schick, Roland E Kälin, Rainer Glass. „Cannabidiol converts NF-κB into a tumor suppressor in glioblastoma with defined antioxidative properties“ Neuro-Oncology, November 2021; Volume 23, Issue 11, Pages 1898–1910, https://doi.org/10.1093/neuonc/noab095

References

Abe, Ichiro, Kentaro Ochi, Yuichi Takashi, Yuka Yamao, Hanako Ohishi, Hideyuki Fujii, Midori Minezaki, et al. 2019. *Effect of denosumab, a human monoclonal antibody of receptor activator of nuclear factor kappa-B ligand (RANKL), upon glycemic and metabolic parameters: Effect of denosumab on glycemic parameters.* Medicine (Baltimore). 98(47):e18067.

Ahmed, KaziT., Md Ruhul Amin, Parv Shah, and Declan W. Ali. 2018. *Motor neuron development in zebrafish is altered by brief (5-hr) exposures to THC (Δ9-tetrahydrocannabinol) or CBD (cannabidiol) during gastrulation.* Scientific Reports 10518 (2018).

Alexander V. Bagaev, corresponding author1,4 Anastasiya Y. Garaeva, Ekaterina S. Lebedeva, Alexey V. Pichugin, Ravshan I. Ataullakhanov, and Fazly I. Ataullakhanov. 2019. *Elevated pre-activation basal level of nuclear NF-κB in native macrophages accelerates LPS-induced translocation of cytosolic NF-κB into the cell nucleus.* Scientific reports. 2019; 9: 4563.

Belmellat, Nadia, Luca Semerano, Noria Segueni, Diane Damotte, Patrice Decker, Bernhard Ryffel, Valérie Quesniaux, Marie-Christophe Boissier, and Eric Assier. 2017. *Tumor Necrosis Factor-Alpha Targeting Can Protect against Arthritis with Low Sensitization to Infection.* Frontiers in immunology 14;8:1533.

Bonnet, Nicolas, Lucie Bourgoin, Emmanuel Biver, Eleni Douni, and Serge Ferrari. 2019. *RANKL inhibition improves muscle strength and insulin sensitivity and restores bone mass.* J Clin Invest. 1; 129(8): 3214–3223.

Boyce, Alison M. 2017. *Denosumab: An Emerging Therapy in Pediatric Bone Disorders.* Curr Osteoporos Rep. 15(4): 283–292.

Bredel, Markus, Denise M. Scholtens, Ajay K. Yadav, Angel A. Alvarez, Jaclyn J. Renfrow, James P. Chandler, Irene L.Y. Yu, et al. 2010. *NFKBIA Deletion in Glioblastomas.* The New England journal of medicine, 364(7), 627-37.

Bremner, Paul, and Michael Heinrich. 2010. *Natural products as targeted modulators of the nuclearfactor-κB pathway.* Journal of Pharmacy and Pharmacology 54(4):453-72, 18 02.

Brito, Cheila, Ana Azevedo, Susana Esteves, Ana Rita Marques, Carmo Martins, Ilda Costa, Manuela Mafra, José M. Bravo Marques, Lúcia Roque, and Marta Pojo. 2019. *Clinical insights gained by refining the 2016 WHO classification of diffuse gliomas with: EGFR amplification, TERT mutations, PTEN deletion and MGMT methylation.* BMC Cancer volume 19, Article number: 968.

Burry, Richard W. 2011. *Controls for Immunocytochemistry: An Update.* Journal of histochemistry & cytochemistry, 59(1): 6–12.

Cahill, Kirk E., Ramin A. Morshed, and Bakhtiar Yamini. 2015. *Nuclear factor-κB in glioblastoma: insights into regulators and targeted therapy.* Neuro-oncology, 18(3), 329-39.

Caron, Gersende, Yves Delneste, Jean-Pierre Aubry, Giovanni Magistrelli, Nathalie Herbault, Aline Blaecke, Anthony Meager, Jean-Yves Bonnefoy, and Pascale Jeannin. 1999. *Human NK cells constitutively express membrane TNF-alpha (mTNFalpha) and present mTNFalpha-dependent cytotoxic activity.* European journal of immunology 29(11):3588-95.

Chakravarti, Bandana, Janani Ravi, and Ramesh K. Ganju. 2014. *Cannabinoids as therapeutic agents in cancer: current status and future implications.* Oncotarget, 5(15): 5852–5872.

Chatterjee, Budhaditya, Payel Roy, Uday Aditya Sarkar, Mingming Zhao, Yashika Ratra, Amit Singh, Meenakshi Chawla, et al. 2019. *Immune Differentiation Regulator p100 Tunes NF-κB Responses to TNF.* Frontiers in immunology. 2019; 10: 997.

Chinder, Pramod Shekarappa, Suraj Hindiskere, Srinath Doddarangappa, and Utkarsh Pal. 2019. *Evaluation of Local Recurrence in Giant-Cell Tumor of Bone Treated by Neoadjuvant Denosumab.* Clin Orthop Surg. 11(3): 352–360.

Christian, Frank, Emma L. Smith, and Ruaidhrí J. Carmody. 2016. *The Regulation of NF-κB Subunits by Phosphorylation.* Cells. 2016 Mar; 5(1): 12.

Christofferson., Dana E, Ying Li, and Junying Yuan. 2014. *Control of Life-or-Death Decisions by RIP1 Kinase.* Annual Review of Physiology 76:129-50.

Colombel, J.-F., B. Jharap, W. J. Sandborn, B. Feagan, L. Peyrin-Biroulet, S. F. Eichner, A. M. Robinson, N. M. Mostafa, Q. Zhou, and R. B. Thakkar. 2017. *Effects of concomitant immunomodulators on the pharmacokinetics, efficacy and safety of adalimumab in patients with Crohn's disease or ulcerative colitis who had failed conventional therapy.* Aliment Pharmacol Ther. 2017 Jan; 45(1): 50–62.

da Nóbrega, FR, O Ozdemir, SCS Nascimento Sousa, JN Barboza, H Turkez, and DP de Sousa. 2018. *Piplartine Analogues and Cytotoxic Evaluation against Glioblastoma.* Molecules. 23(6): 1382.

Dai, Erhei, Lianshan Zhang, Lihong Ye, Shiqing Wan, Lulu Feng, Qi Qi, Fang Yao, and Zhen Li. 2017. *Hepatic expression of cannabinoid receptors CB1 and CB2 correlate with fibrogenesis in patients with chronic hepatitis B.* Vol. 59. International Journal of Infectious Diseases 59:124-130.

Deng, Liting, Josée Guindon, Benjamin L. Cornett, Alexandros Makriyannis, Ken Mackie, and Andrea G. Hohmann. 2014. *Chronic cannabinoid CB2 activation reverses paclitaxel neuropathy without tolerance or CB1-dependent withdrawal.* Biological psychiatry 77(5): 475–487.

Deng, Liting, Lindsay Ng, Tatsuya Ozawa, and Nephi Stella. 2017. *Quantitative Analyses of Synergistic Responses between Cannabidiol and DNA-Damaging Agents on the Proliferation and Viability of Glioblastoma and Neural Progenitor Cells in Culture.* The Journal of pharmacology and experimental therapeutics 360(1):215-224.

Deora, Arun, Subramanya Hegdea, Jacqueline Leea, Chee-Ho Choi, Qing Chang, Cheryl Lee, Lucia Eaton, et al. 2017. *Transmembrane TNF-dependent uptake of anti-TNF antibodies.* mAbs 9(4):680-695.

Devinsky, Orrin, Maria Roberta Cilio, Helen Cross, Javier Fernandez-Ruiz, Jacqueline French, Charlotte Hill, Russell Katz, et al. 2014. *Cannabidiol: Pharmacology and potential therapeutic role in epilepsy and other neuropsychiatric disorders.* Epilepsia 55(6): 791–802.

Diaz-Meco, Maria T., and Jorge Moscat. 2012. *The atypical PKCs in inflammation: NF-κB and beyond.* Immunological reviews 246(1): 154–167, 3.

Dong, Junsheng, Jianji Li, Luying Cui, Yefan Wang, Jiaqi Lin, Yang Qu, and Heng Wang. 2019. *Cortisol modulates inflammatory responses in LPS-stimulated RAW264.7 cells via the NF-κB and MAPK pathways.* BMC Vet Res. 2018; 14: 30.

Duran, Angeles, María T. Diaz-Meco, and Jorge Moscat. 2003. *Essential role of RelA Ser311 phosphorylation by ζPKC in NF-κB transcriptional activation.* EMBO Journal 22(15): 3910–3918.

Elbaz, Mohamad, Mohd W. Nasser, Janani Ravi, Nissar A. Wani, Dinesh K. Ahirwar, Helong Zhao, Steve Oghumu, et al. 2015. *Modulation of the tumor microenvironment and inhibition of EGF/EGFR pathway: Novel anti-tumor mechanisms of Cannabidiol in breast cancer.* Molecular oncology, 9(4): 906–919.

Emal, Diba, Elena Rampanelli, Nike Claessen, Frederike J. Bemelman, Jaklien C. Leemans, Sandrine Florquin, and Mark C. Dessing. 2019. *Calcineurin inhibitor Tacrolimus impairs host immune response against urinary tract infection.* Scientific Reports volume 9, Article number: 106 (2019) .

European Medicines Agency. 2021. *Epidyolex (cannabidiol) An overview of Epidyolex and why it is authorised in the EU.* European Medicines Agency: EMA/191061/2021 - Epidyolex (cannabidiol) An overview of Epidyolex and why it is authorised in the EU, https://www.ema.europa.eu/en/documents/overview/epidyolex-epar-medicine-overview_en.pdf, March.

Evans, Sean M., Kyle G. Rodino, Haley E. Adcox, and Jason A. Carlyon. 2018. *Orientia tsutsugamushi uses two Ank effectors to modulate NF-κB p65 nuclear transport and inhibit NF-κB transcriptional activation.* PLoS Pathog. 2018 May; 14(5): e1007023.

Filippis, Daniele De, Giuseppe Esposito, Carla Cirillo, Mariateresa Cipriano, Benedicte Y. De Winter, Caterina Scuderi, Giovanni Sarnelli, et al. 2011. *Cannabidiol Reduces Intestinal Inflammation through the Control of Neuroimmune Axis.* PLoS One 6(12):e28159.

Fluhrer, Regina, Gudula Grammer, Lars Israel, Margaret M. Condron, Christof Haffner, Elena Friedmann, Claudia Böhland, et al. 2006. *A gamma-secretase-like intramembrane cleavage of TNFalpha by the GxGD aspartyl protease SPPL2b.* Nature Cell Biology 8(8):894-6.

Ghovanloo, Mohammad-Reza, Noah Gregory Shuart, Janette Mezeyova, Richard A. Dean, Peter C. Ruben, and Samuel J. Goodchild. 2018. *Inhibitory effects of cannabidiol on voltage-dependent sodium currents.* The Journal of biological chemistry 293(43):16546-16558.

Gilmore, TD. 2006. *Introduction to NF-jB: players, pathways, perspectives.* Boston: Oncogene 25(51):6680-4.

Greenwich Biosciences, Inc. 2018. "EPIDIOLEX® (cannabidiol) oral solution. Highlights of prescribing information." June. https://www.accessdata.fda.gov/drugsatfda_docs/label/2018/210365lbl.pdf.

Gualtierotti, Roberta, Marco Parisi, and Francesca Ingegnoli. 2018. *Perioperative Management of Patients with Inflammatory Rheumatic Diseases Undergoing Major Orthopaedic Surgery: A Practical Overview.* Adv Ther. 2018; 35(4): 439–456.

Guo, Xiaoxia, Xiaoxi Ling, Fang Du, Qingbing Wang, Wei Huang, Zhongmin Wang, Xiaoyi Ding, Mingfeng Bai, and Zhiyuan Wu. 2018. *Molecular Imaging of Pancreatic Duct Adenocarcinoma Using a Type 2 Cannabinoid Receptor-Targeted Near-Infrared Fluorescent Probe.* Translational Oncology (5):1065-1073.

Hayden, Matthew S., and Sankar Ghosh. 2004. *Signaling to NF-kappaB.* Genes & Development 18(18):2195-224.

Heldin, Carl-Henrik. 2013. *Targeting the PDGF signaling pathway in tumor treatment.* Cell Communication Signal 11: 97.

Helgadottir, Hildur, Paola Ghiorzo, Remco van Doorn, Susana Puig, Max Levin, Richard Kefford, Martin Lauss, et al. 2018. *Efficacy of novel immunotherapy regimens in patients with metastatic melanoma with germline CDKN2A mutations.* Journal of Medical Genetics 2018-105610, 05 10.

Hillger, JuliaM., Beaule Roy, Zi Wang, Thea Mulder-Krieger, DorretI. Boomsma, P. Eline Slagboom, Erik H.J.Danen, AdriaanP.I Jzerman, and LauraH.Heitman. 2017. *Phenotypic screening of cannabinoid receptor 2 ligands shows different sensitivity to genotype.* Biochemical pharmacology 130:60-70.

Hochrainer, Karin, Racchumi, Gianfranco, and Josef Anrather. 2013. *Site-specific Phosphorylation of the p65 Protein Subunit Mediates Selective Gene Expression by Differential NF-κB and RNA Polymerase II Promoter Recruitment.* The Jurnal of Biological Chemistry, 288(1): 285–293.

Horiuchi, Takahiko, Hiroki Mitoma, Shin-ichi Harashima, Hiroshi Tsukamoto, and Terufumi Shimoda. 2010. *Transmembrane TNF-α: structure, function and interaction with anti-TNF agents.* Rheumatology (Oxford) 49(7):1215-28.

Ibeas Bih, Clementino, Tong Chen, Alistair V. W. Nunn, Michaël Bazelot, Mark Dallas, and Benjamin J. Whalley. 2015. *Molecular Targets of Cannabidiol in Neurological Disorders.* Neurotherapeutics. 2015 Oct; 12(4): 699–730.

Ivanov, Vladimir N., Jinhua Wu, and Tom K. Hei. 2017. *Regulation of human glioblastoma cell death by combined treatment of cannabidiol, γ-radiation and small molecule inhibitors of cell signaling pathways.* Oncotarget 8(43):74068-74095.

Jamontt, JM, A Molleman, RG Pertwee, and ME Parsons. 2010. *The effects of Δ9-tetrahydrocannabinol and cannabidiol alone and in combination on damage, inflammation and in vitro motility disturbances in rat colitis.* British journal of pharmacology 160(3): 712–723.

Jesionek-Kupnicka, Dorota, Malgorzata Szybka, Beata Malachowska, Wojciech Fendler, Piotr Potemski, Sylwester Piaskowski, Dariusz Jaskolski, et al. 2014. *TP53 Promoter Methylation in Primary Glioblastoma: Relationship with TP53 mRNA and Protein Expression and Mutation Status.* DNA and Cell Biology 33(4): 217–226.

Kalayanamitra, Ricci, Ibrahim Yaghnam, Ravi Patel, Andrew Groff, and Rohit Jain. 2019. *The Calcium Culprit: A Case of Denosumab-induced Hypocalcemia.* Cureus. 11(5): e4768.

Kinker, Gabriela Sarti, Andrew Maltez Thomas, Vinicius Jardim Carvalho, Felipe Prata Lima, and André Fujita. 2016. *Deletion and low expression of NFKBIA are associated with poor prognosis in lower-grade glioma patients.* Scientific Reports, volume 6, Article number: 24160.

Korc, Murray. 2016. *RelA: a tale of a stitch in time.* J Clin Invest. 2016 Aug 1; 126(8): 2799–2801.

Langford, R. M., J. Mares, A. Novotna, M. Vachova, I. Novakova, W. Notcutt, and S. Ratcliffe. 2013. *A double-blind, randomized, placebo-controlled, parallel-group study of THC/CBD oromucosal spray in combination with the existing treatment regimen, in the relief of central neuropathic pain in patients with multiple sclerosis.* Journal of neurology 260(4):984-97.

Lash, L.H. 2010. *Renal Toxicology.* Comprehensive Toxicology, Volume 7, 2010, Pages 117-150.

Lee, Eun Hee, Soojin Kim, Mi-Sun Choi, Se-Myo Park, Kyoung-Sik Moon, Seokjoo Yoon, and Jung-Hwa Oh. 2019. *Inhibition of PPARα target genes during*

cyclosporine A-induced nephrotoxicity and hepatotoxicity. Molecular & Cellular Toxicology volume 15, pages185–197.

Lee, Eunjee, Raymund L. Yong, Patrick Paddison, and Jun Zhu. 2018. *Comparison of glioblastoma (GBM) molecular classification methods.* Semin Cancer Biol. ;53:201-211.

Lee, Robin E. C., Sarah R. Walker, Kate Savery, David A. Frank, and Suzanne Gaudet. 2014. *Fold-change of nuclear NF-κB determines TNF-induced transcription in single cells.* Molecular cell, 53(6), 867-79.

Leon-Boenig, Gladysde, Krista K.Bowman, Jianwen A.Feng, Terry Crawford, Christine Everett, Yvonne Franke, Angela Oh, et al. 2012. *The Crystal Structure of the Catalytic Domain of the NF-κB Inducing Kinase Reveals a Narrow but Flexible Active Site.* Structure 20(10):1704-14.

Levy, Dan, Alex J. Kuo, Yanqi Chang, Uwe Schaefer, Christopher Kitson, Peggie Cheung, Alexsandra Espejo, et al. 2011. *SETD6 lysine methylation of RelA couples GLP activity at chromatin to tonic repression of NF-κB signaling.* Nature Immunology volume 12, pages29–36(2011).

Liu, Fei, Yifeng Xia, Aaron S. Parker, and Inder M. Verma. 2012. *IKK Biology.* Immunological Reviews 246(1): 239–253.

Liu, Ting, Lingyun Zhang, Donghyun Joo, and Shao-Cong Sun. 2017. *NF-κB signaling in inflammation.* Signal Transduct Target Ther. 2017; 2: 17023.

Louis, David. N., Arie Perry, Pieter Wesseling, Daniel J Brat, Ian A Cree, Dominique Figarella-Branger, Cynthia Hawkins, et al. 2021. *The 2021 WHO Classification of Tumors of the Central Nervous System: a summary.* Neuro-Oncology, Volume 23, Issue 8, August 2021, Pages 1231–1251.

Maguire, Orla, Kieran O'Loughlin, and Hans Minderman. 2015. *Simultaneous assessment of NF-κB/p65 phosphorylation and nuclear localization using imaging flow cytometry.* Journal of immunological methods 423: 3–11.

Malta, Tathiane M, Camila F de Souza, Thais S Sabedot, Tiago C Silva, Maritza S Mosella, Steven N Kalkanis, James Snyder, Ana Valeria B Castro, and Houtan Noushmehr. 2018. *Glioma CpG island methylator phenotype (G-CIMP): biological and clinical implications.* Neuro Oncol. 20(5): 608–620.

Marcu, Jahan P., Rigel T. Christian, Darryl Lau, Anne J. Zielinski, Maxx P. Horowitz, Jasmine Lee, Arash Pakdel, et al. 2010. *Cannabidiol enhances the inhibitory effects of Δ9-tetrahydrocannabinol on human glioblastoma cell proliferation and survival.* Molecular cancer therapeutics, 9(1): 180–189.

Masilamani, A P, R Ferrarese, E Kling, N K Thudi, H Kim, D M Scholtens, F Dai, et al. 2017. *KLF6 depletion promotes NF-κB signaling in glioblastoma.* Oncogene volume 36, pages3562–3575(2017).

Massi, Paola, Marta Solinas, Valentina Cinquina, and Daniela Parolaro. 2013. *Cannabidiol as potential anticancer drug.* British journal of clinical pharmacology, 75(2): 303–312.

McComb, S, H H Cheung, R G Korneluk, S Wang, L Krishnan, and S Sad. 2012. *cIAP1 and cIAP2 limit macrophage necroptosis by inhibiting Rip1 and Rip3 activation.* Cell death and differentiation 19(11):1791-801.

Mitoma, Hiroki, Takahiko Horiuchi, Hiroshi Tsukamoto, and Naoyasu Ueda. 2018. *Molecular mechanisms of action of anti-TNF-α agents – Comparison among therapeutic TNF-α antagonists.* Cytokine 101:56-63.

Mohan, Mohita J., Theresa Seaton, Justin Mitchell, Anne Howe, Kevin Blackburn, William Burkhart, Mary Moyer, et al. 2002. *The Tumor Necrosis Factor-α*

Converting Enzyme (TACE): A Unique Metalloproteinase with Highly Defined Substrate Selectivity. Biochemistry 41(30):9462-9.
Molinaro, Annette M., Jennie W. Taylor, John K. Wiencke, and Margaret R. Wrensch. 2019. *Genetic and molecular epidemiology of adult diffuse glioma.* Nat Rev Neurol.15(7):405-417.
Moreno, Rita, Jürgen-Markus Sobotzik, Christian Schultz, and M. Lienhard Schmitz. 2010. *Specification of the NF-κB transcriptional response by p65 phosphorylation and TNF-induced nuclear translocation of IKKε.* Nucleic acids research 38(18): 6029–6044.
Mussbacher, Marion, Manuel Salzmann, Christine Brostjan, Bastian Hoesel, Christian Schoergenhofer, Hannes Datler, Philipp Hohensinner, et al. 2019. *Cell Type-Specific Roles of NF-κB Linking Inflammation and Thrombosis.* Front Immunol. 2019; 10: 85.
Nabissi, Massimo, Maria Beatrice Morelli, Matteo Santoni, and Giorgio Santoni. 2013. *Triggering of the TRPV2 channel by cannabidiol sensitizes glioblastoma cells to cytotoxic chemotherapeutic agents.* Carcinogenesis, 34(1):48-57.
Nastasio, Silvia, Marco Sciveres, Lorenza Matarazzo, Cristina Malaventura, Francesco Cirillo, Silvia Riva, and Giuseppe Maggiore. 2019. *Long-term follow-up of children and young adults with autoimmune hepatitis treated with cyclosporine.* Digestive and Liver Disease, Volume 51, Issue 5, 712 - 718.
Noursadeghi, Mahdad, Jhen Tsang, Thomas Haustein, Robert F. Miller, Benjamin M. Chain, and David R. Katz. 2008. *Quantitative imaging assay for NF-κB nuclear translocation in primary human macrophages.* Journal of immunological methods 329(1-2): 194–200.
Oeckinghaus, Andrea, and Sankar Ghosh. 2009. *The NF-κB Family of Transcription Factors and Its Regulation.* Cold Spring Harb Perspectives in Biology 1(4): a000034, 10.
Oprea, Alina, Nicolas C. G. Bonnet, Olivier Pollé, and Philippe A. Lysy. 2019. *Novel insights into glucocorticoid replacement therapy for pediatric and adult adrenal insufficiency.* Ther Adv Endocrinol Metab. 2019; 10: 2042018818821294.
Pagano, Ester, Raffaele Capasso, Fabiana Piscitelli, Barbara Romano, Olga A. Parisi, Stefania Finizio, Anna Lauritano, Vincenzo Di Marzo, Angelo A. Izzo, and Francesca Borrelli. 2016. *An Orally Active Cannabis Extract with High Content in Cannabidiol attenuates Chemically-induced Intestinal Inflammation and Hypermotility in the Mouse.* Frontiers in pharmacology 7: 341.
Park, Jiae, Sun-Young Lee, Jeeheun Shon, Koeun Kim, Hyo Jin Lee, Kyung Ah Kim, Boo-Yong Lee, Seung-Hun Oh, Nam Keun Kim, and Ok Joon Kim. 2019. *Adalimumab improves cognitive impairment, exerts neuroprotective effects and attenuates neuroinflammation in an Aβ1-40-injected mouse model of Alzheimer's disease.* Cytotherapy. 2019 Jun;21(6):671-682.
Prescott, Jack A., and Simon J. Cook. 2018. *Targeting IKKβ in Cancer: Challenges and Opportunities for the Therapeutic Utilisation of IKKβ Inhibitors.* Cells. 7(9):115, 08.
Reina-Campos, Miguel, Maria T. Diaz-Meco, and Jorge Moscat. 2019. *The Dual Roles of the Atypical Protein Kinase Cs in Cancer.* Cancer Cell. ;36(3):218-235, 16 09.

Renshaw, Simon. 2017. *Immunohistochemistry and Immunocytochemistry Essential Methods.* 2nd Edition. John Wiley & Sons, Ltd.

Rimessi, Alessandro, Simone Patergnani, Elli Ioannidi, and Paolo Pinton. 2013. *Chemoresistance and Cancer-Related Inflammation: Two Hallmarks of Cancer Connected by an Atypical Link, PKCζ.* Front Oncol. ; 3: 232.

Rog, David J., Turo J. Nurmikko, Tim Friede, and Carolyn A. Young. 2005. *Randomized, controlled trial of cannabis-based medicine in central pain in multiple sclerosis.* Neurology. Neurology 65(6):812-9.

Ruiz-Perera, Lucia M., Lennart Schneider, Beatrice A. Windmöller, Janine Müller, Johannes F. W. Greiner, Christian Kaltschmidt, and Barbara Kaltschmidt. 2018. *NF-κB p65 directs sex-specific neuroprotection in human neurons.* Scientific reports, 8: 16012.

Sator, Paul. 2018. *Safety and tolerability of adalimumab for the treatment of psoriasis: a review summarizing 15 years of real-life experience.* Ther Adv Chronic Dis. 2018 Aug; 9(8): 147–158.

Schoedel, Kerri A., Isabella Szeto, Beatrice Setnik, Edward M.Sellers, Naama Levy-Cooperman, Catherine Mills, Tilden Etges, and Kenneth Sommerville. 2018. *Abuse potential assessment of cannabidiol (CBD) in recreational polydrug users: A randomized, double-blind, controlled trial.* Epilepsy & behavior 88:162-171.

Sekar, Krithiga, and Alison Pack. 2019. *Epidiolex as adjunct therapy for treatment of refractory epilepsy: a comprehensive review with a focus on adverse effects.* Version 1. F1000Res. 2019; 8: F1000 Faculty Rev-234.

Sinigaglia, Mathieu, Tarek Assi, Florent L. Besson, Samy Ammari, Myriam Edjlali, Whitney Feltus, Laura Rozenblum-Beddok, et al. 2019. *Imaging-guided precision medicine in glioblastoma patients treated with immune checkpoint modulators: research trend and future directions in the field of imaging biomarkers and artificial intelligence.* EJNMMI Res. 2019; 9: 78.

Spadazzi, Chiara, Federica Recine, Laura Mercatali, Giacomo Miserocchi, Chiara Liverani, Alessandro De Vita, Alberto Bongiovanni, Valentina Fausti, and Toni Ibrahim. 2019. *mTOR inhibitor and bone-targeted drugs break the vicious cycle between clear-cell renal carcinoma and osteoclasts in an in vitro co-culture model.* J Bone Oncol. 2019 Jun; 16: 100227.

Sundar, Swetha J., Jason K. Hsieh, Sunil Manjila, Justin D. Lathia, and Andrew Sloan. 2014. *The role of cancer stem cells in glioblastoma.* Neurosurgical Focus 37(6):E6.

Szaflarski, Jerzy P., Elizabeth Martina Bebin, Gary Cutter, Jennifer DeWolfe, Leon S.Durec, Tyler E.Gaston, Pongkiat Kankirawatana, et al. 2018. *Cannabidiol improves frequency and severity of seizures and reduces adverse events in an open-label add-on prospective study.* Epilepsy & behavior S1525-5050(18)30473-6.

Tegowski, Matthew, and Albert Baldwin. 2018. *Noncanonical NF-κB in Cancer.* Biomedicines 6(2): 66.

Thiele, Elizabeth, Eric Marsh, Maria Mazurkiewicz-Beldzinska, Jonathan J. Halford, Boudewijn Gunning, Orrin Devinsky, Daniel Checketts, and Claire Roberts. 2019. *Cannabidiol in patients with Lennox-Gastaut syndrome: Interim analysis of an open-label extension study.* Epilepsia. 60(3): 419–428.

Urbano, Paulo César Martins, Vanete Thomaz Soccol, and Valderilio Feijó Azevedo. 2014. *Apoptosis and the FLIP and NF-kappa B proteins as pharmacodynamic criteria for biosimilar TNF-alpha antagonists.* Biologics. 2014; 8: 211–220.

Urits, Ivan, Matthew Borchart, Morgan Hasegawa, Justin Kochanski, Vwaire Orhurhu, and Omar Viswanath. 2019. *An Update of Current Cannabis-Based Pharmaceuticals in Pain Medicine.* Pain Ther. Jun; 8(1): 41–51.

Verhaak, Roel G.W., Katherine A. Hoadley, Elizabeth Purdom, Victoria Wang, Yuan Qi, Matthew D. Wilkerson, C. Ryan Miller, et al. 2010. *An integrated genomic analysis identifies clinically relevant subtypes of glioblastoma characterized by abnormalities in PDGFRA, IDH1, EGFR and NF1.* Cancer Cell 17 (1) 98–110.

Vermeulen, Linda, Gert De Wilde, Petra Van Damme, Wim Vanden Berghe, and and Guy Haegeman. 2003. *Transcriptional activation of the NF-κB p65 subunit by mitogen- and stress-activated protein kinase-1 (MSK1).* EMBO Journal 22(6):1313-24.

Vlahopoulos, Spiros A., Osman Cen, Nina Hengen, James Agan, Maria Moschovi, Elena Critselis, Maria Adamaki, et al. 2015. *Dynamic aberrant NF-κB spurs tumorigenesis: a new model encompassing the microenvironment.* Cytokine Growth Factor Rev. 26(4): 389–403.

Volmar, Marie N M, Jiying Cheng, Haitham Alenezi, Sven Richter, Alisha Haug, Zonera Hassan, Maria Goldberg, et al. 2021. *Cannabidiol converts NF-κB into a tumor suppressor in glioblastoma with defined antioxidative properties.* Neuro-Oncology, Volume 23, Issue 11, Pages 1898–1910, https://doi.org/10.1093/neuonc/noab095 , November.

Wang, Dan, Sandy D. Westerheide, Julie L. Hanson, and Albert S. Baldwin. 2000. *Tumor Necrosis Factor α-induced Phosphorylation of RelA/p65 on Ser529 Is Controlled by Casein Kinase II.* Journal of Biological Chemistry 275(42):32592-7.

Wang, Qianghu, Baoli Hu, Xin Hu, Hoon Kim, Massimo Squatrito, Lisa Scarpace, Ana C. de Carvalho, et al. 2017. *Tumor Evolution of Glioma-Intrinsic Gene Expression Subtypes Associates with Immunological Changes in the Microenvironment.* Cancer Cell. 32(1):42-56.e6.

Wood, Matthew D., Joydeep Mukherjee, and Russell O Pieper. 2018. *Neurofibromin knockdown in glioma cell lines is associated with changes in cytokine and chemokine secretion in vitro.* Scientific Reports volume 8, Article number: 5805.

Wu, Biyu, Jinglu Tong, and Zhihua Ran. 2020. *Tacrolimus Therapy in Steroid-Refractory Ulcerative Colitis: A Review.* Inflamm Bowel Dis. 2020 Jan 1;26(1):24-32.

Yamazaki, Soh, Tatsushi Muta, and Koichiro Takeshige. 2001. *A Novel IκB Protein, IκB-ζ, Induced by Proinflammatory Stimuli, Negatively Regulates Nuclear Factor-κB in the Nuclei.* Journal of Biological Chemistry 276(29):27657-62.

Young, Richard M., Aria Jamshidi, Gregory Davis, and Jonathan H. Sherman. 2015. *Current trends in the surgical management and treatment of adult glioblastoma.* Annals of Translational Medicine 3(9):121.

Zaheer, Sarah, Meryl LeBoff, and E. Michael Lewiecki. 2015. *Denosumab for the Treatment of Osteoporosis.* Expert Opin Drug Metab Toxicol. 11(3): 461–470.

Zajicek, John P., and Vicentiu I. Apostu. 2011. *Role of Cannabinoids in Multiple Sclerosis.* CNS Drugs 25(3):187-201.

Zeligs, Kristen P., Monica K. Neuman, and Christina M. Annunziata. 2016. *Molecular Pathways: The Balance between Cancer and the Immune System Challenges the Therapeutic Specificity of Targeting Nuclear Factor-κB*

Signaling for Cancer Treatment. Clin Cancer Res. 2016 Sep 1; 22(17): 4302–4308.

Zeng, Ailiang, Jianxing Yin, Yan Li, Rui Li, Zheng Wang, Xu Zhou, Xin Jin, Feng Shen, Wei Yan, and Yongping You. 2018. *miR-129-5p targets Wnt5a to block PKC/ERK/NF-κB and JNK pathways in glioblastoma.* Cell Death & Diseasevolume, 9(3): 394.

Zhang, Hongtao, Alan Berezov, Qiang Wang, Geng Zhang, Jeffrey Drebin, Ramachandran Murali, and Mark I. Greene. 2007. *ErbB receptors: from oncogenes to targeted cancer therapies.* The Journal of Clinical Investigation 117(8): 2051–2058, 8.

Zhou, Wen, and Junying Yuan. 2014. *Necroptosis in health and diseases.* Seminars in cell and developmental biology 35:14-23.

Acknowledgment

First and foremost, I would like to express my sincerest gratitude to my supervisor Prof. Dr. Rainer Glass for his limitless support and continual guidance throughout my research progress.

I owe a great debt of gratitude to Dr. Roland Kaelin for the feedback and advice during my laboratory experiments and Mrs. Stefanie Lange for her intensive laboratory efforts and support.

It was a great honour to work alongside such an elite team.

I would like to express my heartfelt thanks to my parents, my sisters and brothers for their endless support. This achievement would not have been possible without them.

Finally, thank you to my friends and colleagues for always being there to encourage and support.

LMU LUDWIG-MAXIMILIANS-UNIVERSITÄT MÜNCHEN

Promotionsbüro
Medizinische Fakultät

MMRS MUNICH MEDICAL RESEARCH SCHOOL

Eidesstattliche Versicherung

Alenezi, Haitham

Name, Vorname

Ich erkläre hiermit an Eides statt,

dass ich die vorliegende Dissertation mit dem Titel

Investigating the Effect of Cannabidiol on NF-κB Phosphorylation and Nuclear Translocation in Glioblastoma Cells.

selbständig verfasst, mich außer der angegebenen keiner weiteren Hilfsmittel bedient und alle Erkenntnisse, die aus dem Schrifttum ganz oder annähernd übernommen sind, als solche kenntlich gemacht und nach ihrer Herkunft unter Bezeichnung der Fundstelle einzeln nachgewiesen habe.

Ich erkläre des Weiteren, dass die hier vorgelegte Dissertation nicht in gleicher oder in ähnlicher Form bei einer anderen Stelle zur Erlangung eines akademischen Grades eingereicht wurde.

Bonn, 30.09.2022

Ort, Datum

Haitham Alenezi

Unterschrift Doktorandin bzw. Doktorand